The Dissertation Committee for Katherine Ann Alfredo Certifies that this is the approved version of the following dissertation:

DRINKING WATER TREATMENT BY ALUM COAGULATION: COMPETITION AMONG FLUORIDE, NATURAL ORGANIC MATTER, AND ALUMINUM

Committee:

Desmond F. Lawler, Co-Supervisor

Lynn E. Katz, Co-Supervisor

Howard M. Liljestrand

Gerald E. Speitel Jr.

James A. Holcombe

DRINKING WATER TREATMENT BY ALUM COAGULATION: COMPETITION AMONG FLUORIDE, NATURAL ORGANIC MATTER, AND ALUMINUM

by

Katherine Ann Alfredo, B.E.; M.S.E.

Dissertation

Presented to the Faculty of the Graduate School of

The University of Texas at Austin

in Partial Fulfillment

of the Requirements

for the Degree of

Doctor of Philosophy

The University of Texas at Austin

December 2012

Dedication

To Mo, my best friend.

Acknowledgements

To the two people who most directly shaped me as a researcher, I want to acknowledge my advisers, Des Lawler and Lynn Katz. I would not feel as confident as I do in my research skills if not for you both. I know it must have been difficult to advise me since I feel I was often proposing a grand-plan, of which were parts that could possibly maybe someday look like a decent proposal. Thanks to the two of you I did eventually adopt blinders, without which I may be proposing another scheme to study abroad. With your continued support and an unflagging determination to see that I remain on course I was able to focus and finish my work as a doctoral candidate.

To Hillary Hart and Jay Banner, who, while they were not my advisers, have influenced me in ways only an adviser can, both inside the lab and out. The support you both have shown me, especially over the last few years, has always made me feel like I could accomplish anything. Hillary, I enjoyed working with you on the research ethics project and really hope that there is an opportunity to collaborate again. Your door was always open and you provided a safe environment for me to discuss anything regarding my research, my travels, my big research proposal plans, anything. Jay, you have had a huge influence on my community involvement and engagement. I truly feel that being involved in the GK-12 program was life-changing for me, once again making me aware of these other paths which intersect the one I continue to travel. You have shown me incredible support. You have both been great mentors and an integral component in my development as a researcher.

My family, both the one which I was born into, and the one I have had the ability to create, has without a doubt been a major support system for me. Mom, Dad, and Alex,

thanks for letting me take over the dining room table this thanksgiving, and allowing me to turn my "visit" into an incessant work session, for allowing me to cancel the plans we had made in advance, and for not calling me out on this. As this is only one instance of your willingness to shape your lives to mine when the occasion calls for it, you should know that I appreciate you having been so very patient through it all. I want to thank Chris and Ellison Carter, my Austin family and one half of *Hillhome*, for dealing with my messiness and allowing me to blame it on stress, for cooking dinner when I forgot to buy groceries, and for taking time to hang out on the couch. *FamilyTime* would not have been the same had you not been there. You two are family, no asterisks or blood required.

Lastly, I want to acknowledge and thank my husband, Mo. Words cannot describe the amount of support you have given me over the last 7 years, to include (but not limited to) quitting your job and moving to Ghana because I had a "hunch." You are a great friend and the person to whom I dedicate my dissertation and all my future work. I would not want to hop all over the world studying water related issues if I could not share the experiences with you. I love you. Thank you for all of your support.

DRINKING WATER TREATMENT BY ALUM COAGULATION: COMPETITION AMONG FLUORIDE, NATURAL ORGANIC MATTER, AND ALUMINUM

Publication No._____

Katherine Ann Alfredo, Ph.D.

The University of Texas at Austin, 2012

Supervisors: Desmond F. Lawler and Lynn E. Katz

Some community water systems using sources containing elevated levels of fluoride, in the United States and worldwide, struggle to treat their drinking water to healthy fluoride concentrations. Many treatment plants in the U.S. currently use aluminum based salts, such as aluminum sulfate and polyaluminium chloride, as coagulants during conventional treatment for removal of particles from drinking water sources. Moreover, enhanced aluminum sulfate, or alum, coagulation requires higher concentrations of aluminum added to the process and has been shown to be effective for removal of disinfectant byproduct precursors, i.e., natural organic matter (NOM). The presence of fluoride may interfere with the formation of aluminum hydroxide precipitates, and interrelationships among NOM, aluminum precipitation and fluoride removal are not well understood.

A fundamental understanding of how fluoride alters the properties of aluminum precipitates and how fluoride and NOM molecules compete as ligands interacting with soluble aluminum species is lacking. As a result, the development of guidelines for implementation and optimization of a treatment scheme that uses aluminum in the presence of fluoride requires a multi-faceted approach in which the development of a mechanistic understanding of these interactions is conducted in concert with macroscopic experiments to identify optimum conditions for simultaneous removal of fluoride and NOM.

To date, little research has looked at the efficiency of removing both fluoride and organics from the perspective of the precipitation process. To provide a foundation for revising treatment techniques, this research evaluated the effect of co-precipitating aluminum in the presence of fluoride, organics, and in multi-ligand systems to characterize the solid precipitate and removal competition. This research verified the formation of a co-precipitate in the presence of fluoride and certain low molecular weight organics. Co-precipitation from organics and fluoride competes for removal, especially at low alum coagulant doses, complicating treatment for resource limited areas.

.

Table of Contents

List of Tables xii

List of Figures xiv

Chapter 1: Introduction 1

1.1: Background 1

1.2 Problem Statement 2

1.3 Approach 3

1.3.1 Evaluate how co-precipitating aluminum solids in the presence of fluoride affects the characteristics of the solid precipitate 4

1.3.2 Evaluate the effect of a co-precipitating solid on removal and competition of low molecular weight organics and fluoride 4

1.3.3 Evaluate the effect of a co-precipitating solid on removal and competition of natural organic matter and fluoride 5

1.3.4 Evaluation of fluoride's impact on the stability of formed co-precipitates in the presence of low molecular weight organics. ... 5

1.4 Summary 5

Chapter 2: Background 7

2.1 Introduction 7

2.2 Fluoride in Drinking Water: History in the United States and Human Health Effects 7

2.3 Fluoride in Drinking Water: Water Treatment Effects and Regulation .. 12

2.4 Natural Organic Matter: Structure and Regulations 20

2.5 Aluminum: Environmental Presence and Health Effects 26

2.6 Drinking Water Treatment: Aluminum, Particles, NOM, and Fluoride . 28

2.7 Summary 34

Chapter 3: Research Approach and Methodology 35

3.1 Research Approach 35

3.2 Methodology 38

3.2.1 Jar Tests: Simulating drinking water treatment at bench scale ... 38

3.2.2 Titrations of precipitates 42

3.2.3 Analysis of aqueous constituent concentrations 43
3.2.4 Precipitate dry analysis 44
3.2.5 Precipitate wet analysis: *In situ* measurements of precipitate physical characteristics 46
3.3 Summary 48

Chapter 4: Fluoride incorporation into aluminum oxide precipitates during alum coagulation 50
4.1 Introduction 50
4.2 Research Approach 53
4.3 Results and Discussion 58
4.4 Conclusion 79

Chapter 5: Competition between fluoride and low molecular weight organics during alum coagulation 82
5.1 Introduction 82
5.2 Background and Selection of NOM surrogates 86
5.3 Research Approach 87
5.4 Results and Discussion 89
5.5 Conclusions 105

Chapter 6: Competition between fluoride and natural organic matter during alum coagulation 108
6.1 Introduction 108
6.2 Research Approach 111
6.3 Results and Discussion 113
6.4 Conclusions 134

Chapter 7: Stability of aluminum precipitates 137
7.1 Introduction 137
7.2 Background 137
7.3 Research Approach 139
7.4 Results and Discussion 140
7.5 Conclusions 166

Chapter 8: Conclusions 168
8.1 Fluoride Co-Precipitation 168
8.2 Effect of a Co-Precipitating Solid on Removal and Competition of Low Molecular Weight Organics 169
8.3 Competition Between Fluoride and Natural Organic Matter and the Ability to Model Removal using a Low Molecular Weight Organic Acid 171
8.4 Stability and Dissolution of Amorphous Aluminum Precipitates 172
8.5 Implications for drinking water treatment plants 173
8.6 Future work 174
Appendix 176
Appendix 1: Fourier Transform Infrared (FTIR) Spectroscopy 176
A-1.1 Background 176
A-1.2 Research Approach 176
A-1.3 Results and Discussion 178
A-1.4 Conclusions 182
References 184
Vita 194

List of Tables

Table 2-1: States containing at least 20 PWS with delivery water exceeding 2.0 mg/L F from natural sources (Department of Health and Human Services 1993) 16

Table 2-2: Molecular Weight Distribution of Aquatic Humus from various sources (from Prakash and MacGregor 1983) 20

Table 2-3: Required removal of total organic carbon by enhanced coagulation for systems using conventional treatment. (EPA 815-R-99-012 1999)..31

Table 3-1: Low molecular weight organic acids of interest 38

Table 3-2: Typical alum doses and initial aluminum concentrations used during jar tests for this study. 40

Table 4-1: Equilibrium constants for dissociated reactions of aluminum minerals and complexes (excerpt of compiled table in Lindsay and Walthall 1996)59

Table 4-2: Formation of aluminum solids dependent on ligand (sulfate and fluoride): aluminum dose ratio (Violante and Huang 1985).....71

Table 4-3: Specific surface area by gas adsorption 74

Table 4-4: SEM/EDX determination of Al:F ratios in precipitates 77

Table 4-5: Stoichiometric ratios normalized by aluminum concentration.....78

Table 4-6: Bonding energy position for flocs formed by 200 mg/L alum.....79

Table 5-1: Low molecular weight organic acids of interest 87

Table 6-1: Required removal of total organic carbon by enhanced coagulation for systems using conventional treatment. (EPA 815-R-99-012 1999)110

Table 6-2: Dominant coagulation mechanism for particle only system (interpreted from Amirtharajah and Mills (1982)) 115

Table 6-3: Zeta potential for pH 6.5 and 20 mg/L alum.....122
Table 6-4: Raw water and NOM Extracts of Lake Austin water.....124
Table 6-5: Zeta potential (from 20 mg/L alum analysis) for optimal precipitation pH range (determined from 100 mg/L alum solubility curves).....131
Table 7-1: Stability constants for formation of complexes and solids.....147

List of Figures

Figure 2-1: Change in dental fluorosis among children 12-15 years old (adapted from Beltran-Aguilar et al. 2010). 11

Figure 2-2: Counties in Texas that contain a PWS with naturally occurring fluoride above 1.5 mg/L (data from Fluoride Action Network and the 1993 Fluoride Census) 17

Figure 2-3: Possible structures for surface complexes of organic acids. (adapted from Evanko and Dzombak 1998).....25

Figure 2-4: Modes of particle destabilization in aluminum coagulation systems (adapted from Amirtharajah and Mills 1982) 29

Figure 3-1: Schematic of proposed research and chemical reactions. L represents ligands in solution, Al represents aluminum and the gray lines represent? 36

Figure 3-2: Schematic of the different jar test methodologies: Co-precipitation (CPT), preform (PRE), and transferred preform (T-PRE). 41

Figure 4-1: Fluoride complexes of aluminum as a function of [F] when $[Al^{3+}]$ is calculated from equilibrium with amorphous $Al(OH)_{3(s)}$ at pH 6.5..60

Figure 4-2: Co-precipitation and adsorption of fluoride by aluminum hydroxides.61

Figure 4-3: XRD images of aluminum precipitates formed at 100 mg/L alum and 200 mg/L alum. (a) and (b) contain no fluoride and (c) and (d) both contain 5 mg/L fluoride. All spectra show a lack of crystalline structure in the formed aluminum precipitates. 63

Figure 4-4: Schematic of proposed changes to aluminum coordination during fluoride co-precipitation at a given pH. 65

Figure 4-5: Titrations of background alkalinity and increasing doses of alum coagulant. 66
Figure 4-6: Titration curves of various alum doses with 0, 5, and 10 mg/L fluoride. 68
Figure 4-7: Titration curves for 50 mg/L alum and the associated precipitation curves. 69
Figure 4-8: XRD patterns of aged precipitates formed without and without fluoride present. 72
Figure 4-9: XRD pattern for alum only precipitates aged 45 days with matching boehmite spectrum peaks. 73
Figure 4-10: Particle size analysis of flocs formed by 100 mg/L alum (a-b) and 200 mg/L alum (c-d) doses with and without fluoride present. 75
Figure 4-11: SEM images of precipitates formed with and without fluoride present at the time of precipitation. 77
Figure 5-1: Common aqueous complexes between aluminum and organic acids (adapted from Vance et al. 1996)....84
Figure 5-2: Removal of LMW organics by alum coagulation 90
Figure 5-3: pH varied salicylic removal. 200 mg/L alum, initial concentrations of salicylic acid=5 mg/L C. 91
Figure 5-4: Impact of fluoride on removal of LMW organics by alum coagulation.94
Figure 5-5: Impact of 5 mg/L C from LMW organics on fluoride removal: Alum doses varied and pH 6.6. 95

Figure 5-6: Potential inner-sphere disruptions caused by fluoride precipitating with alum: Comparing (a) Proposed inner-sphere bonds for pyromellitic acid during alum coagulation and (b) proposed inner-sphere bonds for pyromellitic acid during alum coagulation when fluoride is present.96
Figure 5-7: Effects of the precipitation process on removal at pH 6.6 and varying alum coagulant doses: Comparing CPT and PRE systems for pyromellitic acid and fluoride removal. 98
Figure 5-8: X-ray diffraction patterns for aluminum precipitates formed during CPT and PRE experiments with pyromellitic acid.....100
Figure 5-9: 12-hour x-ray diffraction scan of aluminum precipitates formed in the presence of 5 mg/L C pyromellitic acid, confirming amorphous precipitates. 101
Figure 5-10: Comparison of pyromellitic acid impacts on fluoride removal at varying doses of influent fluoride concentrations: (a) fluoride removal density with 100 mg/L alum (b) fluoride removal density 200 mg/L alum. (c) Comparison of removal densities from varied fluoride on pyromellitic acid removal densities at 100 and 200 mg/L alum. 103
Figure 5-11: Comparison of fluoride impacts on pyromellitic acid removal at varying doses of influent pyromellitic acid concentrations: (a) organic removal density with 100 mg/L alum (b) organic removal density 200 mg/L alum. (c) Comparison of removal densities from varied pyromellitic acid on fluoride removal densities at 100 and 200 mg/L alum 104
Figure 6-1: Critical coagulation dose evaluated for single and dual ligand systems (a) residual turbidity, (b) NOM removal, (c) fluoride removal. 117

Figure 6-2: Residual aluminum for single and dual ligand systems at (a) 20 mg/L alum and (b) 50 mg/L alum. 119
Figure 6-3: NOM and fluoride removal in single and dual ligand systems over a range of coagulant doses. 120
Figure 6-4: Electrophoresis measurements for 20 mg/L alum systems containing various combinations of ligands in single and dual ligand systems123
Figure 6-5: Potentiometric titrations of isolated Lake Austin NOM. 126
Figure 6-6: Titration of 50 mg/L alum in systems with varying combinations of NOM and fluoride (a) Initial concentration of 5 mg/L C NOM and 5 mg/L fluoride, (b) Initial concentrations of 10 mg/L C (NOM) and fluoride. 127
Figure 6-7: Titration of 100 mg/L alum in systems with varying combinations of NOM and fluoride (a) Initial concentration of 5 mg/L C NOM and 5 mg/L fluoride, (b) Initial concentrations of 10 mg/L C (NOM) and fluoride. 128
Figure 6-8: Solubility curves for 100 mg/L alum in the presence of varying ligand combinations. 130
Figure 6-9: Comparison of NOM to LMW organic (pyromellitic) as a model surrogate over the 10-500 mg/L alum coagulant dose range: (a) percent organic removed, (b) percent fluoride removed. 132
Figure 6-10: Comparison of NOM to LMW organic (pyromellitic) as a model surrogate: low dose alum coagulant range: (a) percent organic removed, (b) percent fluoride removed. 133

Figure 7-1: Stability of aluminum during treatment: α-Al_2O_3 ([Al] = 349 μMol, equivalent aluminum concentrations of a 100 mg/L alum dose). (a) Residual aluminum as a function of time, (b) percent organic removed, (c) percent fluoride removed.....142

Figure 7-2: Stability of aluminum during treatment: preformed (PRE) aluminum precipitates using a 100 mg/L alum dose ([Al] = 349 μMol) (a) residual aluminum as a function of time, (b) percent organic removed, (c) percent fluoride removed.....144

Figure 7-3: Solubility diagrams (a) gibbsite (α-$Al(OH)_{3(s)}$), (b) amorphous $Al(OH)_{3(s)}$ (stability constants are presented in Table 7-1). 147

Figure 7-4: Stability of aluminum during treatment: preformed aluminum precipitates, transferred (T-PRE) using a 100 mg/L alum dose ([Al] = 349 μMol) (a) residual aluminum as a function of time, (b) percent organic removed, (c) percent fluoride removed.....149

Figure 7-5: Solubility of aluminum precipitates over a range of coagulant doses with $[F]_i$=5 mg/L: comparison of CPT and PRE (a) dissolution of aluminum CPT, (b) percent fluoride removed by CPT precipitates, (c) residual aluminum of PRE precipitates, (d) percent fluoride removed by PRE precipitates. 152

Figure 7-6: Solubility of CPT aluminum precipitates over a range of coagulant doses, C_i=5 mg/L salicylic acid, F_i = 0 and 5 mg/L (a) residual aluminum concentration F_i = 0 mg/L, (b) percent organic removed F_i = 0 mg/L (c) residual aluminum concentration F_i = 5 mg/L, (d) percent organic removed F_i = 5 mg/L, (e) percent fluoride removed F_i = 5 mg/L...158

Figure 7-7: Solubility of CPT aluminum precipitates over a range of coagulant doses, C_i=5 mg/L pyromellitic acid, F_i = 0 and 5 mg/L (a) residual aluminum concentration F_i = 0 mg/L, (b) percent organic removed F_i = 0 mg/L (c) residual aluminum concentration F_i = 5 mg/L, (d) percent organic removed F_i = 5 mg/L, (e) percent fluoride removed F_i = 5 mg/L...159

Figure 7-8: Solubility of CPT aluminum precipitates over a range of coagulant doses, C_i=5 mg/L phthalic acid, F_i = 0 and 5 mg/L (a) residual aluminum concentration F_i = 0 mg/L, (b) percent organic removed F_i = 0 mg/L (c) residual aluminum concentration F_i = 5 mg/L, (d) percent organic removed F_i = 5 mg/L, (e) percent fluoride removed F_i = 5 mg/L...163

Figure 7-9: Comparison of CPT aluminum solubility for select coagulant doses: 100 mg/L (a, b) and 200 mg/L (c, d) alum doses. Residual aluminum concentrations in the phthalic acid systems are plotted separately to highlight the dissolution effects of a phthalic and fluoride CPT system (b, d).....165

Figure A1-1: FTIR spectra for corundum and precipitated aluminum solids from 200 mg/L alum.....179

Figure A1-2: FTIR spectra of the pressed KBr pellets for precipitates formed by 200 mg/L alum. (a) 200 mg/L alum only, (b) CPT with 5 mg/L C from pyromellitic acid, (c) CPT with 5 mg/L F, (d) PRE with 5 mg/L C from pyromellitic acid, and (e) CPT dual ligand system with 5 mg/L F and 5 mg/L C from pyromellitic acid. 181

Chapter 1: Introduction

The goals of this study were to (1) evaluate how co-precipitating aluminum solids in the presence of fluoride affects the characteristics of the solid precipitate, (2) evaluate the effect of a co-precipitating solid on removal and competition of low molecular weight organics and fluoride, (3) evaluate the effect of a co-precipitating solid on removal and competition of natural organic matter and fluoride, and (4) evaluate the stability of co-precipitated aluminum in the presence of low molecular weight organics and fluoride.

1.1: BACKGROUND

Today, few utilities in North America are concerned about excessive fluoride (F) in their drinking water, but this situation is likely to change in the coming years. Many municipalities fluoridate their water to reach a dose in the range of 0.7-1.2 mg/L F to promote healthy teeth and bone development. In 2011, the Department of Health and Human Services and the U.S. Environmental Protection Agency (EPA) recommended changing the fluoridation practice from the above range to a level of 0.7 mg/L F (Isa 2011); however, the regulated limit for fluoride still remains at 4.0 mg/L. When fluoride is present at levels greater than 1.5 mg/L, it can have negative health effects through incorporation into growing enamel crystals (Aoba and Ferjeskov 2002) and substitution for hydroxyl ions in the apatite structure (Elliot 1994). A March 2010 announcement by EPA Administrator Lisa Jackson included fluoride among the contaminant regulations requiring more research (Jones 2010). This announcement, along with the more recent reduction in recommended fluoridation levels, drives the anticipation that the EPA will reduce the fluoride maximum contaminant level (MCL) in the coming years from its current limit of 4.0 mg/L F. As a result of these recent announcements, many utilities currently in compliance regarding naturally occurring fluoride in their water would suddenly face problems meeting a lower standard, and other systems currently blending

groundwater with surface water to meet standards would have to reconsider their strategy.

According to the EPA, more than 90% of all public water systems are small (less than 10,000 people). Similarly, many of the counties in the United States with naturally occurring fluoride levels above the EPA MCL are served by small public water systems (PWS) (Department of Health and Human Services 1993). According to the Center for Disease Control (CDC) 2006 Water Fluoridation Statistics, 69.2% of the U.S. population on PWSs receives fluoridated water. Of these PWSs, 20% are naturally fluoridated at or above optimal levels. The health effects of fluoride on these smaller, often more rural populations are a concern. Many small drinking water utilities have limited human resources and funds to conduct the required research to optimize treatment. Furthermore, if/when the EPA fluoride MCL is adjusted to reflect the standards of the rest of the world (most adhere to the 1.5 mg/L F guideline set by the World Health Organization), many more municipalities, including those serving larger communities, will be affected.

1.2 PROBLEM STATEMENT

Fluoride, while relatively non-reactive with most water constituents, has a high reactivity with aluminum. Many drinking water treatment plants in the U.S. use aluminum sulfate (alum) or polyaluminum chloride (PACl) as coagulants in the removal of both particles (turbidity) and natural organic matter (NOM); however, since most utilities are unconcerned with fluoride's effect on treatment, the interactions between fluoride and aluminum in complex, natural waters are not adequately understood.

A fundamental understanding of how fluoride alters the properties of aluminum precipitates and how fluoride and NOM molecules compete as ligands interacting with

soluble aluminum species is lacking. As a result, the development of guidelines for implementation and optimization of a treatment scheme that uses aluminum in the presence of fluoride requires a multi-faceted approach in which the development of a mechanistic understanding of these interactions is conducted in concert with macroscopic experiments to identify optimum conditions for simultaneous removal of fluoride and NOM. To date, little research has looked at the efficiency of removing both fluoride and organics from the perspective of the precipitation process. To fill this gap and provide a foundation for revising treatment techniques for water containing fluoride, this research is based around the following goals:

1. Evaluate how co-precipitating aluminum solids in the presence of fluoride affects the characteristics of the solid precipitate
2. Evaluate the effect of a co-precipitating solid on removal and competition of low molecular weight organics and fluoride
3. Evaluate the effect of a co-precipitating solid on removal and competition of natural organic matter and fluoride
4. Evaluate the stability of co-precipitated aluminum in the presence of low molecular weight organics and fluoride

1.3 APPROACH

The experimental approach to understanding the efficiency of removing both fluoride and natural organic matter during alum coagulation and the evaluation of each of the four research goals are organized into four experimental sections.

1.3.1 Evaluate how co-precipitating aluminum solids in the presence of fluoride affects the characteristics of the solid precipitate

This research goal was designed to verify the presence of a co-precipitate in the presence of fluoride at alum doses that are relevant to water treatment processes. The precipitates formed in the presence of fluoride were analyzed using particle size analysis, x-ray diffraction, and titration of the forming precipitates to determine the structural changes in a proposed Al-F precipitate as compared to an aluminum hydroxide precipitate formed under identical conditions without fluoride. Scanning electron microscopy and x-ray photoelectron spectroscopy both provided information regarding precipitate stoichiometry and chemistry. Conclusions regarding the precipitate are only possible after the analysis of the combined results since the amorphous characteristics of the precipitates often obfuscate many of the results or conclusions from particular analyses.

1.3.2 Evaluate the effect of a co-precipitating solid on removal and competition of low molecular weight organics and fluoride

The second research goal was aimed at the determination of the impact of a co-precipitate on the removal of low molecular weight organics and fluoride and the associated primary removal mechanisms. The research evaluated the treatment efficiency of systems with multiple ligands. Using three structurally different low molecular weight organic acids in co-precipitating, competing systems with fluoride allowed for the broad analysis of the type of ligand surface bonds. A more in depth study of the co-precipitating impacts of pyromellitic acid and fluoride on removal in sole and dual ligand systems were tested to further explore co-precipitation mechanisms in dual ligand systems.

1.3.3 Evaluate the effect of a co-precipitating solid on removal and competition of natural organic matter and fluoride

The third research goal evaluated the impact of a co-precipitate in systems most closely resembling a treatment plant. The research determined the impact of NOM and fluoride on particle removal, aluminum precipitation, and the primary removal mechanisms of multiple ligand systems. Analyses comparing removals of pyromellitic acid in sole and dual ligand systems with fluoride to those using natural organic matter assessed the ability to predict natural organic matter removal with a surrogate, low molecular weight organic.

1.3.4 Evaluation of fluoride's impact on the stability of formed co-precipitates in the presence of low molecular weight organics.

The fourth and final research goal evaluated the impact of fluoride on co-precipitate stability through ligand promoted dissolution. Analyses comparing the aluminum dissolution of oxides, aluminum precipitates, and co-precipitates formed in the presence of multiple ligand systems were used to further assess the removal mechanisms concluded in the previous chapters. The dissolution of the precipitates assisted in further assessment in the coordination of the LMW organics as inner- or outer-sphere bonding.

1.4 SUMMARY

The remainder of this document is organized into seven chapters. Chapter 2, Background, outlines concerns and difficulties of drinking water treatment to remove NOM and fluoride alone and when both constituents are present in the source water. Chapter 3, Research Approach and Methodology, explains the experimental methods and gives the motivation behind the experimental design. The experimental results and

discussion are located in Chapter 4 through Chapter 7, each building on the previous chapter's analysis in pursuit of determining the effects of a formed co-precipitate on contaminant removal as outlined in the problem statement and research approach. The final chapter, Chapter 8, summarizes the major findings from this research and outlines possible future research that is still needed to fully recommend a treatment regimen for a plant struggling to meet both fluoride and organics removal using alum coagulation.

Chapter 2: Background

2.1 Introduction

The motivation of this research is to understand how fluoride effects and is affected by drinking water treatment operations currently using aluminum sulfate as a coagulant. The outlined goals all involve evaluating the treatment process through an in-depth analysis of the formed precipitates in multi-ligand systems to evaluate the competition between fluoride and natural organic matter during removal. To accomplish these goals, the history, occurrence, and regulated concentration limits for drinking water are presented for fluoride, natural organic matter, and aluminum. The existing research studies that have investigated one or two of these components are presented throughout this chapter, but despite the depth and breadth of previous research, a knowledge gap persists. To achieve the aforementioned research goals, an investigation of competition during alum coagulation and the precipitation process is needed. It was from this viewpoint that past research was analyzed and the following sections are presented.

2.2 Fluoride in Drinking Water: History in the United States and Human Health Effects

The most common health-effect associated with long-term ingestion of fluoride is fluorosis of the teeth and bones. Both dental and skeletal fluorosis involve a replacement of hydroxyl ions with fluoride in the growing apatite structure. Dental fluorosis is a change in the mineralization of the dental hard tissues (enamel, dentin, and cementum) from prolonged ingestion of fluoride while the teeth are still developing and have not erupted into the mouth (Beltran-Aguilar 2010). The timeframe for these reactions is typically constrained to the first eight years of life. After the tooth erupts, dental fluorosis is classified into categories based on visually detectable changes in enamel according to

the Dean's Fluorosis Index developed by H.T. Dean in the 1930s. The criteria for categorization include (Beltran-Aguilar et al. 2010; Dean 1934):

- *Unaffected:* Enamel is translucent with a smooth, glassy surface of a pale white color.
- *Questionable:* Enamel shows slight changes from a few white flecks to white spots.
- *Very mild*: Small opaque white areas are more common but are less than 25% of the surface.
- *Mild*: More extensive coverage of white opaque areas, but still covers less than 50% of the tooth surface. The surfaces of molars, pre-molars, and incisors exhibit bluish shades as a result of the top layers having worn off.
- *Moderate*: White opaque areas cover more than 50% of the enamel surface.
- *Severe*: All enamel surfaces are impacted with pitting. Pits are deeper and stains are widespread ranging from brown to black with the form of the teeth possibly affected.

Documented cases of fluorosis and the prevalence of fluoride in drinking water of the United States began in 1901 with studies conducted by a series of dentists. Fredrick McKay first studied severe cases of fluorosis in Colorado Springs, Colorado. After moving to the area, McKay noticed many of his patients' teeth contained brown stains. The affliction, called "Colorado Brown Stain," affected most residents, but McKay noticed that the residents had few dental caries despite these brown stains (Black and McKay 1916). McKay observed similar conditions in Oakley, Idaho where only residents consuming piped water had brown stains on their teeth. The case in Oakley is significant

for several reasons. First, it marks an instance where residents became political activists, voting on water quality issues because of dental afflictions. The residents of Oakley successfully convinced the town government to abandon the pipe supply and find a more suitable source (McKay 1925). Oakley also represented a case study where a comparison was possible between residents growing up in the area drinking piped water and those who moved to the area after their teeth already formed, allowing McKay to link mottled teeth to consumption of the piped water as a child (McKay 1925).

Despite this link to the piped water, the cause still eluded dentists and researchers. In 1926, McKay was sent two incisors of a young boy in Oakley pulled for unrelated dental reasons, making it possible to run laboratory analyses on the teeth. The test results linked the stains to manganese, but McKay believed that manganese did not cause the brown statins, but rather stained the teeth after eruption (McKay 1927). McKay traveled across the United States surveying teeth to understand the relationship between mottling and cavities. He noted that while teeth appeared corroded, there was no marked increase in cavities when compared to the teeth of residents without brown teeth (McKay and Black 1929). Late in the 1920s, McKay was appointed to the Public Health Service in Bauxite, Arkansas to determine the cause of mottling in the residents. It was here that McKay sampled and tested the water to find fluoride present. Retracing his steps to the other locations, McKay demonstrated the presence of fluoride in drinking water at levels above 2 mg/L in all cases (Churchill 1931). In light of this discovery, several municipal water supplies across the United States were surveyed for the presence of fluoride. Churchill (1931), however, emphasized that the coinciding occurrences of fluoride and dental mottling were not sufficient enough to draw definitive conclusions. It was the extensive characterization of teeth by H.T. Dean in the 1930s and research directed toward relating fluoride levels to caries and enamel markings that conclusively verified

the linkage between fluoride levels and dental deformities. Dean proposed a recommended fluoride concentration of 1.2 mg/L to promote healthy tooth development; further, he recommended that for the concentrations not exceed 2.0 mg/L because, at such levels, the detrimental effects of fluoride outweigh the benefits (Dean et al. 1942). In response, many community water fluoridation programs were developed to add fluoride to community water and reduce tooth decay for the local populations (Beltran-Aguilar et al. 2010).

Using data from the 1999-2004 National Health and Nutrition Examination survey, a report published in 2010 described the prevalence of dental fluorosis in the United States. Fluorosis was limited to 25% of the population aged 6-49 and the cases were predominantly mild (Beltran-Aguilar et al. 2010). Within this 25% of the population, dental fluorosis is higher in adolescents, especially those 12-15 years old, than in adults. The study also compared the 1999-2004 national survey to the 1986-1987 National Survey of Oral Health in U.S. School Children and analyzed trends in fluorosis as presented in Figure 2-1 below.

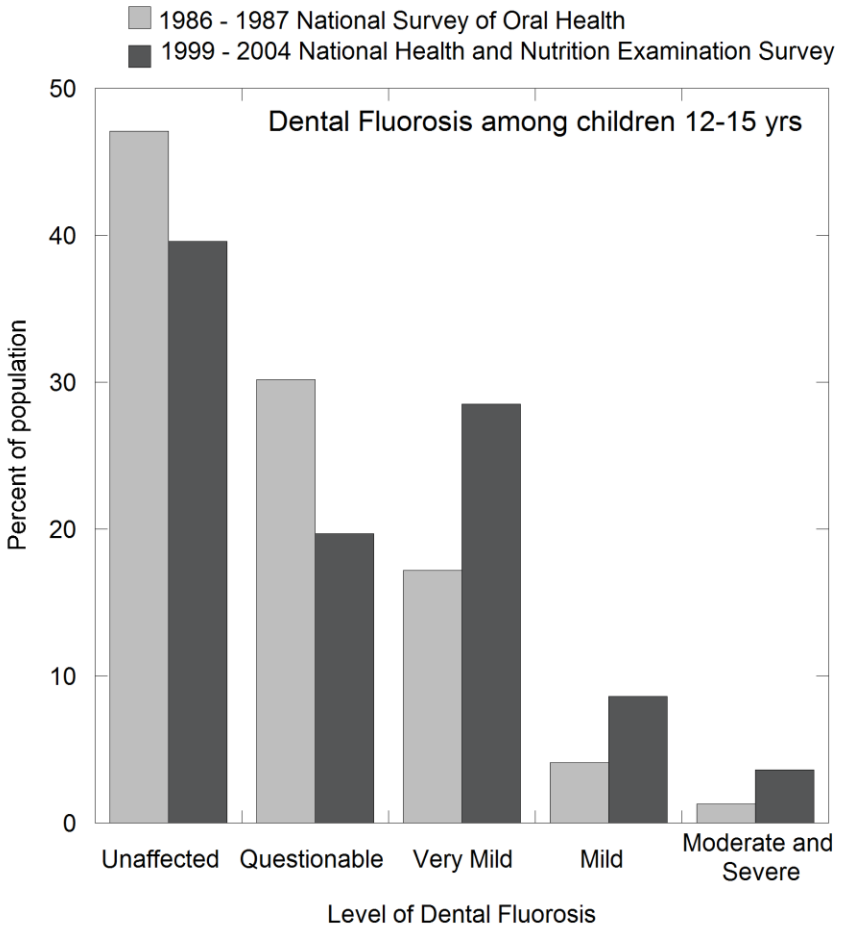

Figure 2-1: Change in dental fluorosis among children 12-15 years old (adapted from Beltran-Aguilar et al. 2010).

The occurrence of fluorosis in children has increased since the 1980s and is likely attributable to the availability of fluoride in dental care products and food. Typically, low levels of fluoride are contained within fruits and vegetables, but grains, especially barley and rice, and root vegetables such as taro, yams, and cassava have been reported to contain levels of approximately 2 mg/kg (Fawell et al. 2006). Tea leaves contain varying amounts of fluoride, ranging from over 100 mg/kg in Asia and Hungary to less than

1 mg/kg in areas of Germany (Fawell et al. 2006); such variation complicates the determination of daily intake across a population. As fluoride becomes more ubiquitous in a population's diet, the desirable concentrations in drinking water and associated regulated limits are called into question. In the next section, the regulation of fluoride in the United States, the determination of exposure, and an examination of fluoride occurrence in Texas and the resulting impact on treatment are discussed.

2.3 Fluoride in Drinking Water: Water Treatment Effects and Regulation

Fluoride is regulated in the United States as part of the National Drinking Water Regulations. All regulated contaminants receive different levels of enforcement that correspond to distinct health related regulatory levels explained below.

In regulating a drinking water contaminant, the EPA first sets a Maximum Contaminant Level Goal (MCLG). The MCLG is a non-enforceable, public health goal meant to mark the concentration at which no known adverse health effects occur. The MCLG does not take into account treatment possibilities or cost and, therefore, solely reflects health concerns with ingesting the contaminant. The enforceable Maximum Contaminant Level (MCL) is the regulated limit that a contaminant in water can be delivered to a user of a public water system. A third standard, the Secondary Maximum Contaminant Level (SMCL), exists as a non-enforceable guideline for contaminants in drinking water that may cause cosmetic or aesthetic effects. The MCL and SMCL are based on both health concerns and achievable treatment.

Despite the recommendations by H.T. Dean in the 1930s, it was not until 1985 that the U.S. Environmental Protection Agency (EPA) set the primary, enforceable MCL for fluoride in drinking water at 4.0 mg/L. This established limit is not based on the

dental-related effects catalogued by Dean, but rather on the oral reference dose for crippling skeletal fluorosis (EPA 2003). The EPA considers dental fluorosis largely cosmetic and set the SMCL of 2.0 mg/L to recognize fluoride's effect on the development of tooth enamel (EPA 2007). The MCLG, from which the MCL and SMCL are derived, is set at a level equivalent to the MCL at 4.0 mg/L F. This value seems to violate the purpose of a contaminant goal level based solely on health effects, as indicated below. The apparent contradiction between setting the MCLG at 4.0 mg/L F and the documented announcements by the EPA (Jones 2010) and Department of Health and Human Services (Isa 2011) leads one to expect an eventual lowering of the MCL.

The MCLG value of 4.0 mg/L F was recently reviewed by the National Research Council in 2006 and, excluding mild fluorosis from the "detrimental to health" stance, they found that occurrence of severe dental fluorosis can occur in populations once the threshold of 2 mg/L fluoride is exceeded (Carton 2006). The committee also agreed that populations exposed to a drinking water concentration of 4 mg/L F over a lifetime are likely to have a greater number of bone fractures than a population exposed to 1 mg/L or less. The MCL and MCLG levels currently target preventing "crippling skeletal fluorosis" or the most severe, Stage III condition of skeletal fluorosis. Skeletal fluorosis can occur undetected over decades while the skeleton is continuously accumulating fluoride. The accumulation transforms a "normal" bone through the stages of fluorosis, beginning with sporadic pain and stiffness of the joints and increasing in severity until Stage III is reached. At that point, calcification of the ligaments in the neck and vertebral column create crippling deformities in the spine and major joints. Accompanying these conditions is often muscle wasting and compression of nerves, thereby causing neurogenic symptoms (Reddy 2009).

The EPA calculates non-carcinogenic contaminant MCLGs using a reference dose (RfD) shown in Eq. 2-1 and

Eq. 2-2 (EPA 2010b). Typically, the relative source contribution (RSC) for drinking water is assumed to be 20% for EPA calculations; however, back calculating a MCLG of 4 mg/L given the other parameters reported (RfD 0.11, UF 2.5, adult body weight 70kg, intake 2 L/day) (EPA 822-R-03-008 2003), the RSC for fluoride is equivalent to 1.0. This higher RSC of 1.0 assumes that 100% of the RfD for fluoride is obtained from drinking water sources. While high fluoride levels are found in black tea, milk, some vegetables, and a specific cooking oil in Tanzania (Trona), the contribution of fluoride through food to a Western diet is minimal; therefore it is reasonable to assume 100% of the RfD is from drinking water sources. Higher protein diets of Westerners produce a more acidic urine and researchers suspect this condition could lead to an increased retention of fluoride; however, present effects of vegetarian vs. non-vegetarian diet on fluoride retention remains unclear (Fawell et al. 2006).

Eq. 2-1 $$\mathrm{MCLG} = \frac{\mathrm{RfD}(\mathrm{BW})(\mathrm{RSC})}{\mathrm{I}}$$

Eq. 2-2 $$\mathrm{RfD} = \frac{\mathrm{BMD\ or\ LOAEL}}{(\mathrm{UF})(\mathrm{MF})}$$

RfD: Oral Reference Dose (mg/kg/day)
BW: Body weight (70kg adults; 10 kg children)
I: Intake (2 L/day adults; 1 L/day children)
LOAEL: lowest-observed-adverse-effect level (mg/kg/day)
BMD: benchmark dose adjusted for bodyweight (mg/kg/day)
UF: uncertainty factor
MF: modifying factor
RSC: relative source contribution

A recent epidemiological study in China indicated that increased risk to the skeleton occurs at total fluoride intake values above 6 mg/day (IPCS 2002). According to the EPA MCLG equations above, this reference dose of 6 mg/day for an adult weighing 70 kg and all other parameters as listed above would decrease the MCLG to 1.2 mg/L F. This lower level is in close agreement with the World Health Organization's (WHO) maximum safe concentration guideline of 1.5 mg/L F (Fawell et al. 2006). While most countries in the world adhere to the WHO guidelines in setting their own drinking water standards, the U.S. MCL is currently higher. Similarly, if in Eq. 2-1 only the RSC was changed to reflect the suggested value of 20%, the MCLG would equal 0.8 mg/L; a value in close agreement with the new recommended fluoridation limits by the EPA and Department of Health and Human Services (HHS) set in early 2011 (Isa 2011). It would be only conjecture to try to predict where the US EPA MCL will be set in the coming years, but it does seem clear that a maximum concentration of 1.5 mg/L F would be a safer target for drinking water.

Naturally occurring fluoride is found in groundwater worldwide. Geologic areas containing marine sedimentary rocks (usually in mountains), volcanic rocks, and igneous and metamorphic rocks such as granites and gneisses rich with fluorite, apatite and/or mica typically contain groundwater with high levels of fluoride. A belt of sedimentary rock located from Iraq through Turkey and also in Morocco influences groundwater concentrations of fluoride throughout that region. The most well-known case of volcanic rocks causing high fluoride levels is in the Rift Valley of East Africa where fluoride levels of over 2000 mg/L are present in some lakes. Regions with granites and gneisses include India, Pakistan, China, West Africa, Thailand and Southern Africa (Fawell et al. 2006).

Several areas throughout the U.S. also overlay geologic areas that contribute to high fluoride levels in corresponding groundwater sources. The Center for Disease Control (CDC) and U.S. HHS collected information on all the operating public water systems (PWSs) in the United States in 1993. The data were used to produce a Fluoridation Census report (Department of Health and Human Services 1993). The census reported more than 14,000 systems with fluoridated water, over 3,000 of which had naturally occurring fluoride at or above optimal levels of approximately 1.0 mg/L F. Fluoride occurs in clusters throughout the lower 48 states, with many PWSs in several states providing water with naturally occurring fluoride at levels greater than 2 mg/L (Table 2-1).

Table 2-1: States containing at least 20 PWS with delivery water exceeding 2.0 mg/L F from natural sources (Department of Health and Human Services 1993)

State	Number of PWSs, [F] > 2 mg/L	Average size of PWS (pop. served)
Arizona	28	1202
Colorado	54	6670
Illinois	43	931
Iowa	43	675
New Hampshire	46	167
New Mexico	27	1994
South Carolina	38	6198
South Dakota	37	24
Texas	29	2336
Virginia	92	1790

Fluoride in Texas naturally occurs in two main areas, the Northwest region around the city of Midland (but extending over a wide swath of west Texas) and a belt

running in a NNE to SSW direction from north of Dallas to an area of the hill country around Bandera County (just west of San Antonio). According to the 1993 Census, clusters of PWSs using source water with fluoride concentrations > 1.5 mg/L exist in these two areas of Texas (Figure 2-2). In Northwest Texas, possible sources of the elevated fluoride levels include marine shale in the underlying bedrock and volcanic-ash deposits in the southern part of the Ogallala Formation aquifer (also referred to as the High Plains Aquifer) (Gurdak et al. 2009). Some plants are purchasing treated surface water to blend with groundwater in order to adhere to the regulated limits. In some of the affected areas, it appears a blend of groundwater with elevated levels of fluoride and surface water is treated using aluminum-based coagulation; this practice makes it critical to understand the chemical competition between fluoride and natural organic matter in the precipitation of and the adsorption onto aluminum hydroxide.

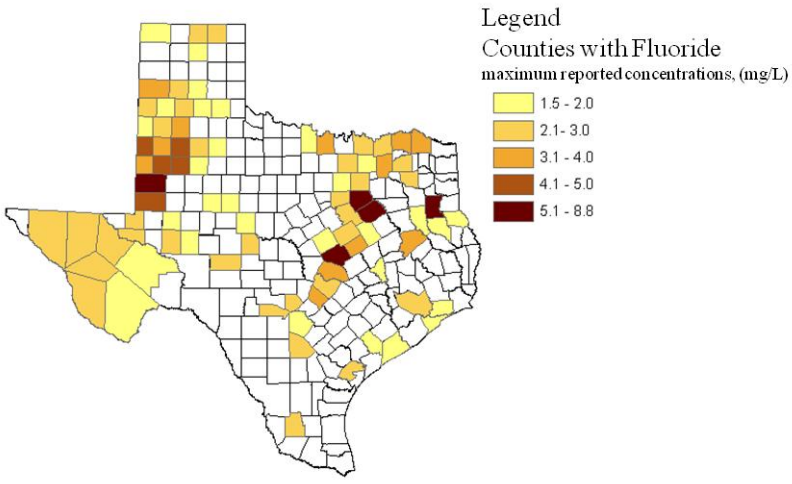

Figure 2-2: Counties in Texas that contain a PWS with naturally occurring fluoride above 1.5 mg/L (data from Fluoride Action Network and the 1993 Fluoride Census)

The average population served by the municipalities in Texas with fluoride levels above 2 mg/L is 3,200 people (Department of Health and Human Services 1993). The City of Midland is the largest PWS in the state reporting high fluoride levels. This PWS serves a population of 106,000, thereby classifying it as a large system (population >10,000). According to the City of Midland's water quality reports over the past several years (2004-2008), the finished water exceeded the secondary SMCL of 2.0 mg/L for fluoride with one source (the Paul Davis Well field) exceeding 4.0 mg/L. Samples from wells no longer used for drinking in nearby Gaines County in northwest Texas have levels over 10 mg/L, and older community members frequently display symptoms of dental fluorosis. A recent analysis of 634 wells in the Ogallala Aquifer underlying northwest Texas found that 59% of the wells exceeded the SMCL and 19% were in violation of the MCL. These wells supply a variety of users including individual households, irrigation, public supply, and livestock (Hudak 2009). Currently, Andrews County's groundwater has levels of both fluoride and arsenic violating their respective MCLs and limited treatment options. Andrews County presently supplies residents with drinking water at a centralized filling station.

Since this 1993 Fluoridation Census report, the number of PWSs with high natural fluoride levels has increased. In Texas, for example, the number of water systems with fluoride levels greater than 2 mg/L F has increased from 29 in 1993 to 49 in 2011 (TCEQ 2011). Currently, these Texas PWSs are using at least one surface water source and delivering water to users above 2 mg/L; 26% of them use surface water as their primary water source. While most counties with high naturally occurring fluoride are using groundwater as their sole water source, high levels of fluoride have also been detected in surface water. Several drinking water treatment plants in Virginia are using surface water sources containing greater than 2.0 mg/L of fluoride, and several counties

in South Carolina reported values hovering around 4.0 mg/L F. Many of these sources also have sufficient TOC concentrations that it is difficult to meet the disinfection byproduct regulations.

A common solution to high fluoride levels in smaller communities is blending groundwater with a surface water source purchased from a nearby municipality. Many PWSs in Texas use this approach; however, even these PWSs practicing blending regularly deliver water to users exceeding 2 mg/L. The surface water can contain high TOC levels, especially in high alkalinity areas. According to the same 2008 Water Quality Report for Midland discussed earlier, the bicarbonate concentrations average 181 mg/L as $CaCO_3$ and influent TOC levels exceed 5 mg/L C. In 2008, Midland achieved an average of 10% TOC removal, a level less than the enhanced coagulation regulations requires for source waters with alkalinity levels above 120 mg/L as $CaCO_3$, as described in Section 2.6 of this chapter.

When both fluoride and natural organic matter are present in source water, these smaller PWSs face a treatment challenge to use common drinking water treatment practices to achieve removal of both. The importance of achieving natural organic matter carbon removal, the structure or organic matter, and the drinking water regulations for organic matter are discussed in the next section. Given the distribution of PWSs in Texas supplying users with water elevated in levels of fluoride, it is necessary to understand the chemical interactions between fluoride, organic matter present in surface waters, and aluminum salts typically used during drinking water treatment.

2.4 NATURAL ORGANIC MATTER: STRUCTURE AND REGULATIONS

Natural organic matter (NOM), the product of plant and biological decay, is present in all natural water. The composition varies spatially and temporally and depends on the origin (e.g., autocthonous, allocthonous, wastewater), age, fate and season (Aiken et al. 1992) and is present as dissolved, colloidal, and organic detrital states (Prakash and MacGregor 1983). Particulate NOM and NOM adsorbed to clay and other mineral particles can settle to the bottom of a water body as stable, insoluble organic matter. The soluble fractions impart the characteristically yellowish-brown color of lakes, rivers, and other natural water bodies. The color is almost entirely due to the large prevalence of the relatively lower molecular weight humic acid and fulvic acid fractions (Table 2-2).

Table 2-2: Molecular Weight Distribution of Aquatic Humus from various sources (from Prakash and MacGregor 1983)

Molecular Weight Range	Soil Extract, Aqueous (%)	River Water (%)
< 700	43.8	63.0
700 – 1500	56.2	25.8
1500 – 5000	0.0	11.2
> 5000	0.0	0.0

NOM undergoes both photo- and bio-degradation in the natural environment and can attenuate the toxicity of heavy metals and other toxic compounds. The most biologically active portions of humus are the lower molecular weight compounds (Prakash and MacGregor 1983). The low molecular weight fractions are able to complex more metal ions than higher molecular weight fractions, leading researchers to investigate

the degree of cellular penetration of metals via organic fractions (Prakash and MacGregor 1983).

The efficacy and efficiency of almost all water treatment processes are impacted by the presence of natural organic matter in the source water. NOM reacts with common disinfectants (e.g., chlorine, chloramines, and ozone) to produce a range of potentially carcinogenic disinfection by-products (Richardson 1998; Arora et al. 1997), fouls membranes used for reverse osmosis and ultrafiltration (Cho et al. 1999), blocks activated carbon pores used for micropollutant removal (Li et al. 2003; Ding et al. 2006; Srinivasan et al. 2008), consumes oxidants used for contaminant destruction (Huang et al. 2005), and competes for adsorption sites with taste and odor producing compounds (Zoschke et al. 2011; Jacangelo et al. 1995). In post-treatment, organics can deposit in water mains as "humic muds." These depositions have been linked to both discoloration of drinking water (red and black in color) and chemical corrosion in the distribution systems (Prakash and MacGregor 1983). As a result, a significant fraction of water treatment research, treatment plant design and operation, and utility cost is devoted to removal of NOM from drinking water.

The structure of NOM is large and varies with location, environmental conditions, and seasonal weather. NOM is a label given to a wide group of materials including dissolved organic matter and particulate organics. Particulate organics can include bacteria, algae, and organic waste, but they represent a small fraction of the total organic carbon comprising NOM. The dissolved fraction is operationally defined as the portion of dissolved carbon that passes through a 0.45 μm filter. This portion of NOM can undergo further classification by chemical nature to hydrophobic- and hydrophilic- acids, bases, and neutrals. Most aquatic NOM is composed of dissolved hydrophobic acids such as fulvic and humic acids (Rebhun and Lurie 1993; Edzwald 1993; Prakash and MacGregor

1983). For the remainder of this document, NOM will be used to refer to the dissolved fraction unless otherwise specified.

Some proposed structural models of NOM include large, cumbersome molecular structures (Burdon 2011). While the representations are different, the models of NOM structure contain specific, repeated features including aromatic rings, carboxylic groups, phenolic groups, and aliphatic chains of varying lengths. In most waters, the large molecules are partially deprotonated, in anionic form, and can be considered polyanions (Rebhun and Lurie 1993). The EPA started requiring treatment of NOM in the 1998 Disinfectant/Disinfectant By-Product Rule because of NOM's ability to react with disinfectant chemicals to form trihalomethanes (THMs) and haloacetic acids (HAAs), two potential carcinogenic groups of disinfection by-products (DBPs). Research characterizing the formation potential of DPBs concluded that the aromatic ring structure of the NOM compound is the most important precursor (Kitis 2002; Wu et al. 2000). Nevertheless, the 1998 Disinfectant/Disinfectant By-Product (D/DBP) Rule specifically addresses removal of total organic carbon (TOC) which is one surrogate measure for the concentration of NOM. Although other treatment methods are occasionally used, "enhanced coagulation" (the use of coagulation to remove NOM in addition to its traditional use of particle removal) is the most common process for NOM removal.

To facilitate the comparison of experimental results and the analysis of chemical reactions, simpler, low molecular weight (LMW) organic acids are often selected as surrogates for NOM. LMW organic acids adsorb to the surface of well-ordered metal oxides through the formation of complexes between the phenolic, carboxylic, or amino groups and the metal ions of the oxide surface. These surrogates often contain a mixture of carboxylic and phenolic groups varying in number and position.

For this research, the aromatic ringed compounds phthalic acid, pyromellitic acid, and salicylic acid were selected as surrogates, based on the depth of research conducted using these organics, and for the lack of work investigating the removal efficiencies and mechanisms during alum coagulation. Evanko and Dzombak (1998) studied the removal of 28 LMW organics by goethite (α-FeOOH) to look at the effect of (1) varying number and position of carboxylic groups, (2) varying number and position of phenolic groups, (3) aliphatic chain length on benzene monocarboxylic acids, and (4) ring sizes. These authors concluded that increasing number of carboxylic groups correlated with increasing removal, providing a base of work for comparison. Another important characteristic to improved removal was the position of a phenolic group ortho to a carboxylic group, influencing the choice of salicylic acid for this study.

Adsorption of salicylic acid on aluminum oxides has been investigated in the past with varying results (Szekeres et al. 1998; Biber and Stumm 1994; Ainsworth et al. 1998). The use of salicylic acid in many of these studies is due to the hypothesis that it is a model organic to use for NOM comparison. Many of these adsorption studies showing high removal efficiencies for salicylic acid are performed under acidic conditions, and so the ability of an amorphous aluminum solid at neutral pH to removal salicylic is still undetermined. The complexes formed with phthalic acid and hematite were extensively studied by Hwang and Lenhart (2009; 2008; Hwang et al. 2007) and by Persson et al. (1998). At high pH, outer sphere bonding is proposed to dominate, but also depends on surface coverage on the hematite surface. The research by Persson et al. (1998) proposes the formation of inner-sphere, mononuclear bidentate, chelating rings at acidic conditions where ligand promoted dissolution is also greatest. The investigation of phthalic acid in terms of attachment to aluminum and stability of the association during drinking water

treatment at near neutral conditions is important in predicting residual aluminum concentrations.

The final organic acid chosen for this study is pyromellitic acid. Work by Pommerenk and Schafran (2005) reported high percent organic removed by preformed aluminum precipitates. Work of adsorbing organics onto freshly precipitated aluminum solids is common (Pommerenk and Schafran 2005; Guan et al. 2007; Guan et al. 2006), but many use aluminum chloride and not alum to form the solids. Pommerenk and Schafran (2005) reported low doses of sulfate had nearly 100% removal, yet the background competition of sulfate is not considered if alum is not used.

Working with LMW organic acids, the attachment and interaction of the molecules with oxide surfaces is less complicated and, therefore, more easily understood than when working with NOM. Organic acids can form electrostatic outer-sphere bonds or inner-sphere complexes with the surface of metal oxides (Figure 2-3). The type of bonds formed can drastically change dissolution behavior and competition with other constituents.

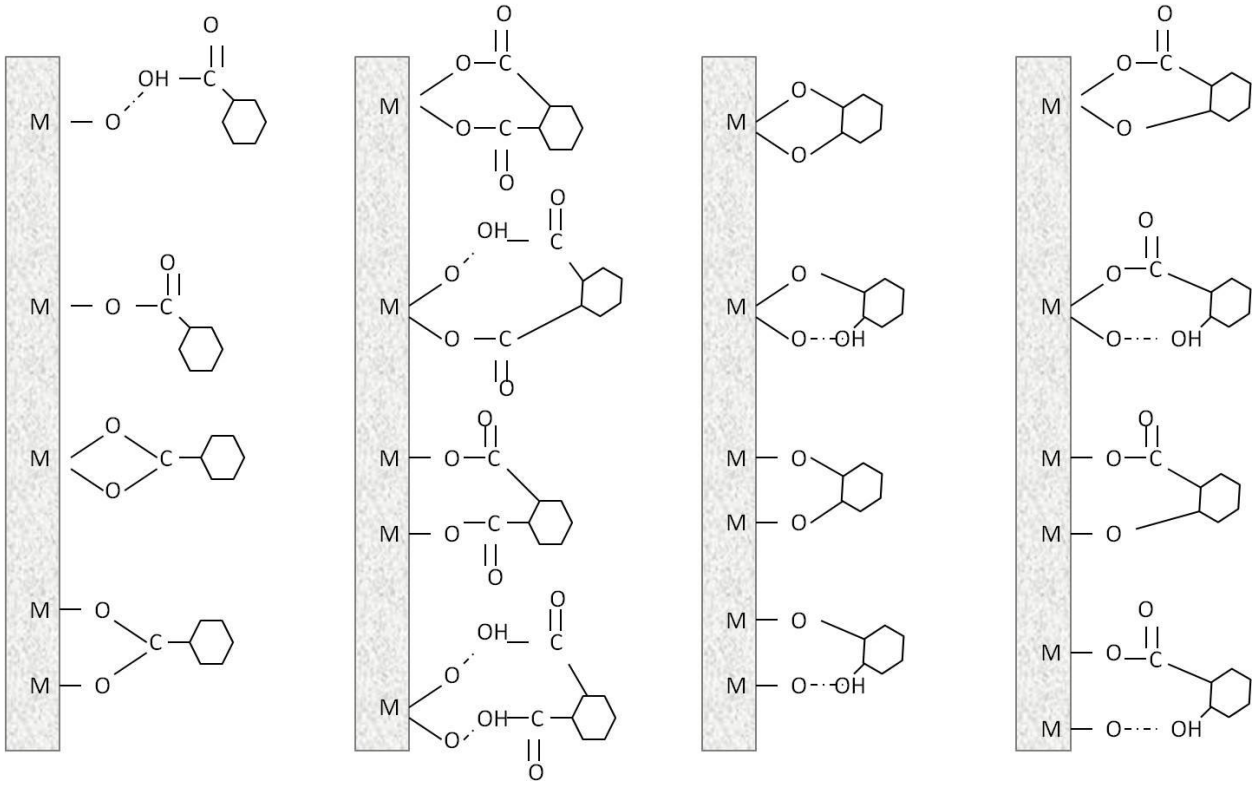

Figure 2-3: Possible structures for surface complexes of organic acids. (adapted from Evanko and Dzombak 1998)

The schematic of surface reactions with oxides presented in Figure 2-3 includes (from left to right) a monocarboxylic benzoic acid, a dicarboxylic benzoic acid, a dihydroxybenzoic acid with adjacent phenolic groups, and dihydroxybenzoic acids with a phenolic group in ortho position relative to the carboxylic group. Physical and thermodynamic factors dictate the likelihood that each of these structures can form. In general, four membered rings are not very stable and can promote the dissolution of oxide surfaces after formation (Persson et al. 1998). In researching the impact organic acids can have on silicate mineral dissolution, Drever and Stillings (1997) narrowed the mechanism of dissolution to the ability of organic acids to affect the rate of reaction far from equilibrium, affect the saturation state of the mineral oxide, and affect the speciation

of dissolved metal ions in solution. In their work, NOM lowered the pH and accelerated dissolution significantly once the pH decreased below pH 5.

While the literature is full of studies classifying bonding mechanisms on oxide structures and extrapolating adsorption densities to larger treatment plants, few consider how a co-precipitating aluminum solid in the presence of multi-ligand systems affect the removal and competition of low molecular weight organics and fluoride. Classifying the bonding mechanisms used in the presence of fluoride will facilitate in the optimization of treatment. Central to the study is the coordination differences in bonding during a co-precipitation of aluminum and those formed on the surface after the aluminum precipitate is formed. To better understand the importance of aluminum, the next section provides a brief background.

2.5 Aluminum: Environmental Presence and Health Effects

Aluminum is a reactive metal and has several polymorphs composed of the same basic structural unit stacked in different sequences and classified based on coordination polyhedral (Hemingway and Sposito 1996). Two common oxides used in research are corundum (α-$Al_2O_{3(s)}$, octahedral oxide) and gibbsite (α-$Al(OH)_{3(s)}$, octahedral hydroxide) (Goldberg et al. 1996). The availability of bonding sites on an oxide/hydroxide surface determines its reactivity.

Many treatment plants in the United States use aluminum based salts as coagulants during drinking water treatment; however, residual aluminum concentrations are only regulated by the EPA's SMCL of 0.05-0.2 mg/L. Aluminum is categorized as an aesthetic concern in drinking water treatment, causing color concerns when the SMCL is exceeded (EPA 2010). There is definitive research linking the accumulation of aluminum

in the human brain and diseases associated with Alzeimer's Disease (AD). Due to the ubiquitous nature of aluminum in the environment, it is difficult to perform epidemiological studies on exposure as it relates to AD. Speculation as to the cause of the elevated concentrations relies mainly on genetic explanations related to defects in barriers to aluminum accumulating in areas of the brain. Aluminum as a cause of AD is still argued in the literature with researchers calling for a greater comprehension of the disease and improved understanding of molecular interactions of aluminum in the brain (Crapper McLachlan 1986). Even though there is a positive correlation between AD and concentrations of aluminum in drinking water, it is not strong enough to warrant regulation on a health basis due to the complicated nature of isolating exposure from water (Flaten 2001).

The use of aluminum in drinking water treatment is only one reason that aluminum chemistry has been studied extensively. Aluminum is also one of the most abundant elements in soils, comprising nearly 7% of solid matter in a soil sample (Lindsay and Walthall 1996). The prevalence of aluminum in soil has led to significant research examining aluminum weathering, dissociation, and environmental speciation by soil scientists (i.e., Violante and Huang 1985, Violante and Huang 1992, Kwong and Huang 1981). Acid rain and acidic environments in soils are of great concern for the transport of aluminum through the natural environment (Lindsay and Walthall 1996). In the Adirondack Mountain Range of NY, low pH values were observed in lakes in the late summer and autumn after rainfall and snowmelt, increasing total aluminum levels in the observed lakes (Driscoll 1980). These increased levels of aluminum were cited as the cause for trout deaths in the Adirondack lakes. Evaluation of aluminum speciation in the acidified water also indicated that aluminum was primarily organically complexed even though inorganic species (fluoride, hydroxide, sulfate) were present (Driscoll 1980).

More recently, researchers are investigating the emerging link between possible aluminum-fluoride aqueous complexes and related health effects. It has recently been proposed that the action of AlF_X increases the potential to develop of AD (Strunecka and Patocka 2002). In the presence of fluoride, aluminum ions were shown to accelerate impairment to the nervous system functions.

Fluoride is also increasing in abundance in the natural environment. In a study conducted in Austin, TX, where fluoride is not present at high concentrations in source waters or underlying minerals, increasing fluoride concentrations in streams has been positively correlated with increasing urbanization (Christian et al. 2011). In China and India, high concentrations of both fluoride and aluminum are reported in teas (Strunecka and Patocka 2002). Due to the common practice of treating drinking water with aluminum salts, background fluoride concentration, aqueous complexes with aluminum, and competition for removal with NOM is extremely important to monitor in the future. Understanding the chemistry during treatment, from precipitation to adsorption, as proposed in this research is necessary to further inform aluminum and aluminum-fluoride dose exposures from water.

2.6 Drinking Water Treatment: Aluminum, Particles, NOM, and Fluoride

Influent water at common drinking water treatment plants undergoes rapid mixing, coagulation/flocculation, sedimentation, filtration, and disinfection prior to entering the distribution system. Flocculation, or the act of smaller particles aggregating to form larger ones, began as an essential component for particle removal but has also become an important process for treating NOM and other organic and inorganic constituents. As it became apparent that aluminum coagulation had potential for removal

of THM precursors and inorganic contaminants, many treatment plants increased aluminum doses in the coagulation process to target removal of these other contaminants.

Particle removal occurs by destabilization through the addition of a destabilizing agent, also known as a coagulant as pictured in Figure 2-4. Aluminum based destabilization agents mainly use two different methods to achieve particle removal: (1) charge neutralization of negatively charged particles by the positively charged metal hydrolysis species followed by the aggregation of destabilized particles and (2) sweep flocculation in which the formation of aluminum hydroxide precipitate leads to adsorption and enmeshment of contaminants and particles (Benjamin and Lawler 2012; Shin et al. 2008).

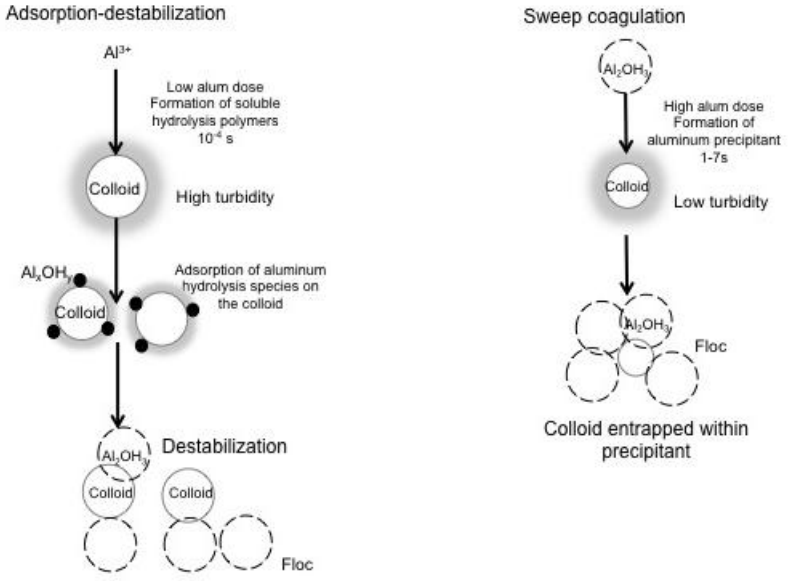

Figure 2-4: Modes of particle destabilization in aluminum coagulation systems (adapted from Amirtharajah and Mills 1982)

After the aluminum hydrolyzing metal salt is added to solution, it undergoes a series of hydrolysis reactions. The positively charged species interact with the negatively charged particles in the two pathways described above and pictured in Figure 2-4. The right side of Figure 2-4 depicts the dominant coagulation mechanism in turbid waters. Higher concentrations of particles allow for sufficient particle interaction after destabilization and, therefore, can undergo treatment at lower chemical concentrations. The interaction between positively charged metal hydrolysis species and the negatively charged particles is stoichiometric (Shin et al. 2008). At the critical coagulation dose, the charge requirement for destabilization is satisfied and the colloids can aggregate as long as the time and mixing provided yield sufficient particle collisions. The left side of Figure 2-4 depicts the reactions in low turbidity waters. Fewer particles require the formation of precipitates to cause interaction and allow for sweep floc to occur (Shin et al. 2008). The particle removal is no longer a stoichiometric relationship between the hydrolyzed metal salts and the colloids; it is the chemistry related to metal hydroxide precipitation that determines removal. The optimum pH to achieve sweep flocculation through precipitation of aluminum hydroxide is consistent with the minimum solubility of aluminum (Amirtharajah and Mills, 1982).

The process of removing NOM by coagulation with aluminum salts involves aluminum hydrolysis, aluminum complexation with the organics, precipitation, and adsorption reactions on the precipitate (Edzwald and Van Benschoten 1990). Organics with phenolic and carboxylic groups are successfully removed by coagulation-flocculation treatment (Licsko 1993). The establishment of bonds between the metal hydroxide and organic acid relies on the organic's charge, allowing for the development of intramolecular hydrogen bonds (Licsko 1993). Along with the hydrogen bonds formed, electrostatic interactions and surface complexation are important in the removal

of NOM from water by coagulation-flocculation treatment. Because effective treatment requires high concentrations of aluminum, the NOM removal process is referred to as enhanced coagulation; that is, the process uses more aluminum (or iron) salts than would be required for particle removal alone to create additional adsorption sites (surface area of the precipitated metal hydroxide) for NOM removal.

As concern regarding the presence of DBPs in drinking water increased in the 1990's, the EPA started requiring treatment of total organic carbon (TOC, a common measure of NOM) as part of the 1998 Disinfectant/Disinfectant By-Product (D/DBP) Rule. TOC removal goals are dictated by U.S. EPA regulations; utilities are required to reduce the TOC by a fixed percentage according to a matrix dependent on the raw water TOC and alkalinity, as shown in Table 2-3.

Table 2-3: Required removal of total organic carbon by enhanced coagulation for systems using conventional treatment. (EPA 815-R-99-012 1999)

Source Water TOC (mg/L)	Source Water Alkalinity (mg/L as $CaCO_3$)		
	0-60	60-120	>120
2.0-4.0	35%	25%	15%
4.0-8.0	45%	35%	25%
>8.0	50%	40%	30%

The regulations allow water utilities an exception to this rule if they reach the "point of diminishing returns," defined as less than 0.3 mg/L TOC removal per 10 mg/L addition of coagulant (EPA 815-R-99-012 1999). As other constituents in the water, such as fluoride, impart a demand on the coagulant, more consideration must be paid to optimizing chemical doses. Indeed, previous research has shown that fluoride has a high affinity for forming aqueous aluminum-fluoride bonds (Hoa and Huang 1986; Lopez Valdiviesco et al. 2006), thus reducing available aluminum for NOM interactions. With

competition from fluoride, the point of diminishing returns might be reached far earlier than if no fluoride were in the water; that is, the fluoride competes for sites with the organics, so less TOC removal per addition of coagulant would occur.

The water quality reports for the City of Midland show that the water not only contains high fluoride levels (an average of 2.8 mg/L and a maximum of 5.1 mg/L in 2008), but also contains relatively high influent levels of NOM (>4.5 mg C/L measured as dissolved organic carbon, DOC). The data suggest that the reduction in NOM is only approximately a 10% reduction through treatment, far less than the drinking water regulations require (Water System Data Sheet 2009; EPA 815-R-99-012 1999). Poor removal of DOC is possibly the result of elevated fluoride levels in the influent water.

Along with their adsorption work with preformed aluminum chloride, Pommerenk and Schafran (2002, 2005) researched the effects that fluoride can have on the coagulation of NOM when plants practice what is termed "prefluoridation," fluoridation at any point preceding filtration. Using aluminum sulfate (alum) as the destabilizing agent, Pommerenk and Schafran demonstrated when fluoride is present at levels up to 3 mg/L fluoride at the point of alum injection, formation of aqueous aluminum-fluoride complexes dominated. To achieve NOM removal results similar to levels when no fluoride was present, the alum dose required doubling. Moreover, the quality of the effluent water was compromised due to loss of more than 1 mg/L of the added fluoride during flocculation. Pommerenk and Schafran did not investigate the microscopic effects of fluoride on the treatment process, only the overall treatment efficiencies. To understand the degree of fluoride's influence on the formed co-precipitate, more than a comparison of residual aluminum and fluoride values is needed.

In investigating the chemical competition between organic acids, fluoride, and aluminum during drinking water treatment, understanding the stability and dissolution of

the aluminum precipitate throughout the process is essential. Fluoride has been shown to enhance the dissolution rates of preformed amorphous aluminum oxides in the presence of organic acids under acidic conditions (Zutic and Stumm 1984; Plankey and Patterson 1988; Kraemer et al. 1998). The dissolution rate, involving the four steps of ligand attachment to surface sites, detachment of surface aluminum species, transport of the aluminum complex into the bulk solution, and regeneration/protonation of the active sites, is typically calculated according to Furrer and Stumm's (1986) kinetic model:

Eq. 2-3 $$R_H=k_H(\equiv AlOH_2^+)^n = k_H(C_H^S)^n$$

Eq. 2-4 $$R_L=k_L(\equiv AlL) = k_L C_L^S$$

Eq. 2-5 $$R_{tot}= R_H+R_{L1}+R_{L2}$$

The first equation listed above, Eq. 2-3, describes a proton promoted dissolution rate where k_H is a rate constant, C_H^S is the surface proton concentration (mol/m^2), and n is the number of protons attached per reaction site prior to detachment of aluminum during dissolution. Eq. 2-4 describes the ligand promoted dissolution rate where k_L is the ligand rate constant and C_L^S is the surface concentration of adsorbed ligands (mol/m^2). The above model for acidic regions also assumes that the reactions are independent and parallel, and therefore additive (Eq. 2-5), which includes the possibility of two different ligands). Typically, C_L^S is determined by a constant capacitance model (CCM); however, due to the variety of possible structures for surface complexes of organic acids at near neutral pH, this method of approximating the surface coverage of ligands seems less than accurate.

A more in depth understanding of the types of competing reactions and removal densities are achieved at near neutral pH is needed in order to predict residual aluminum concentrations after alum coagulation. Evaluation of the precipitating aluminum solid in

multi-ligand systems and associated competing ligand removal efficiencies are needed for co-precipitated solids to verify a CCM approach to dissolution analysis.

2.7 SUMMARY

To evaluate an adequate treatment approach for fluoride, NOM, and particles, it is important to both quantify the extents of removal through understanding the types of bonds formed at the surface and quantify their stability as a function of the surface reactions of competing ligands. Most studies regarding fluoride removal have only considered the adsorption of fluoride onto aluminum oxide precipitates (Pommerenk and Schafran 2005; Tripathy et al. 2006) and use the adsorption based removal efficiencies to predict treatment. A gap exists in the understanding of the competition between NOM, fluoride, and aluminum when modeled after an alum coagulation treatment scheme. To properly predict the effectiveness of treatment at a treatment plant using alum coagulation, experiments must be conducted in the same manner. The research approach in the following section addresses three objectives that represent key chemical reactions during the coagulation process: precipitation, adsorption, and dissociation/desorption. To understand the competition among fluoride, NOM, and aluminum during drinking water treatment, these three processes and associated chemical reactions must be understood.

Chapter 3: Research Approach and Methodology

3.1 Research Approach

The coagulation of NOM by aluminum salts involves a suite of chemical processes including aluminum hydrolysis, complexation, precipitation, and adsorption (Edzwald and Van Benschoten 1990). The removal of fluoride involves the formation of a co-precipitate and/or the adsorption onto the precipitating aluminum (oxy)hydroxide. Competition between ligands for removal exists throughout the process: during both the formation of the precipitate and during the formation of complexes on the precipitate surface. To understand the co-precipitation process, the competition for co-precipitation with fluoride and organic acids, and the competition for adsorption onto the formed precipitate, the research used an experimental matrix of jar tests combined with spectroscopic analysis of precipitates and surfaces to elucidate a macroscopic and molecular level understanding of the treatment process.

The research plan framed the analyses around the removal mechanisms of coagulation processes—specifically complexation, co-precipitation, and adsorption. Figure 3-1 shows a basic schematic of the steps in the coagulation process that occur during jar tests and include rapid mixing, slow mixing, and quiescent settling. In the rapid mix stage, the destabilizing agent is added and distributed throughout the jar. After a short rapid mix period, the mixing is slowed to promote particle interaction and floc formation during the slow mix stage. Lastly, the process concludes with a period of no mixing to allow for settling of flocs and particles. The chemical interactions of interest to this research occur after the systems are dosed with aluminum sulfate (alum), the coagulant used in this research.

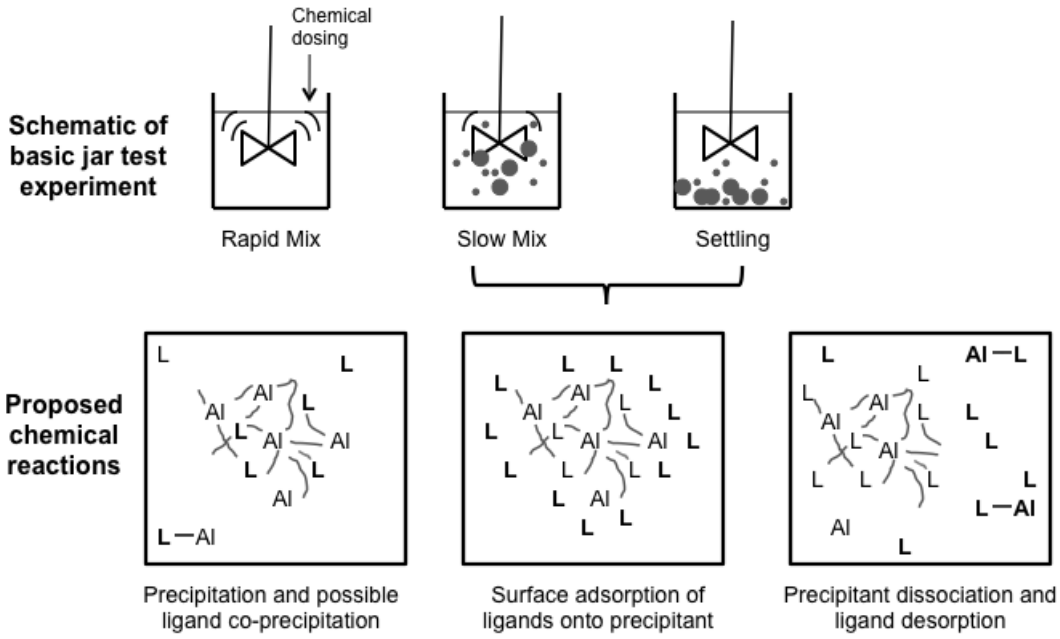

Figure 3-1: Schematic of proposed research and chemical reactions. L represents ligands in solution, Al represents aluminum and the gray lines represent?

The proposed chemical reactions in Figure 3-1 are divided into three distinct categories. The "L" represents the ligand (organic acid, fluoride, and/or Lake Austin NOM) and is in bold when involved in the chemical reaction portrayed. After alum dosing, the aluminum can form aqueous complexes with ligands in the system and incorporate these complexed ligands into the forming precipitate.

NOM molecules, even isolated fractions, are large complicated molecules comprised of aromatic rings, aliphatic chains, carboxylic groups, phenolic groups, and other structural components. Focus was placed on understanding competition from aromatic compounds with carboxylic and phenolic groups and the large, complex NOM molecules was modeled through the use of three low molecular weight (LMW) organic acids in Table 3-1 as NOM surrogates along with NOM isolates from Lake Austin,

Texas. The use of LMW organic acids and a natural NOM isolate aided in evaluating the practicality of using surrogates to understand the chemistry of complex NOM during flocculation treatment. The surrogates were chosen based on their removal efficiencies, functional group types, and functional group positions.

Salicylic acid is an aromatic compound commonly found in natural waters. Ainsworth et al. (1998) investigated the binding of salicylic acid to alumina and found a mixed monodentate and bidentate inner-sphere complexation. The position of the phenolic group with an ortho carboxylic group has previously been concluded to enhance removal on goethite (Evanko and Dzombak 1998) and the use of salicylic acid as a surrogate in this study will help determine the importance of this relationship. Phthalic acid has been shown to exhibit chelating effects when binding with oxide surfaces (Lindegren and Persson 2010). This chelation is important when considering competition with fluoride and removal by non-crystalline materials. Finally, pyromellitic acid was selected since it has been reported to most closely represent humic acid in adsorption studies (Evanko and Dzombak 1998).

Table 3-1: Low molecular weight organic acids of interest

Name	Chemical Formula	Structure	pKa [a]
Salicylic Acid	$C_7H_6O_3$	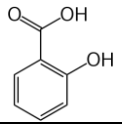	2.88, 13.56
Phthalic Acid	$C_8H_6O_4$	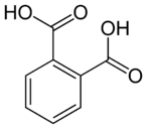	2.87, 5.23
Pyromellitic Acid	$C_{10}H_6O_8$	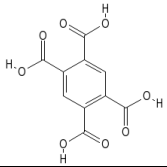	1.52, 2.95, 4.65, 5.89

[a] Taken from Martell and Smith (1974) and corrected for an ionic strength of 0.01M.

The experimental chapters of this document are broken down into major themes. The processes of precipitation and ligand incorporation of fluoride are investigated in Chapter 4. After a precipitate is formed, ligands can also bond to the surface of the solid and compete with other ligands for removal; this adsorption is the focus of Chapters 5-6. In Chapter 6, the use of LMW as surrogates for NOM is also evaluated. Finally, in Chapter 7, the stability of the formed precipitates and adsorbed ligands are investigated.

3.2 METHODOLOGY

3.2.1 Jar Tests: Simulating drinking water treatment at bench scale

All jar tests followed the base time parameters of 2 minutes rapid mix after alum dosing, 30 minutes slow mix (18-20 rpm, estimated to yield a velocity gradient, G, value

of 12-15 s^{-1}), and 40 minutes settling. The coagulant was added at approximately pH 3 to prevent nucleation upon dosing and then raised to the desired pH during the 2 minute rapid mix using 2.5 N NaOH. Lake Austin NOM and LMW organic acid concentrations varied to bracket values of 5 mg/L of carbon (0.42 mMol C). Fluoride concentrations reflected levels found in Texas from moderate concentrations of 2 mg/L (0.11 mMol F) to higher concentrations of 5 mg/L-10 mg/L F (0.26 mMol F-0.53 mMol F). A synthetic water composition of 3 meq/L alkalinity from $NaHCO_3$ and 3 meq/L hardness from $CaCl_2$ comprised the background matrix for all experiments unless otherwise stated. When included in experimentation, the initial turbidity was set at a concentration of 13-18 NTU with Min-u-sil 5 silica particles. The silica particles were tested for reactivity with fluoride and revealed no influence over fluoride removal. Acid and base pH adjustments were made with 1.0 N HCl and either 1.0 N or 2.5 N NaOH.

Alum stock was made from aluminum sulfate salt calculated to have the average chemical formula $Al_2(SO_4)_3*12.8H_2O$. The following alum doses and corresponding aluminum concentrations in Table 3-2 were used throughout the research and are presented below for reference.

Table 3-2: Typical alum doses and initial aluminum concentrations used during jar tests for this study.

Alum dose (mg/L)	$(Al)_i$ (mg/L)	$(Al)_i$ (mMol)	Log $[Al]_i$ (M)
10	0.9	0.035	-4.457
20	1.9	0.070	-4.155
30	2.8	0.105	-3.980
40	3.8	0.140	-3.855
50	4.7	0.175	-3.758
100	9.4	0.349	-3.457
150	14.1	0.524	-3.281
200	18.9	0.699	-3.156
300	28.3	1.048	-2.980
400	37.7	1.397	-2.855
500	47.2	1.746	-2.758

The basic jar tests imitate a drinking water treatment plant where coagulant doses are added to influent water streams containing the contaminants (ligands). These tests are referred to as "co-precipitation" (CPT) throughout this study and are described in the top diagram in Figure 3-2. Two additional jar test procedures were used during this research to understand the influence of precipitation and adsorption on the removal process. The second set of jar tests, called "preformed" tests (PRE), isolated the adsorption process (middle diagram in Figure 3-2). Aluminum precipitates were created by first dosing each jar with alum while free of ligands. These jars underwent the typical 2 min rapid mix followed by a 30 min slow mix to allow the precipitate to form. After the first 30 min slow mix, the jars underwent ligand dosing at a low speed to distribute the ligand throughout the jar but limit the breakage of formed flocs. After ligand dosing, the jars were mixed for a second 30 min slow mix and then settled for 40 min.

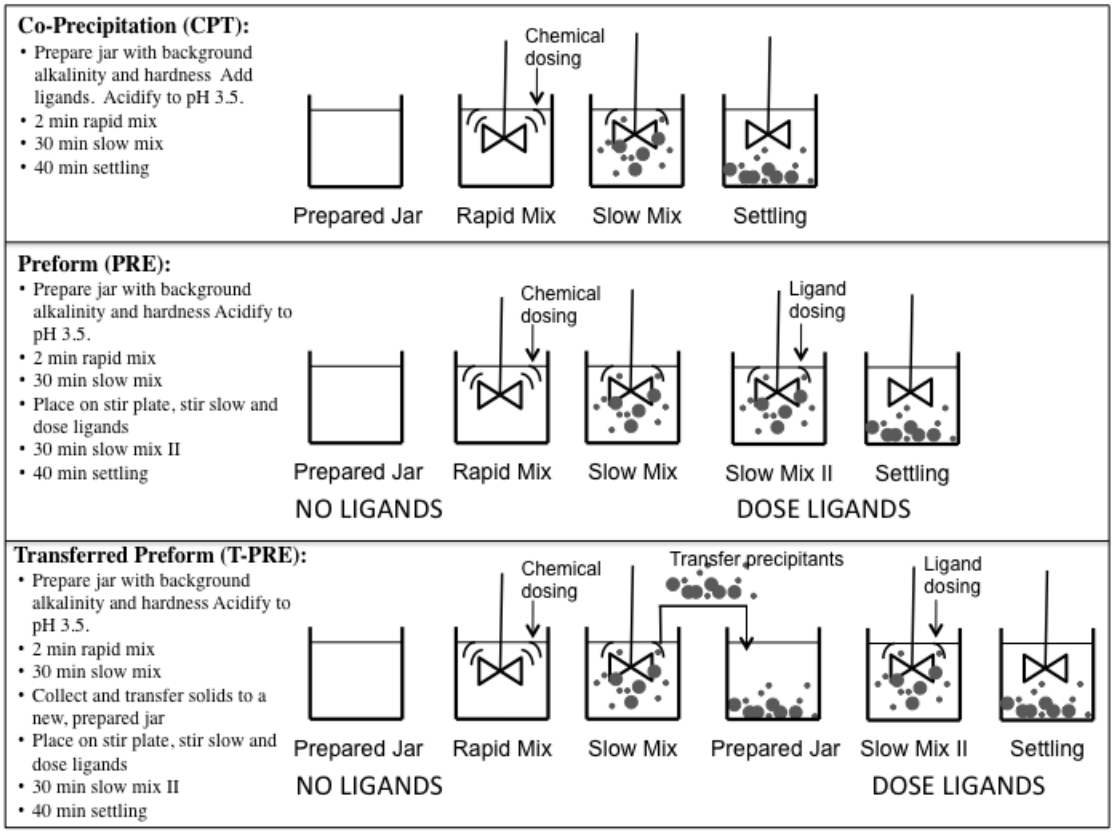

Figure 3-2: Schematic of the different jar test methodologies: Co-precipitation (CPT), preform (PRE), and transferred preform (T-PRE).

The final jar test experimental procedure used was a modification on the PRE jar test methodology. After the aluminum precipitates formed without any ligands present, the jars were filtered and the precipitate collected on 0.45 μm filter paper and washed with 10 mL of deionized water (DI). The collected solids were then transferred to a new jar that contained the background water matrix without ligands and pre-adjusted to pH 6.5. After adding the solids, the jars were stirred and the ligands dosed into the system. This set of experiments is referred to as "transferred preform" (T-PRE).

Solubility/dissolution experiments were conducted following the co-precipitation and pre-formed adsorption jar test methodologies outlined above. Aliquots sampled at 30 min, 3 hr 20 min and 7 hr 20 min were transferred to polypropylene vials and allowed to settle for 40 min prior to filtration at 1 hr 10 min, 4 hr, and 8 hr analysis times. Collected filtrate from solid liquid separation with a 0.45 μm membrane filter was analyzed for residual ligand and aluminum concentrations.

3.2.2 Titrations of precipitates

To understand the role of ligand replacement for OH^- during precipitation, a series of titrations were performed. Background synthetic water as explained above was present during all the titration tests. Using a 100 mL sample volume, the background synthetic matrix was titrated from an initial pH of 2.0 to above 10 using a standardized 1.1N NaOH. Following a background titration, a series of CPT titrations were performed. The alum only titrations received a pre-determined alum dose and pH adjustment using 1N HCl to pH 2.0 prior to titration with NaOH. After each addition of NaOH, 30 sec were allotted for the pH meter to stabilize before adding the next volume of titrant. The titrations used sequential aliquots of NaOH in order to compare the resulting pH at exactly the same concentration of added OH^-.

In a separate set of 50 mL vials, equal concentrations of coagulant, ligands, and base were added to represent a complete titration curve. The vials were placed in an end-over-end rotator for 30 min to simulate slow mixing and allowed to settle for 40 min before filtration and analysis of residual aluminum and ligand concentrations.

3.2.3 Analysis of aqueous constituent concentrations

All samples were filtered through 0.45 μm membrane filters at the end of each experiment. The collected filtrate was divided for cation, anion, and organic analysis. Filtrate for cation analysis was acidified with 100 μL concentrated HNO_3 per 10 mL sample and placed in a 4°C storage room if not analyzed immediately. The filtrate was analyzed for aqueous aluminum concentrations using inductively coupled plasma spectroscopy (ICP) (Agilent Varian 710-ES, CA) at 237.12 nm, 308.215 nm, and 394.401 nm wavelengths for concentrations above the 40 μg/L detection limit. Furnace atomic adsorption spectroscopy (Perkin Elmer AAnalyst 600, MA) was used for all concentrations below the ICP detection limit. All analyses included measurements of a blank and a standard from the calibration curve every 12-18 samples to check the accuracy of the machine throughout the analysis period.

Aqueous fluoride was measured using a fluoride ion selective electrode (Thermo Electron Corporation, MA). All samples were mixed with a total ionic strength adjustment buffer (TISAB) to increase the ionic strength and allow for steady, reliable measurements. The precision associated with the ion selective electrode was tested during each experiment by measuring all five calibrating standards every 12-18 samples. The published +/- 2% reproducibility of the electrode was confirmed as, on average, a 2-4% variability in measurements over 1 hour. The type of TISAB used in this study either contained an aluminum complexing agent (either CDTA or EDTA) for total fluoride measurements or lacks this complexing agent to measure free fluoride.

Residual natural organic matter (NOM) and low molecular weight (LMW) organic acids were measured by UV-Vis spectroscopy (Agilent 8453, CA) using a 1 cm quartz cell. All LMW samples were acidified using 5 μL of 1N HCl per milliliter of sample prior to UV-Vis spectroscopic measurement to acquire consistent protonation

states. NOM measurements occurred at a wavelength of 254 nm, salicylic acid at 296 nm, phthalic acid at 277 nm, and pyromellitic acid at 294 nm. All constituent measurements were preceded by a five-point calibration curve for sampling accuracy.

NOM is a large, complicated compound. Isolation of NOM fractions are separated based on molecular size and hydrophobicity, but this is not a characterization of functional groups. Direct potentiometric titrations of 100 mg/L C solutions of the Lake Austin isolated NOM with a 0.10 M NaCl background electrolyte were performed in a CO_2 free environment to further elucidate the dominant properties of the Lake Austin NOM. All prepared solutions of NOM were purged with nitrogen gas for 4 hours prior to titration to remove any background carbonate from the solution.

3.2.4 Precipitate dry analysis

Precipitates collected on the 0.45 μm filter membranes were then prepared for dry analysis. The precipitates were immediately transferred to small, solids handling vials and frozen at -81^{o}C followed by vacuum freeze-drying at temperatures below -40^{o}C and pressures of 60 millitorr. Freeze dried solids were stored in desiccators for analysis by X-ray diffraction (XRD) (Philips Diffractometer and Scintag theta-theta Diffractometer), scanning electron microscope (Model Quanta 650 FEG), surface area (Quantachrome Autosorb-1), porosity (Quantachrome Autosorb-1), and X-ray photoelectron spectroscopy (Kratos Analytical Company). Precipitates were also analyzed by Fourier Transfer Infrared (FTIR) transmission and diffuse reflectance spectroscopy. The methodology and analyses of the FTIR results are located in Appendix 1.

XRD analysis used freeze dried precipitates ground to a fine powder and powder-mounted on a glass, silica, or quartz slide using acetone. Samples were first analyzed

using the Philips automated vertical scanning general powder diffractometer (PANalytical Inc., Westborough, MA). XRD patterns were recorded from 4 to 60^{o}2θ min^{-1} to determine if any crystalline aluminum oxide was present or confirm the presence of an amorphous precipitate through the lack of spectra peaks. Yu et al. (2007) were able to obtain crystalline precipitates after 1 day of aging; however this timescale needs more testing. After aging, the Yu et al. (2007) precipitate contained bayerite and gibbsite with the peaks increasing in intensity as the aging period increased. To test the minor differences in patterns, a Scintag X1 (Thermo ARL, Switzerland) theta-theta diffractometer was used with long dwell times.

The surface area and the porosity of the precipitates analyzed using Brunauer-Emmet-Teller (BET) liquid nitrogen adsorption isotherm allow for quantification of specific surface area and average pore diameter of the precipitates (Quantachrome A-1, FL). At least 0.5 mg of sample were used for analysis, degassed for 72 hours under vacuum at 110^{o}C prior to the analysis.

For further analysis of the bulk precipitate, a Model Quanta 650 FEG (FEI Company Inc, Oregon) electron scanning microscopy (SEM) operated under environmental, low vacuum, and high vacuum modes was used for its capability to image amorphous materials (Maurice 2009). Paired with energy dispersive spectroscopy (EDX) (Bruker XFlash Detector 5010, MA) this technique provided qualitative results and was used to corroborate stoichiometric analysis of the X-ray photoelectron spectroscopy. Precipitates were not ground prior to mounting on double-sided carbon tape on the sample holder. A spot size of 3 nm and beam energy of 10 kV were used for the two lower vacuum settings to minimize charging of the particles for imaging. Particles were also coated using a platinum sputtering technique and analyzed under high vacuum mode for comparison and more resolved EDX concentrations.

The final technique used to analyze the precipitates was X-ray photoelectron spectroscopy (XPS) (Kratos Analytical Company, Kyoto) to analyze bonding energy on the surface of the precipitate and stoichiometric ratios of elements. Powder samples were placed on the sample bar contained within copper washers. The sample bar and samples were heated overnight (for at least 10 hours) at temperatures near 80^{o}C and flushed with nitrogen gas to purge absorbed water from the solids. The samples required electrical grounding and charge neutralization. The original charge neutralization with a filament current of 1.8 A and a charge balance of 2.0 V produced noisy peaks. Incremental adjustments determined that a filament current of 1.905 A and a charge balance of 3.682 V produced clean peaks. The amorphous characteristic of the precipitates complicated the XPS analysis of the samples especially when obtaining spectra for fluoride (F 1s). Further adjustments to create well-defined peaks included reducing the dwell time to 800 s^{-1} and setting the pass energy to 40 eV. This set of operating parameters produced the cleanest spectra even when fluoride was present at low concentrations. All samples were analyzed for Al (2p), and O (1s). Data for C (1s) is also collected as a measure of shifting binding energy (considering background carbon contamination to be located at a binding energy of 285 eV).

3.2.5 Precipitate wet analysis: *In situ* measurements of precipitate physical characteristics

Turbidity analyses of precipitates were performed without collecting and freeze-drying the formed solids using a Hach 2100N Laboratory Turbidimeter (Hach Company, Loveland, CO). After 40 min of settling, a 50 mL aliquot of sample was slowly extracted from the top layer of the jar using a wide-mouth glass pipette. Caution was used to ensure not to draw the sample into the pipette too quickly and inadvertently mix the solution, re-

suspending the settled solids. The turbidimeter was calibrated using a set of StablCal Turbidity Standards.

The second *in situ* analysis of precipitates was performed using the Coulter Counter Multisizer III (Hialeah, FL) to measure the particle size distribution. The Coulter Counter was calibrated using four standards added in succession in each of the four apertures used for analysis. Jar tests were conducted with a single jar for analysis according to the jar test experimental design explained above. The suspensions were never allowed to settle, with the jars remaining on slow mix the entirety of the experiment. After 30 min of slow mixing, a desired amount of sample was removed using a wide-mouth pipette to prevent floc breakage. The sample was extracted from the center of the jar to ensure a representative sample was selected and added to particle free water with a background 2% NaCl concentration. The particle free water was confirmed as "particle free" by passing the minimum particle thresholds required for the analysis. After adding the sample to the particle free water, the vial was carefully and slowly inverted and rotated twice to mix the solution. Due to the large, visible nature of the flocs, this sampling technique achieved adequate mixing and distributed the flocs throughout the vial and did not significantly break or alter their form. Sampling apertures of 30, 100, 200, and 400 μm were used for the analysis. The largest aperture, 400 μm, was used when either too few particles were present to achieve the minimum required count using the 30 μm apertures or frequent blockage of the smaller apertures forced the use of larger apertures in order to conduct the analysis.

The final *in situ* analysis of precipitates was the electrophoretic mobility using the Zetaphoremeter IV (CAD, France). This microscopic electrophoresis instrument is equipped with an automatic particle tracking function using digital imaging. The digital tracking eliminates operator error associated with tracking and counting particles. All

measurements were conducted in the stationary layers where particle movements are not impacted by flow induced by electro-osmosis. The stationary layer used was closest to the microscope. The upper cell wall was located following the manufacturers suggestions of using a very diluted dispersion of milk (CAD Instruments 2008). Once the upper wall was located, the stationary layer was calculated for flat cells of finite width to depth ratios using the Komagate equation (Hunter 2001):

Eq. 3-1 $$\frac{S_L}{d} = 0.500 \pm \left[0.0833 + \frac{32d}{\pi^5 l}\right]^{\frac{1}{2}}$$

S_L = Stationary layer position

d = cell thickness

l = cell width

The cell used with the Zetaphoremeter IV is 2.0 mm (thickness) by 5 mm (width), placing the stationary layer at 0.146d or 0.292 mm from the upper wall. The zeta potential is approximated from the measured electrophoretic mobility, using the Smoluchowski equation (Eq. 3-2) (Hunter 2001):

Eq. 3-2 $$\zeta = \frac{U\mu}{\varepsilon_w}$$

U = measured electrophoretic mobility

ε = permittivity of water

μ = absolute viscosity of the water

3.3 SUMMARY

To successfully determine the competition between fluoride and organic matter on the co-precipitation and adsorption in multi-ligand systems, an in depth analysis of the formed solid precipitate was necessary. The potential of an alum coagulation treatment

system to co-precipitate Al-F during drinking water treatment can only be determined when ligand concentrations and coagulant doses that are environmentally relevant are used during the analysis. This research uses a suite of analyses to attempt to answer whether or not fluoride and organics can co-precipitate in single and multi-ligand systems during alum coagulation. Verification of the ability to co-precipitate in a fluoride system establishes the framework to discuss the competition in multi-ligand systems containing simple, low molecular weight organics and subsequently a system containing NOM. Each chapter builds on the results and conclusions of the previous to create a complete picture of this multi-faceted competition.

Chapter 4: Fluoride incorporation into aluminum oxide precipitates during alum coagulation

4.1 INTRODUCTION

Today, few utilities in North America are concerned about excessive fluoride (F) in their drinking water, but this situation is likely to change in the coming years. Many municipalities fluoridate their water to reach an optimum dose of 0.7-1.2 mg/L F to promote healthy teeth and bone development. The Department of Health and Human Services and the U.S. Environmental Protection Agency (EPA) recently recommended changing the fluoridation practice from the above range to a level of 0.7 mg/L F (Isa 2011); however, the regulated limit for naturally occurring fluoride still remains at 4.0 mg/L. When fluoride is present at levels greater than 1.5 mg/L, it can have negative health effects through incorporation into growing enamel crystals (Aoba and Ferjeskov 2002) and substitution for hydroxyl ions in the apatite structure (Elliot 1994). The recent reduction in recommended fluoridation levels drives the anticipation that the EPA will reduce the fluoride maximum contaminant level (MCL) in the coming years from its current limit of 4.0 mg/L F. If the regulatory limit is changed, many utilities will suddenly face problems meeting a lower standard, and other systems using a water blending approach to meet standards will have to reconsider their current strategy.

To understand the relevance of fluoride research concerning drinking water treatment operations currently using aluminum sulfate (alum) as a coagulant, the work of past researchers concerning the coagulation processes are reviewed. Pernitsky and Edzwald (2006) conducted a study to determine optimal alum and polyaluminum chloride doses for a variety of natural waters ranging from low alkalinity, low natural organic matter (NOM), and low turbidity to high values for all three parameters at a pH

range of 6.6-7.8. The study concluded that a proposed range of 0.5-0.8 mg Al/mg TOC is optimal to encompass the variety of proposed case studies. Shin et al (2008) compared the required stoichiometry for coagulation of waters with NOM and those with only turbidity to find the minimum effective alum doses required for adequate removal ranged from 8 mg/L to 30 mg/L alum ($Al_2(SO_4)_3$*$18H_2O$) depending on the initial turbidity. Their study only considered alum doses of 140 mg/L alum and less. The work by Amirtharajah and Mills (1982) expanded on this alum dose range and developed a set of guidelines for particle removal based on aluminum concentration and pH using alum doses as high as 300 mg/L alum ($Al_2(SO_4)_3$*$14.3H_2O$). In the EPA enhanced coagulation guide, a maximum alum dose of 100 mg/L alum ($Al_2(SO_4)_3$*$14\text{-}18H_2O$) is considered for discussion within the document (EPA 1999). Based on the above research, a coagulant dose range from 20-300 mg/L alum ($Al_2(SO_4)_3$*$12.8H_2O$) was used with a focus at pH 6.6 typical for treatment.

Fluoride, while relatively non-reactive with most water constituents, has a high reactivity with aluminum. Many drinking water treatment plants in the U.S. use aluminum sulfate (alum) or polyaluminum chloride (PACl) as coagulants for the removal of both particles (turbidity) and natural organic matter (NOM); however, since most utilities have not focused on fluoride's effect on treatment, the interactions between fluoride and aluminum in complex waters are not adequately understood.

The precipitate formed during the coagulation process when fluoride is present is still under investigation. Hu et al (2005) proposed a fluoride and hydroxide precipitate can form with Al (III) ions:

Eq. 4-1 $$n\mathrm{Al}^{3+}_{(aq)} + 3n - m\mathrm{OH}^{-1}_{(aq)} + m\mathrm{F}^{-1}_{(aq)} \rightarrow \mathrm{Al}_n n\mathrm{F}_m(\mathrm{OH})_{(3m-n)}$$

However, they state that this precipitate is only stable when [F] is needed to make the molar ratio of ([F]+[OH])/([Al]) > 3. When [OH]/[Al]>3, the coordination between

fluoride and aluminum is replaced by hydroxide ions. Hu et al. (2005) used aluminum concentrations ranging from 1-5 mMol Al, an equivalent alum dose of approximately 300-1600 mg/L alum (well above doses used in water treatment), and did not add carbonate alkalinity in most of their experiments, performing the tests in distilled water. Gong et al. (2012) also investigated the co-precipitation process with fluoride and concluded that an aluminum-fluoride co-precipitate is potentially forming during alum coagulation; however, the experiments were conducted at concentrations not relevant to treatment operation. The initial aluminum concentrations were equivalent to an alum dose of 490 mg/L alum ($Al_2(SO_4)_3$*$18H_2O$, 40 mg/L Al) and over a fluoride concentration range of 5-80 mg/L fluoride; concentrations irrelevant to traditional treatment plants. The experiments also did not add background carbonate alkalinity and hardness, but rather used distilled water as the synthetic background water. Building on Gong et al. (2012) and Hu et al. (2005), this work considered aluminum and fluoride at environmentally and treatment relevant concentrations and examined the effects of fluoride on the physical formation of flocs during alum coagulation.

Traditionally, research focused on aluminum precipitation and stability in the presence of various inorganic ligands was a focus of geochemists and soil scientists. The research groups of Huang and Violante investigated the disruption in the crystalline development of aluminum precipitates when formed in the presence of organic and inorganic ligands (Kwong et al. 1981; Violante and Huang 1985, 1992; Violante et al. 1998; Xu et al. 2010; Yu et al. 2007); however, most of these studies were framed in the time scale of 30 to over 100 days for precipitate aging to occur. The longer timescales allowed for the investigation of aluminum precipitation and stability in soils; however, th time scale used does not correlate to the morphology of precipitates formed during typical detention times for drinking water treatment of hours. Fluoride was shown to

inhibit the formation of crystalline aluminum oxides during the longer timescales studied by Violante and Huang (1985). Aside from the longer timescales, chemical concentrations were often well above typical doses experienced during treatment. The equivalent alum dose corresponding to the 2 mMol/L aluminum concentrations used during Violante and Huang's investigation exceed 500 mg/L alum. In the framework of drinking water treatment, it is necessary to understand how fluoride affects the precipitation processes of aluminum within a more relevant detention time and concentration range for precipitate aging and reactions.

The goal of this research was to evaluate the presence of a co-precipitate in the presence of fluoride at alum doses that are relevant to water treatment processes. Investigating the effects of fluoride on water treatment using aluminum chemicals at low concentrations is important when ensuring high quality treated effluent. This study is aimed at understanding how fluoride effects the formation of aluminum precipitates during alum coagulation based drinking water treatment.

4.2 Research Approach

Determining the structure and chemical composition of amorphous precipitates requires a multifaceted approach using a variety of indirect analytical techniques; the structure and chemistry are not tested directly. To start, the removal efficiencies in a co-precipitated (CPT) versus a preformed (PRE) system were analyzed using a series of jar tests. The CPT system allows for the precipitate to form in the presence of the contaminant (fluoride) while the PRE system doses the ligand after the amorphous precipitate has formed and a residual aluminum concentration is present. Comparison of the two experiments and differences in gathered results elucidates the dominant removal

mechanism. The complete explanations of the experimental procedures for these two types of jar tests are located in Chapter 3.2.1—Jar Tests: Simulating drinking water treatment at the bench scale.

To test the differences in structure between precipitates formed with and without fluoride present, several experimental analyses were used. The outline below details the analyses used, what each analysis tested, and justification for using the specified approach. The detailed methodology description from Chapter 3: Research Approach and Methodology is in the parenthesis following the analysis section name.

Co-precipitation and Preformed jar tests (3.2.1)

To determine the removal efficiency differences for fluoride by alum in systems limited to adsorption and those where the precipitates form in the presence of fluoride, the preformed precipitate (PRE) and co-precipitation (CPT) jar test experimental methods were used. Unless otherwise specified, all tests contain a background synthetic water matrix comprised of 3 meq/L alkalinity and 3 meq/L hardness. Jar test experiments were conducted at a target pH of 6.5 and only adjusted at the beginning of an experiment using 1.0 N HCl and 1.0 N NaOH unless indicated differently in the text or on the figure. Alum stock of 11.63 mMol and 23.26 mMol alum ($Al_2(SO_4)_3$*$12.8H_2O$) were used to dose the jars with coagulant at the beginning of the experiment.

Aged precipitates created during jar tests (3.2.2)

After the settling period of the selected jar test (methodology completely explained in Chapter 3.2.1), the precipitates and solution were transferred to a polypropylene container, minimizing headspace during transfer, and allowed to age for 45 days at 25^{o}C. Before placement in the container, the pH was adjusted to 6.6 and

allowed to age without additional pH adjustment. The purpose of this experiment was to test the degree of disruption by fluoride in the formed aluminum precipitate.

X-Ray Diffraction Spectroscopy (XRD) (3.2.4)

XRD is an extremely useful analytical tool for studying crystalline samples as it is capable of identifying the solid and providing crystalline structure in well formed materials or size of crystalline particles in those starting to form crystalline layers. For example, it is frequently used to distinguish rapidly precipitated non-crystalline iron hydroxide precipitates as either 1-line, 2-line, or 6-line ferrihydrite (Martinez and McBride 1998; Eggleton and Fizpatrick 1988). In this research, XRD was used to evaluate the amorphous phase of the precipitates at the conclusion of the experiment and solids handling.

Titrations of forming precipitates (3.2.2)

Titrations of the systems with and without fluoride were conducted by starting at an acidic pH and titrating with NaOH until a pH > 10 was reached. Measurements of pH were recorded after the electrode measurement stabilized after each base addition (approximately 0.5 min after each addition of strong base). It was hypothesized that differences in the amount of base required to achieve higher pH values, through the pH range of optimal precipitation, would signify a change in precipitate chemistry. A titration of the background water matrix was used as a baseline from which to compare the alum only and alum with fluoride systems.

Scanning electron microscopy and energy dispersive spectroscopy (SEM/EDX) (3.2.4)

SEM has the ability to image the precipitates at a magnification as high as 500,000X, although a magnification of only 500X was used in this analysis. SEM imaging allowed for the qualitative analysis of the shape and size of the precipitates formed with and without fluoride at 100 mg/L and 200 mg/L alum doses. SEM paired with EDX was used to determine the stoichiometry of the precipitates to a depth of 2 μm below the surface. EDX has effectively been used to analyze stoichiometry but does have limitations in resolving the spectroscopic peak of oxygen (Leng 2008). For this reason, EDX was used to both gain a general understanding of concentration ratios of aluminum to fluoride (when present during precipitation) and then as a comparison to data collected from X-ray photoelectron spectroscopy.

X-ray photoelectron spectroscopy (XPS) (3.2.4)

XPS is typically able to provide a more precise analysis of a material's stoichiometry (van der Heide 2011); however, when applied to the amorphous precipitates analyzed as a part of this research, additional preparation was required. Aluminum oxides are often used as desiccants due to their ability to absorb water, but this trait was detrimental to the analysis of the precipitates using XPS. To overcome the interference from absorbed and lattice bonded water molecules, the samples were heated for at least 10 hours prior to analysis and purged with nitrogen gas. By using this type of pre-treatment, double-sided copper tape was no longer a viable sample holder due to the adhesive. Instead, particles were placed inside small copper washers directly on the sample stage, requiring additional spacing between samples to account for particles bouncing during loading of the sample holder and potential cross-contamination. For proof of method, each measurement of experimentally formed precipitate was

accompanied by the measurement of purchased α-$Al(OH)_{3(s)}$ (gibbsite) as the first sample analyzed for stoichiometric verification.

Gas adsorption-desorption experiments (3.2.4)

Nitrogen gas adsorption-desorption onto particle surfaces and analysis of the resulting isotherm provided information on the specific surface area and pore size distribution of the precipitates. Using the Brunauer, Emmett, and Teller (BET) theory (Gregg and Sing 1967), the number of molecules required to achieve monolayer coverage was calculated and directly correlated to specific surface size through knowledge of molecular cross-sectional area of nitrogen gas (the adsorbent used in this research). The linear range of the BET plot selected for analysis was, on average, P/Po values of 0.20 – 0.32 +/- 0.07. Using BET derived specific surface area allowed for the comparison of precipitates formed with and without fluoride and determination of physically differences in formed precipitates.

Particle size distribution analysis (3.2.5)

Particle size distribution analysis was performed on the precipitates after the allotted 30 min of slow mixing prior to settling. Paired with the BET analysis above, the particle size distribution analysis allowed for a more in depth understanding of fluoride's impact on particle size. Volume distributions of the measure particle and floc diameters were plotted and used to determine the impacts of fluoride on floc formation and growth.

Each of the above mentioned analyses are unable to conclusively identify the impact fluoride might have on aluminum precipitation, floc formation, and treatment efficiencies; however, when used in combination, results from these analytical tools can

be used to build a consistent set of conclusions as to the impact of fluoride on precipitates formed during alum based drinking water treatment. The work in this study was restricted to environmentally relevant concentrations of alum, initial fluoride, and contained background alkalinity and hardness to simulate real water conditions in a treatment plant.

4.3 RESULTS AND DISCUSSION

The majority of investigations on fluoride removal have only considered the adsorption of fluoride onto aluminum oxide precipitates (Pommerenk and Schafran 2005; Tripathy et al. 2006) and use the adsorption based removal efficiencies to predict treatment. When in an aqueous solution, aluminum hydroxides tend to dissolve and form various alumina complexed species presented in the list of equations below (Hoa and Huang 1986; Valdiviesco, et al. 2006).

Eq. 4- 2 $Al^{3+} + F^{-} \leftrightarrow AlF^{2+}$

Eq. 4- 3 $Al^{3+} + 2F^{-} \leftrightarrow AlF_2^{+}$

Eq. 4- 4 $Al^{3+} + 3F^{-} \leftrightarrow AlF_3$

Eq. 4- 5 $Al^{3+} + 4F^{-} \leftrightarrow AlF_4^{-}$

Eq. 4- 6 $Al^{3+} + OH^{-} \leftrightarrow Al(OH)^{2+}$

Eq. 4- 7 $Al^{3+} + 2OH^{-} \leftrightarrow Al(OH)_2^{+}$

Eq. 4- 8 $Al^{3+} + 3OH^{-} \leftrightarrow Al(OH)_3$

Eq. 4- 9 $Al^{3+} + nOH^{-} \leftrightarrow Al(OH)_n^{3-n}$

In acid and neutral solutions, complexation of fluoride with alumina occurs resulting in very little free fluoride. At pH > 8, complexation with hydroxyl ions will

dominate, marked by higher values of free fluoride remaining in the solution (Hoa and Huang 1986). To understand the impact of aluminum-fluoride complexes on aqueous aluminum in alum coagulation experiments at pH 6.5, the assumption that the available aluminum is from an amorphous aluminum precipitate at pH 6.5. This aluminum concentration is then used to calculate the resulting Al-F complexes under varying fluoride conditions (Table 4-1). Plotting the complexes and varied influent fluoride concentrations, the speciation of aluminum-fluoride complexes is presented in Figure 4-1. From Figure 4-1, an initial fluoride concentration of 5 mg/L ($10^{-3.58}$ Mol) and pH 6.5 is dominated by the aqueous species AlF_3. For free Al^{3+} to exist as the dominant species in solution, $F^- < 0.0019$ mg/L.

Table 4-1: Equilibrium constants for dissociated reactions of aluminum minerals and complexes (excerpt of compiled table in Lindsay and Walthall 1996)

Reaction	Log K^0
$Al(OH)_{3(s)}$ (amorphous) + $3H^+ \leftrightarrow Al^{3+} + 3H_2O$	9.66
$Al(OH)_{3(s)}$ (gibbsite) + $3H^+ \leftrightarrow Al^{3+} + 3H_2O$	8.04
$Al^{3+} + F \leftrightarrow AlF^{+2}$	6.98
$Al^{3+} + 2F \leftrightarrow AlF_2^+$	12.60
$Al^{3+} + 3F \leftrightarrow AlF_3^0$	16.65
$Al^{3+} + 4F \leftrightarrow AlF_4^-$	19.03

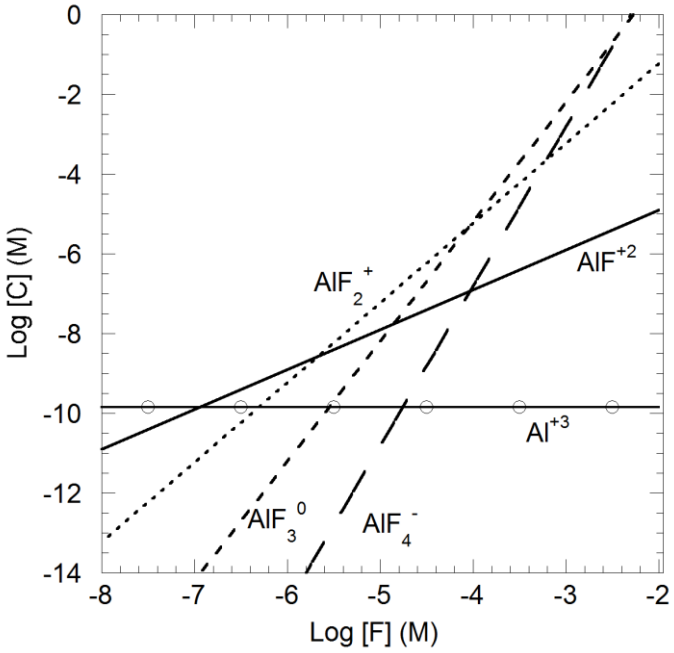

Figure 4-1: Fluoride complexes of aluminum as a function of [F] when $[Al^{3+}]$ is calculated from equilibrium with amorphous $Al(OH)_{3(s)}$ at pH 6.5.

To gain an understanding of how treatment of fluoride is impacted by the precipitation process, jar tests run in a method that employed co-precipitation (CPT) of solids in the presence of fluoride were compared to jar tests conducted using a method that employed fluoride adsorption onto preformed (PRE) solids (Figure 4-2). The results presented in Figure 4-2 clearly show that when fluoride is present at the time of precipitation, more fluoride removal occurs than when fluoride ions are dosed into a system already containing preformed aluminum hydroxide flocs. Focusing on the 100 mg/L and 200 mg/L alum doses, fluoride removal is decreased by approximately 25% when removal is limited to adsorption processes. Since fluoride forms strong aqueous complexes with aluminum, the residual aluminum concentration is important to consider.

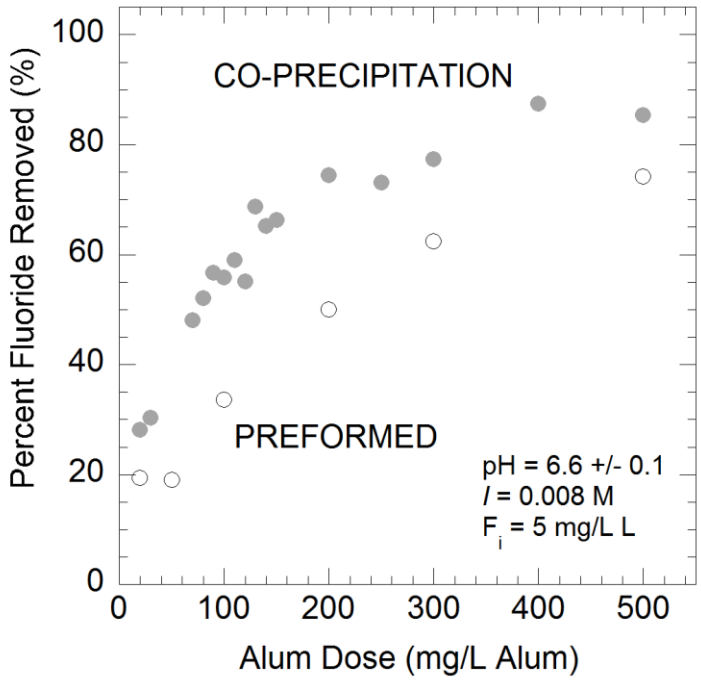

Figure 4-2: Co-precipitation and adsorption of fluoride by aluminum hydroxides.

At the conclusion of the jar tests with fluoride present, CPT with 100 mg/L alum resulted in only 79% aluminum precipitation versus 99% in the PRE system, yet, the removal density of fluoride on the preformed aluminum solids (0.269 mMol F/mMol Al) is only half that of the fluoride removed with the co-precipitated solids (0.533 mMol F/mMol Al). At 200 mg/L alum, residual aluminum concentrations at the conclusion of the CPT and PRE experiments were low, over 99% of the added aluminum precipitated regardless of experimental set up (CPT vs. PRE). The co-precipitation system still had a higher aremoval density (0.275 mMol F/mMol Al) than adsorption onto PRE precipitates (0.200 mMol F/mMol Al). Even though the presence of fluoride during precipitation causes slightly less aluminum solids to form due to the aqueous complexes presented in

Figure 4-1, increased removal of fluoride still occurred. The increased removal indicates surface adsorption is not the sole removal mechanism and that a closer investigation of the formed precipitate is warranted. It is hypothesized that fluoride is forming a co-precipitate with aluminum based on the results in Figure 4-2.

To understand the effects of fluoride on the precipitates formed during alum coagulation, X-ray diffraction (XRD) was used to first determine the crystalline nature of the precipitates. In all samples, with and without the initial contaminant concentration of 1 - 10 mg/L fluoride, amorphous precipitates were created (Figure 4-3a-d). Regardless of coagulant dose tested, all precipitate XRD analyses produced no spectrum peaks, thus confirming amorphous solids after 1 hr 10 min. In samples that exceeded 30 mg/L of fluoride, fluorite (CaF_2, $Ksp=10^{10.4}$ at 25^oC) was precipitated during the coagulation process. In the background synthetic water matrix of 3 meq/L hardness and 3 meq/L alkalinity, fluoride concentrations in excess of 2.7 mg/L F are needed to precipitate fluorite according to equilibrium calculations; however, in these experiments in which aluminum was present, only when the initial fluoride concentration $F^-_i = 30$ mg/L was fluorite observed in the XRD patterns. By not considering background concentrations of alkalinity and hardness, research conducted at extremely high fluoride concentrations is not immediately applicable to real-world treatment conditions. Initial fluoride concentrations in all subsequent experiments in this research were limited to fluoride concentrations less than 10 mg/L fluoride, both to model influent drinking water conditions most commonly encountered in the United States and to limit removal due to fluorite precipitation.

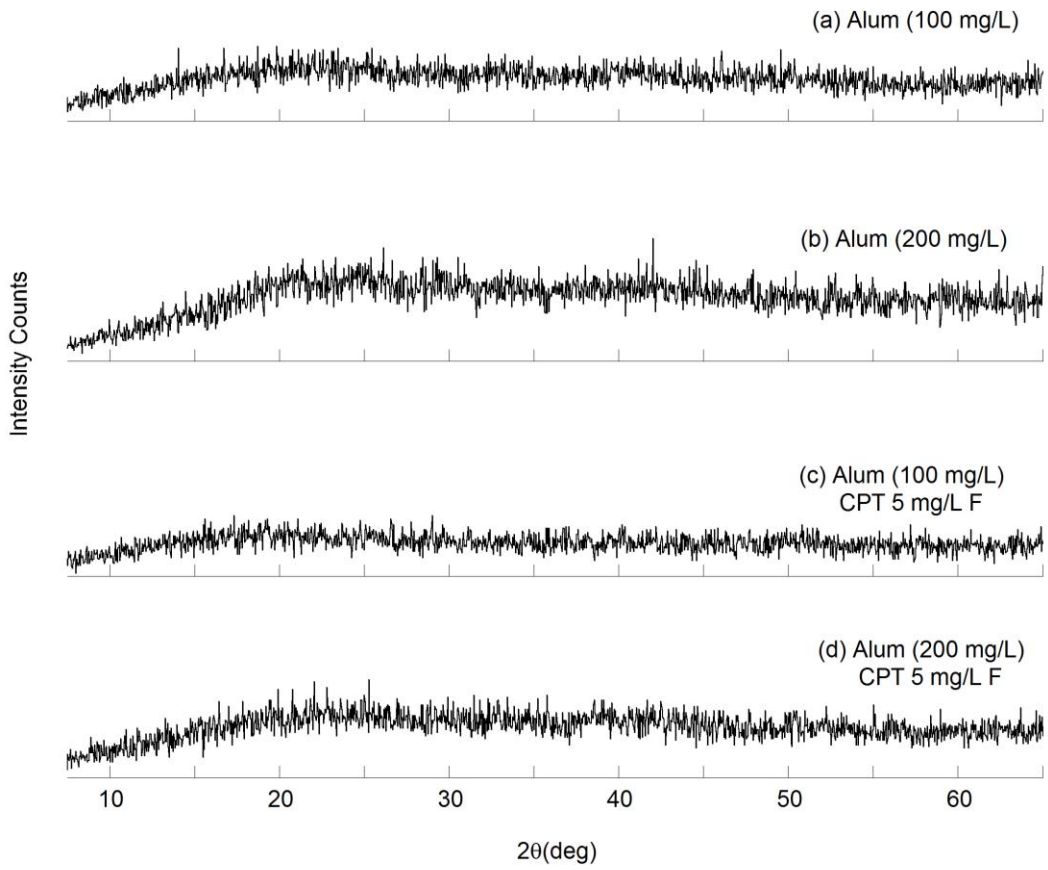

Figure 4-3: XRD images of aluminum precipitates formed at 100 mg/L alum and 200 mg/L alum. (a) and (b) contain no fluoride and (c) and (d) both contain 5 mg/L fluoride. All spectra show a lack of crystalline structure in the formed aluminum precipitates.

The fact that the precipitates remain amorphous during the allocated treatment detention time eliminated the use of analytical techniques such as XRD to directly test for fluoride incorporation into formed precipitates and determination of co-precipitation. Instead, a series of tests to understand the alteration of the precipitate was conducted to enable conclusions on fluoride's effect on aluminum precipitation.

To fully understand the influence of fluoride on the formed solids, it is first important to consider the process of forming an aluminum precipitate. After alum is dosed into solution, the free aqueous aluminum ion is octahedrally coordinated by six water molecules. Incrementally, the hydration shell loses protons to the bulk water solution during hydrolysis as shown in Eq. 4-10:

Eq. 4-10 $Al(H_2O)_6^{3+} + H_2O \leftrightarrow Al(H_2O)_5OH^{2+} + H_2O$

This process is typically abbreviated to not include the waters of hydration Eq. 4-11:

Eq. 4-11 $Al^{3+} + H_2O \leftrightarrow AlOH^{2+} + H_2O$

The fluoride ion has the same charge (-1) and approximately the same ionic radius as the hydroxyl ion; therefore, fluoride can completely coordinate and exist as octahedrally coordinated to aluminum (AlF_6^{3-}) (Nordstrom and Kay 1996).

When, at a given pH, the solution is oversaturated with respect to aluminum, thermodynamics favor precipitation. If the hypothesis that fluoride-aluminum co-precipitation is occurring within these systems is correct and can explain the increased removal of fluoride, then as the pH of a solution containing a given aluminum concentration is increased to promote precipitation, the fluoride ions contained in the octahedral coordination will not undergo replacement by OH^- and will remain in the precipitate structure, as represented in the schematic in Figure 4-4. When fluoride is not present, Figure 4-4a, precipitation of a pure aluminum hydroxide phase will proceed until equilibrium is achieved. In the fluoride system, Figure 4-4b, coordinated fluoride replaces OH^-, increasing the solution pH for the same concentration of base added due to the increased concentration of residual, unbound, hydroxyl ions.

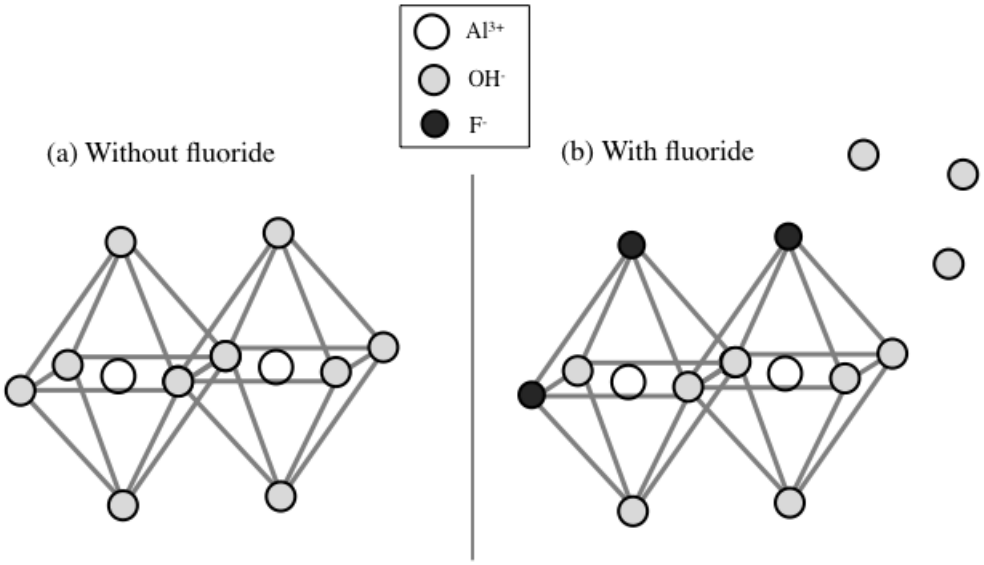

Figure 4-4: Schematic of proposed changes to aluminum coordination during fluoride co-precipitation at a given pH.

To test the above hypothesis, a series of titrations incrementally adding strong base were performed. The pH values after each OH^- addition were compared. To first test the ability to measure slight changes in pH given the background alkalinity, a series of systems with increasing alum doses were titrated and the results are presented in Figure 4-5. It is clear from this figure that even with background alkalinity present, differences in titration curves as the alum doses increase are possible.

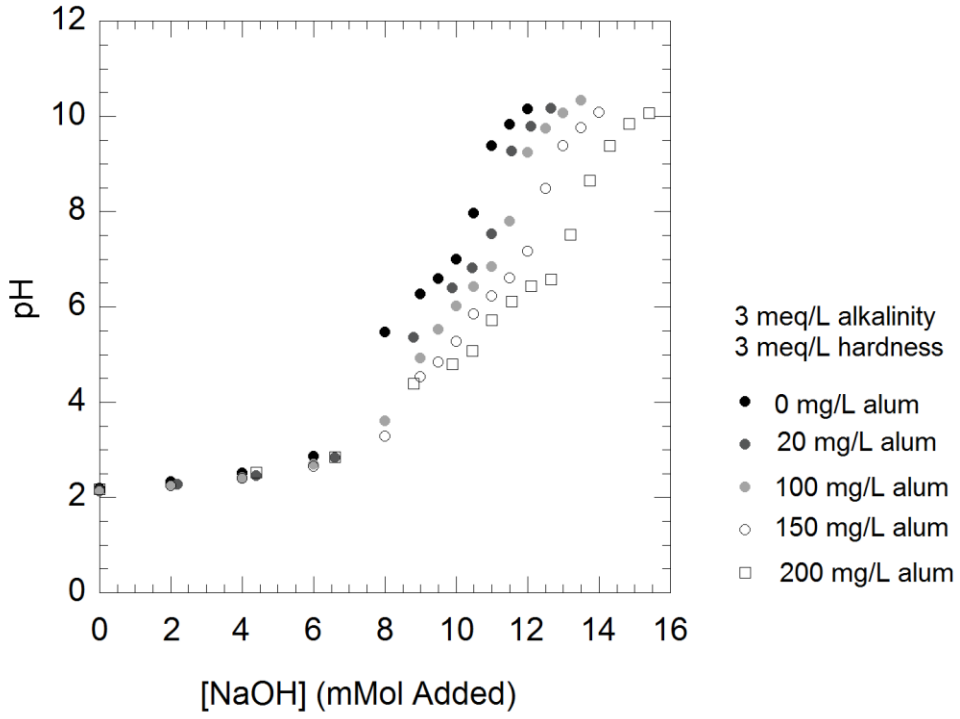

Figure 4-5: Titrations of background alkalinity and increasing doses of alum coagulant.

Precipitation began after a pH of 4 was exceeded in these experiments, above which the titration curves diverge. As alum doses increased, more hydroxyl ions are needed to complex with the aluminum ions, resulting in less increase in pH with each incremental addition of base.

If aluminum-fluoride co-precipitation does not occur, then, as fluoride doses vary, no difference is expected in the titration curves acquired in the presence and absence of fluoride. However, as the concentration of fluoride increased, the same small additions of hydroxyl ions led to larger increases in pH, especially for the 50 mg/L alum and 100 mg/L alum coagulant doses (Figure 4-6b and c). It should be noted that the difference in the pH between the systems occurs at pH values greater than the pKa of 3.17 for

hydrofluoric acid. Above this pH, the fluoride available for complexing with aluminum increased.

Little variation between the curves was observed for both the low dose of alum, 20 mg/L alum (Figure 4-6a), and the highest doses tested, 150-200 mg/L alum (Figure 4-6d-e). At the low alum dose, the system was aluminum-limited and, therefore, no variation in the curves was observed. There was not enough aluminum to distinguish any differences between the titration curves even at the highest fluoride doses of 10 mg/L F. Even the 50 mg/L alum system (Figure 4-6b) was aluminum limited at the fluoride dose of 10 mg/L F as there is no difference between the 5 and 10 mg/L F curves in the 50 mg/L alum system. At the highest alum doses, the 150 mg/L and 200 mg/L alum doses, it is believed that the system was now fluoride limited in this reaction. The curves, again, show no distinguishable differences between those containing fluoride and those without fluoride due to the limited available fluoride to complex to aluminum ions. Each system precipitates aluminum oxide solids regardless of the presence of a co-precipitate forming as well, but in the fluoride-limited systems, the amount of aluminum oxide precipitated obscures the co-precipitate formed.

Researchers who work at environmentally irrelevant levels of aluminum will not observe co-precipitating effects. The [Al]:[F] molar ratio required to see observed effects during the titrations were 1:1.5. When compared to previous research, this ratio is near the upper end of the researched concentration ratios and is typically achieved through high doses of fluoride rather than low aluminum concentrations (Gong et al. 2012; Pommerenk and Schafran 2002; Violante and Huang 1985).

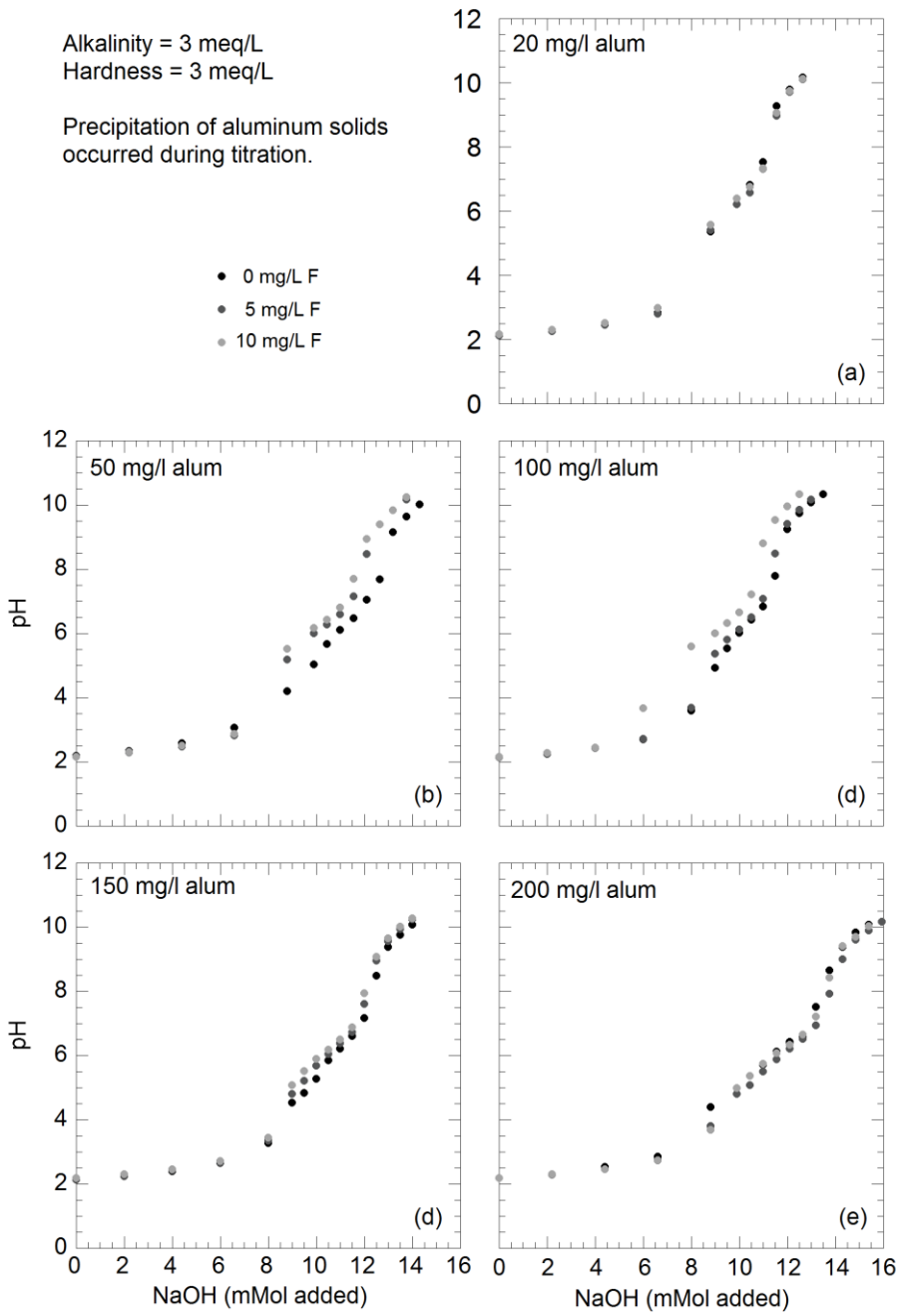

Figure 4-6: Titration curves of various alum doses with 0, 5, and 10 mg/L fluoride.

The presence of an increased pH for the systems containing fluoride in comparison to those systems without fluoride during titration with a strong base suggests that less pure aluminum hydroxide precipitation is occurring. To ensure it is not due to aqueous complexation of aluminum and is from precipitation, the percent aluminum precipitated is plotted alongside the titration curve in Figure 4-7 for the 50 mg/L alum dose. The solid line at pH 7 in Figure 4-7b marks the pH of over 95% precipitation for all three curves and is repeated on Figure 4-7a for ease of comparison. If the associations were solely due to complexation, above this line the titration curves would all intersect in Figure 4-7a, with the stoichiometry for precipitation fully satisfied; however, this is not observed. A similar correlation exists for the 100 mg/L alum dose solubility curve (not shown), further confirming that even though complexation is important, it is not the sole contribution.

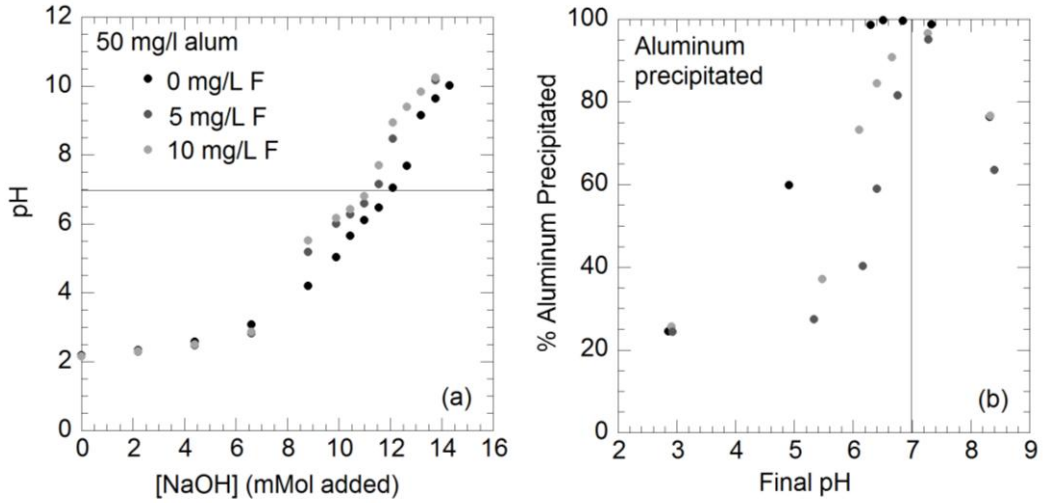

Figure 4-7: Titration curves for 50 mg/L alum and the associated precipitation curves.

If fluoride formed a co-precipitate as proposed here, fluoride is either blocking the formation of aluminum hydroxide precipitates or the fluoride ligand is preferentially incorporated into the solid phase compared to the hydroxide ion. Data from the CPT and PRE experiments suggests that in some cases less aluminum was removed from solutions, suggesting that a blocking mechanism was at least in part responsible for the reduced hydroxide ion consumption. This type of precipitation blockage can occur throughout the structure or localized to edge sites. Nordin et al. (1999) suggested that fluoride mainly occupies edge sites of boehmite and can occupy edge and kink sites in bayerite. Considering the possibility of occupying an edge sites, it is possible that fluoride inhibits the formation of double hydroxide bridges, thus preventing the formation of a crystalline solid and alters the formed precipitate.

If the hydroxyl bridges are inhibited and fluoride is not eventually replaced by hydroxyl ions in the precipitate over time, then aged precipitates containing fluoride should result in a different structure. Violante and Huang (1985) investigated the inhibition of oxide formation by organic and inorganic ligands at varying [Ligand]/[Al] molar ratios and found that the presence of ligands altered the crystallinity and structure of the solids formed during precipitation of aluminum. While the $[Al]_T$ used in their research is greater than the equivalent $[Al]_T$ from a 500 mg/L alum dose, their use of high concentrations of fluoride create an overlap in [F]/[Al] ratios of their experiments and this study and are summarized in Table 4-2.

Precipitates formed by CPT from a 200 mg/L alum dose, with and without fluoride, were aged for 45 days. A 200 mg/L alum dose equals an $[Al]_T$=0.873 mMol Al, and $[SO_4^-]_T$=1.31 mMol SO_4^-, and a $[SO_4^-]$/[Al] = 1.5. When 5 mg/L of fluoride is present, [F]/[Al] = 0.3. Bracketing these concentrations with the ratios used by Violante

and Huang (1985), Table 4-2 summaries their results after aging precipitates for 5 months.

Table 4-2: Formation of aluminum solids dependent on ligand (sulfate and fluoride): aluminum dose ratio (Violante and Huang 1985)

[Ligand]/[Al] ratio, (R)	Sulfate	Fluoride
0.1	Bayerite and small amounts of gibbsite	Bayerite
0.2	Bayerite and gibbsite	Bayerite
0.5	Bayerite and gibbsite	Amorphous
1.0	Gibbsite and small amounts of bayerite and pseudoboehmite	Amorphous
3.0	Gibbsite and small amounts of bayerite and pseudoboehmite	Amorphous

According to their results, aged precipitates form crystalline solids in systems precipitating in the presence of fluoride and sulfate individually at the concentrations used in this study. When aliquots of precipitates were aged for 45 days for this study, the x-ray diffraction patterns in Figure 4-8a and b show very little variation or peak presence. The scans of Figure 4-8a and b were quick scans using short dwell times; however, the alum only system exhibited small, ill-defined peaks (Figure 4-8a) while the precipitates formed in the presence of fluoride do not show any peaks (Figure 4-8b), signifying that the solid is still amorphous.

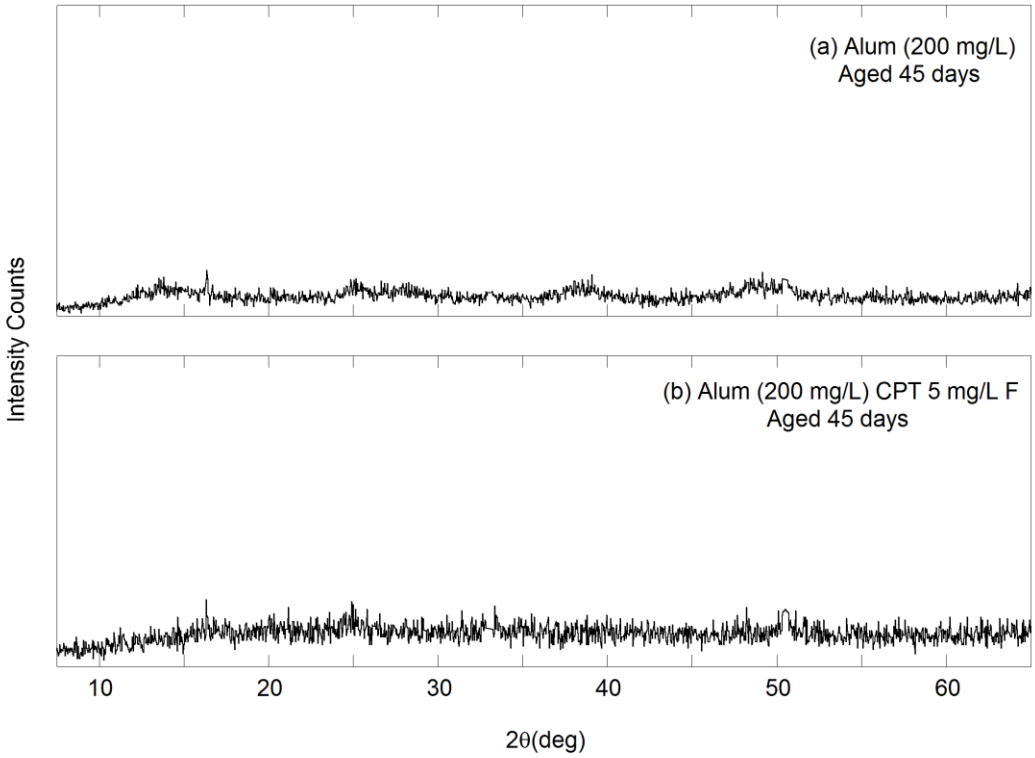

Figure 4-8: XRD patterns of aged precipitates formed without and without fluoride present.

To achieve better resolution, diffraction patterns using the Scintag theta-theta diffractometer and a longer dwell time were obtained for both aged precipitates. The XRD pattern from the more precise diffractometer and increased dwell time enhanced the peaks observed in Figure 4-8a (Figure 4-9) while the CPT solid remained amorphous (pattern not shown). Matching the peaks to catalogues of oxide peaks, it was determined that the aged precipitates contain boehmite with a crystallite size of around 25 angstroms.

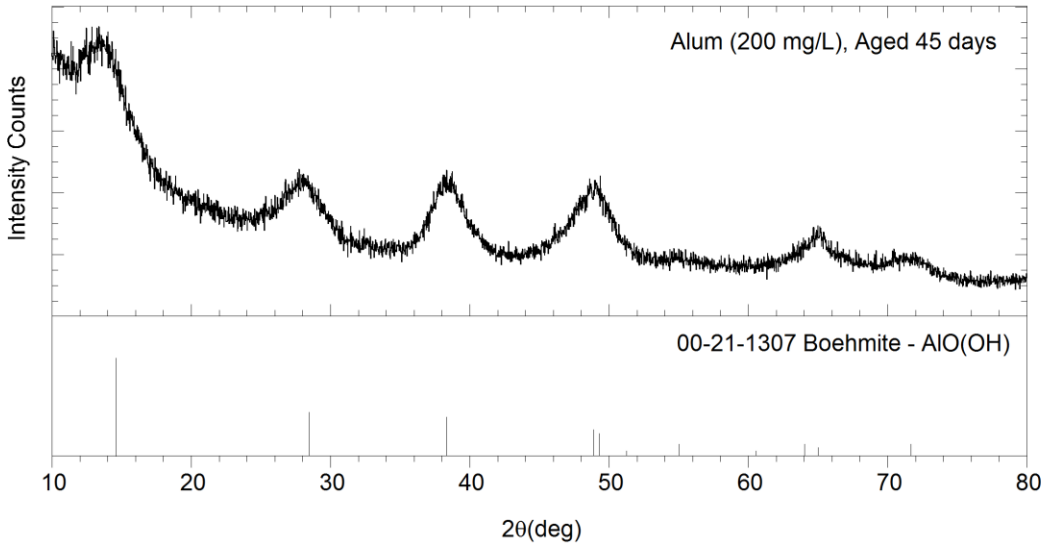

Figure 4-9: XRD pattern for alum only precipitates aged 45 days with matching boehmite spectrum peaks.

The lack of crystallinity from the precipitates formed in the presence of fluoride suggests that fluoride is in fact disrupting the bonds of the precipitate. Violante and Huang (1985) report the lowest [F]/[Al] ratio for precipitates to remain amorphous after 5 months of aging is 0.4. The results obtained by this study show that boehmite is well resolved after only 45 days of aging when only sulfate is present. This result is contradictory to the gibbsite results obtained by Violante and Huang (1985). When both sulfate and fluoride are present only amorphous precipitates were present after 45 days of aging.

If fluoride is preventing the double hydroxide bridges from forming in the precipitate, it is essentially preventing the formed floc and precipitate from growing as well. A smaller solid should, therefore, possess a higher specific surface area. Using gas absorption and the Brunauer-Emmett-Teller method of analysis (BET), the specific

surface area of solids formed in the presence of 0, 5, and 10 mg/L fluoride were calculated and are compared in Table 4-3.

Table 4-3: Specific surface area by gas adsorption

Sample	BET surface area (m^2/g)
200 mg/L alum	186
200 mg/L alum, CPT 5 mg/L F	294
200 mg/L alum, CPT 10 mg/L F	330

As fluoride concentrations increase at the time of precipitation, the solid appears to become smaller. The limit of this trend and the linearity cannot be analyzed without more data points; however, the consistency of increasing specific surface area with increasing fluoride is observed suggesting that more sites can be occupied by fluoride as long as enough fluoride is available.

During the experiments, qualitatively smaller flocs were observed for co-precipitation experiments with fluoride over those formed in the absence of fluoride. To quantify this observed difference, particle size distribution analysis was performed for two alum doses. Looking at the results in Figure 4-10, graphs a and b, stacked vertically on the left, are log size distributions for the 100 mg/L alum dose without (b) and with (a) 5 mg/L fluoride. A 0.2 decrease in peak volume of log d_p resulted when fluoride was included in the experiments. This decrease is equivalent to the formation of flocs that are 1.6 μm smaller when fluoride is present. When the alum dose was increased to 200 mg/L alum (Figure 4-10c-d) the peak volume of particle diameter decreased again between systems without and with fluoride by 0.1 log d_p, or 1.3 μm in diameter. Considering that the majority flocs formed without fluoride in the 200 mg/L alum system are 7.9 μm in

diameter and when fluoride is present at the time of precipitation, a reduction in peak volume diameter to 6.31 μm is significant.

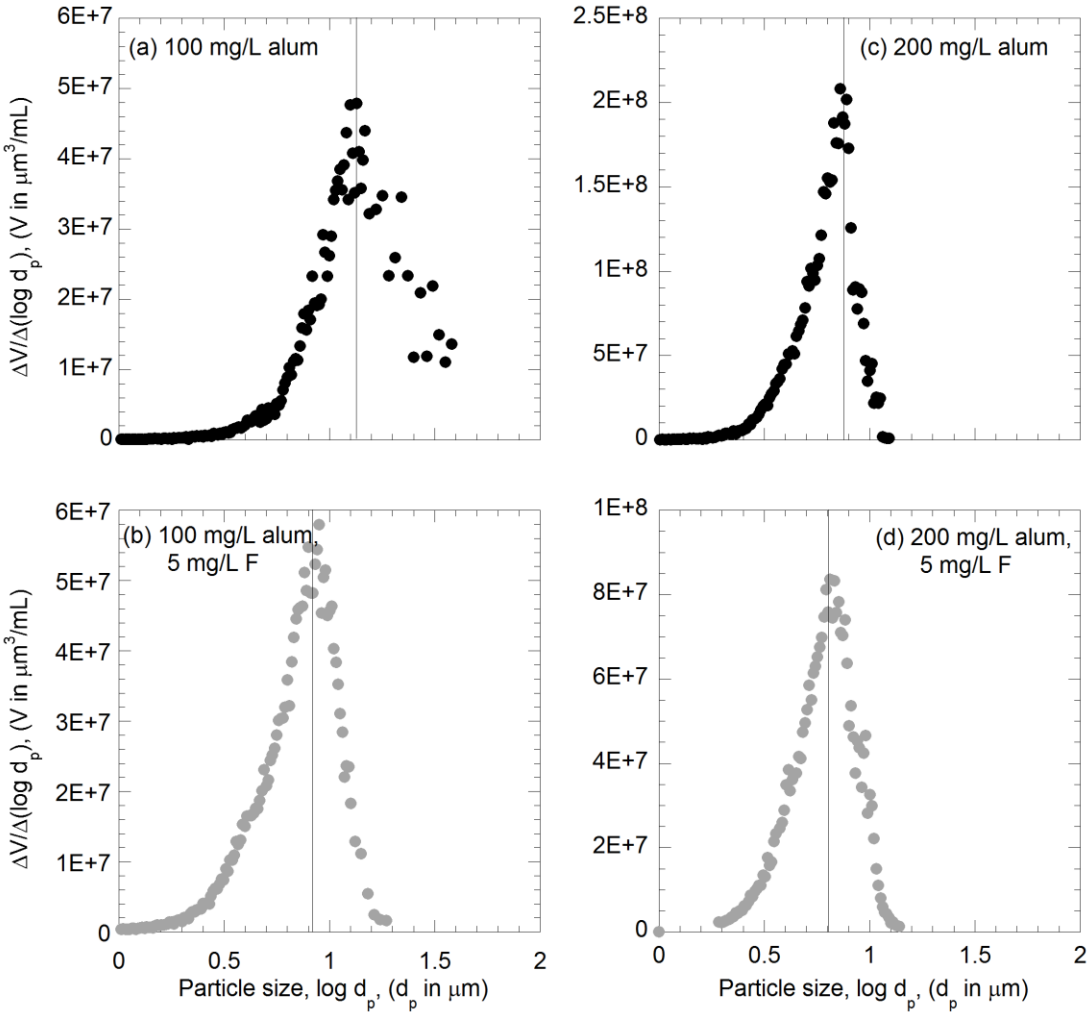

Figure 4-10: Particle size analysis of flocs formed by 100 mg/L alum (a-b) and 200 mg/L alum (c-d) doses with and without fluoride present.

From the results presented thus far, the titration data, specific surface area analysis, and the particle size distribution, it appears that fluoride is replacing hydroxyl ions in the precipitate structure at concentrations as low as 5 mg/L F. To understand

stoichiometry and morphology impacts of fluoride replacement in the precipitate, Scanning Electron Microscopy (SEM) and X-ray photoelectron spectroscopy (XPS) analysis were performed on the formed solids. Both XPS and SEM, when paired with energy-dispersive electron spectroscopy (EDX), allow for localized chemical analysis; however, XPS only has a spectral depth of 2-20 atomic layers while SEM/EDX is able to analyze up to 2 μm in depth below the surface. Using both techniques for analysis enables a more complete understanding of the surface concentrations and bulk concentrations of the material.

The SEM data further confirms the presence of visibly smaller precipitates when fluoride is co-precipitated with aluminum (Figure 4-11). The top two images are those formed without fluoride and show a mixture of several particles sizes with the largest approximately 173 μm and 150 μm in the longest direction for the 100 mg/L and 200 mg/L alum doses, respectively. For the experiments containing fluoride (bottom row of Figure 4-11), the largest precipitates decrease to approximately 63 μm and 100 μm in the longest direction for the 100 mg/L and 200 mg/L alum dose respectively. These particle sizes exceed the maximum particle diameters measured by the particle size distribution analysis; however, particle size measurements by the Coulter Counter are expected to be smaller than those calculated by SEM as the Coulter Counter counted solid volumes.

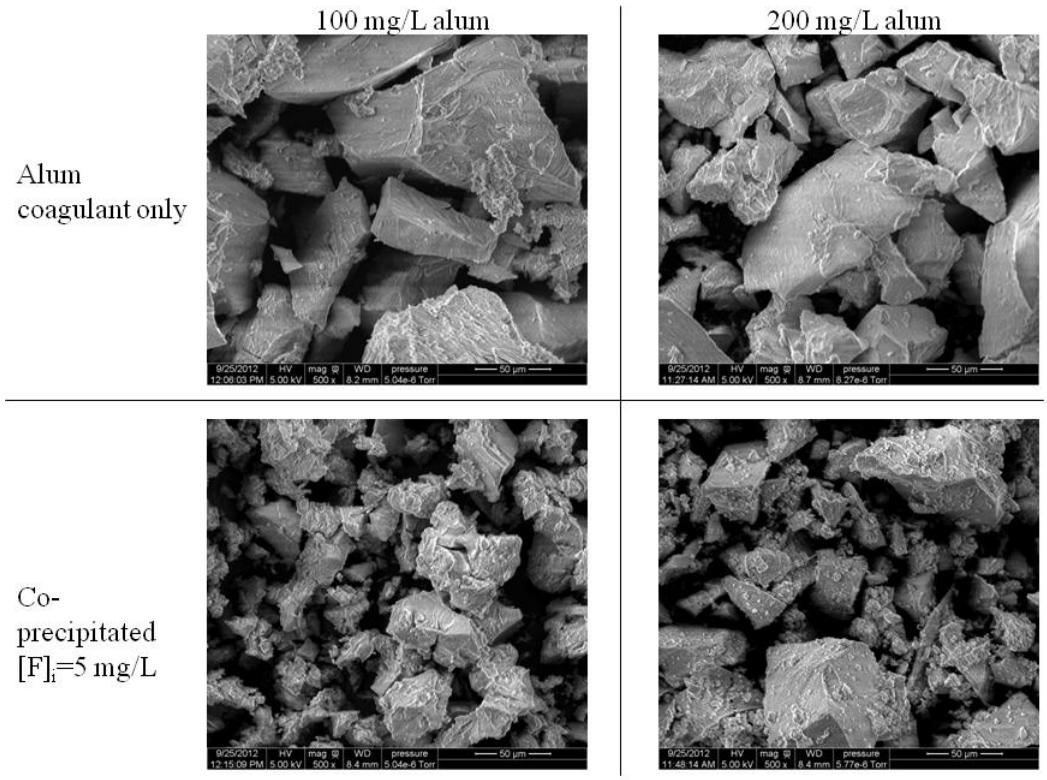

Figure 4-11: SEM images of precipitates formed with and without fluoride present at the time of precipitation.

Since SEM/EDX analysis cannot accurately resolve oxygen concentrations, EDX correlation of Al:F ratios are considered for this analytical procedure and are presented in Table 4-4. More fluoride is incorporated into the aluminum precipitate at the lower alum dose since the [F]/[Al] ratio is greater. Using XPS, the 200 mg/L results were further analyzed for stoichiometric ratios of Al:O:F.

Table 4-4: SEM/EDX determination of Al:F ratios in precipitates

	Al	F
200 mg/L alum, CPT 5 mg/L F	1	0.43
100 mg/L alum, CPT 5 mg/L F	1	0.50

To avoid residual water measurements, the precipitates were heated inside the XPS chamber and flushed with nitrogen gas overnight. A sample of α-$Al(OH)_{3(s)}$ (gibbsite) was used as a reference material to verify the results. Looking first at the calculated stoichiometry of the formed precipitates (Table 4-5), α-$Al(OH)_{3(s)}$ produced an Al Al:O ratio of 1:1.6 as expected, verifying the elimination of almost all extraneous surface bound water from the system. The amorphous precipitates formed during the coagulation process are expected to most closely resemble a psuedoboehmite given the presence of boehmite after 45 days of precipitate aging.. This expectation was confirmed by the measured Al:O ratio of 1:2, the stoichiometric ratio of boehmite, for the fluoride free system. A higher Al:F ratio by a factor of two is observed in the SEM/EDX analysis of the bulk precipitate compared to the XPS results, suggesting that incorporation of fluoride into the material extends below the 2-20 atomic layer limit of the XPS.

Table 4-5: Stoichiometric ratios normalized by aluminum concentration

Sample Name	Al	O	F
Gibbsite	1	1.6	---
200 mg/L alum	1	2.0	---
200 mg/L alum (PRE), 5 mg/L F	1	1.8	0.23
200 mg/L alum (CPT), 5 mg/L F	1	1.7	0.25
200 mg/L alum (CPT), 10 mg/L F	1	1.6	0.42

The Al:O ratio decreases when fluoride is adsorbed to the surface during the PRE experiments since XPS is primarily a surface analysis instrument and accounts for fluoride occupation on the surface. The Al:O ratio continues to decrease in the two CPT systems until a 1:1.6 ratio is reached in the CPT, 10 mg/L fluoride system. The precipitate achieves the same 1:1.6 ratio as gibbsite, but it remains amorphous indicating

a different structure is present. XPS also allows for the analysis of bond strength (Table 4-6). The F 1s bond shows a slight strengthening from 685.6 eV in a PRE system to 685.7 eV when a CPT system is used and 5 mg/L fluoride are used in both. If the decreasing Al:O ratios were only attributed to increasing surface concentrations of fluoride, then the F 1s bond should have remained constant. The bond increases again to 686.0 in the CPT, 10 mg/L fluoride experiment, further proving the trend of increased bond strength with increased fluoride incorporation.

Table 4-6: Bonding energy position for flocs formed by 200 mg/L alum

	Binding Energy (eV)		
Sample Name	O 1s	Al 2p	F 1s
200 mg/L alum	529.81	72.71	
200 mg/L alum (PRE), 5 mg/L F	529.41	72.51	685.6
200 mg/L alum (CPT), 5 mg/L F	529.51	72.41	685.7
200 mg/L alum (CPT), 10 mg/L F	529.51	72.51	686.0

This slight increase in bond strength is consistent with the increase observed by Gong et al. (2012) in their research using aluminum doses more than double of that used in this research. While there is no definitive trend associated with the O 1s and Al 2p binding energy positions as we move from preformed to co-precipitated samples, both have the highest binding energies for the precipitates formed without any fluoride in the system.

4.4 CONCLUSION

Determination of precipitate structure from an amorphous solid is not a straightforward process. Conclusions regarding the precipitate were only possible after the analysis of the combined results since the amorphous characteristics of the precipitates often render the results as undeterminable from analyses used to test oxide

surfaces. Analysis of the results indicated that fluoride is altering the aluminum precipitate when both are present at environmentally relevant concentrations. The increased surface area and decreasing particle sizes of the formed floc suggest that fluoride is blocking the growth of aluminum precipitates due to replacement of hydroxyl ions in the aluminum structure. XPS analysis of the precipitates confirms the replacement of hydroxyl ions with fluoride ions by a measured decrease in the Al:O ratio and stronger F 1s bond in the fluoride co-precipitate.

Co-precipitation with fluoride is important to consider during drinking water treatment for several reasons. First is the tendency of researchers to extrapolate adsorption data to coagulation practices for prediction of removal efficiencies. Following this practice will result in an underestimation of removal and, most likely, excess chemicals being used during treatment. The other important result is the importance of the Al:F ratio in the experiments. Even in this work, when alum doses were increased from 100 mg/L to 200 mg/L alum, changes in precipitate particle size, hydroxyl replacement during titration, and the ratio of aluminum to fluoride measured in the bulk precipitates were evident. Fluoride promoted differences in pH during the titration experiments and particle sizes using the particle counter were more difficult to observe in systems using 200 mg/L alum. It is believed that the differences still exist but because of aluminum hydroxide concentration, the effects are small compared to the changes in solution chemistry and formed precipitates due to aluminum hydroxide reactions.

The changing particle and floc sizes caused by fluoride incorporation into the precipitate can potentially lead to detrimental water quality with regard to parameters other than high residuals of fluoride in treated water. The decreased particle size has the potential to limit particle-particle collisions in systems, leading to less floc growth and a potential decrease in the ability of the flocs to settle.

Fluoride, however, is rarely the only ligand present in drinking water. Alum coagulation is typically used for treating turbidity and natural organic matter in the source water and the interactions between fluoride, aluminum, and the other constituents in the water also requiring treatment must also undergo investigation. To understand the impact of fluoride on alum coagulation, the effects of a co-precipitating solid on removal and competition of low molecular weight organics and fluoride are considered in the next chapter. By considering the impacts of a dual ligand system on the co-precipitate, more complexity is added to the overall discussion of fluoride's impact on drinking water treatment.

Chapter 5: Competition between fluoride and low molecular weight organics during alum coagulation

5.1 INTRODUCTION

Natural organic matter (NOM), the product of plant and biological decay, is present in all natural water. The composition varies spatially and temporally and depends on the origin (e.g., autocthonous, allocthonous, wastewater), age, fate, and season (Aiken et al. 1985). NOM produced from aquatic algae is low in aromatic carbon and phenolic content, whereas terrestrially derived NOM is high in aromatic carbon and phenolic content. NOM undergoes both photo- and bio-degradation in the natural environment and exists in both dissolved and particulate form.

The efficacy and efficiency of almost all water treatment processes are impacted by the presence of natural organic matter in the source water. NOM reacts with common disinfectants (e.g., chlorine, chloramines, and ozone) to produce a range of potentially carcinogenic disinfection by-products (DBPs) (Richardson 1998; Arora et al. 1997), fouls membranes used for reverse osmosis and ultrafiltration (Cho et al. 1999), blocks activated carbon pores used for micropollutant removal (Li et al. 2003; Ding et al. 2006; Srinivasan et al. 2008), consumes oxidants used for contaminant destruction (Huang et al. 2005), and competes for adsorption sites with taste and odor producing compounds (Zoschke et al. 2011). Ozonation of surface waters containing NOM can produce smaller organic acids such as benzoic acids, salicylic acid (2-hydroxylbenzoic acid), and phthalic acid when low ozone doses are applied (Huang et al. 2005). As a result, a significant fraction of water treatment research, treatment plant design and operation, and utility cost is devoted to removal of NOM from drinking water (Jacangelo et al. 1995).

Due to the complexity of NOM chemistry and structural variation depending on location, it is common to use surrogate compounds to model NOM and understand the impact of specific functional groups on treatment. Research characterizing the formation potential of DPBs concluded that the aromatic ring structure of the NOM compound is the most important precursor (Kitis 2002). Furthermore, carboxylic acids and acidic groups comprise approximately 90% of all organic carbon in natural waters (Nordstrom and May 1996). Aluminum complexation with organics primarily occurs with the oxygen atoms within the carboxylic moiety. Figure 5-1 contains several common complexation forms: (A) water bridging, (B) electrostatic attraction, (C) coordination with a single donor group, (D) coordination with a dual donor group. The coordination structures shown form stable complexes with aluminum (Vance et al. 1996).

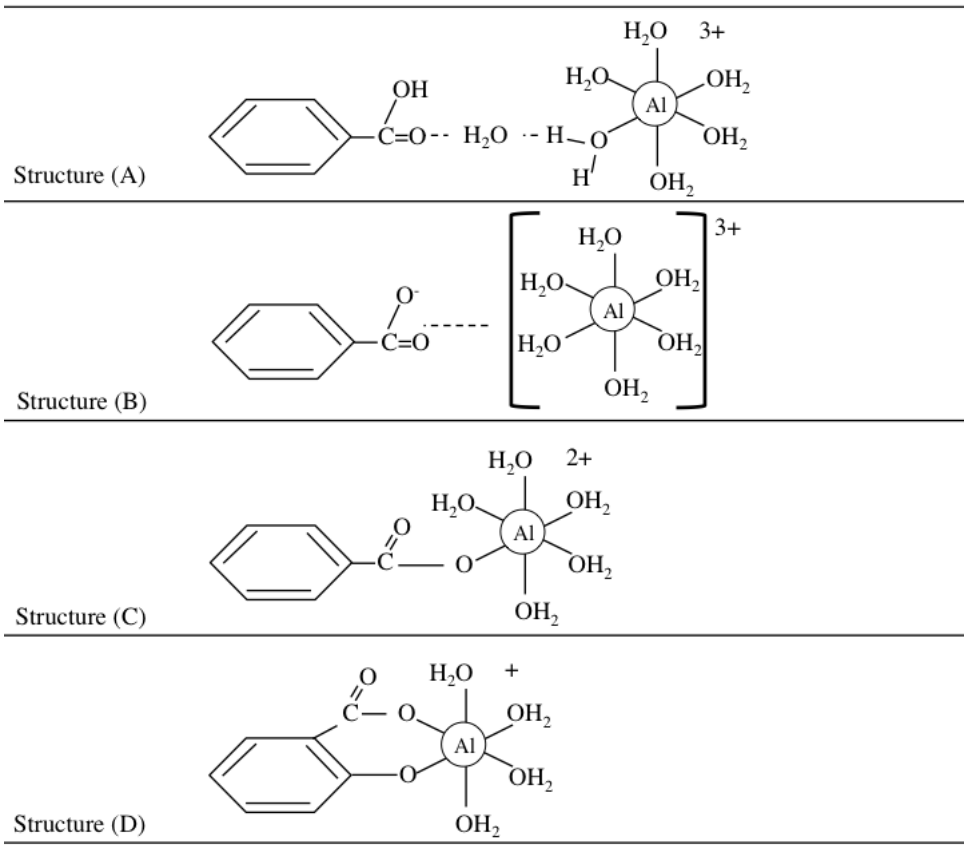

Figure 5-1: Common aqueous complexes between aluminum and organic acids (adapted from Vance et al. 1996)

Xu et al. (2010) showed that organic acids can occupy aluminum coordination sites, thus interfering with the formation of crystalline Al (oxy)hydroxide even after 80 days. Increased incorporation of low molecular weight (LMW) organic acids into the structural network of the aluminum precipitation product occurs through the complexation of the LMW organic acids with aluminum. In the Xu et al. (2010) study, the structure of the LMW organic was important in determining the aged coordination structure of aluminum in the precipitates; however, these findings were after 80 days and do not offer information about the structure of the precipitate immediately after

precipitation. The shortest timescale used by the research group was 1 day. For experiments free of tannate, the precipitates were a bayerite and gibbsite mix. When tannate was present, contaminant concentration was very important in the disruption of forming crystalline aluminum oxides. Molar ratios of tannate/Al of 0.001 produced a mix of crystalline and amorphous aluminum precipitate, but when increased to 0.01, crystalline aluminum peaks in the XRD analysis disappeared (Yu et al. 2007).

Research investigating the importance of molecular structure and surface bonding typically use crystalline oxides (e.g. Evanko and Dzombak 1998; Guan et al. 2006; Lindegren and Persson 2010; Johnson et al. 2005; Johnson et al. 2004a; Johnson et al. 2004b; Noren and Persson 2007) leaving a void in the knowledge base on how these ligands react with a mixed or non-crystalline surfaces. In the framework of drinking water treatment, it is necessary to understand how these ligands, alone and in tandem, affect the precipitation processes of aluminum within a more relevant timescale. As concluded from Chapter 4, molar ratios of [F]/[Al] of 0.3 produced amorphous precipitates, but beyond the influence on the precipitate the impact of this structure on the removal of organic acids is important to understand.

When engineering a treatment system that involves precipitation, it is important to understand the degree of adsorption occurring on the precipitates formed during the process. Bose and Reckhow (1998) noted the importance of NOM properties such as size and charge density in adsorption to aluminum flocs formed with alum, but since they did not use surrogate compounds, they could not comment specifically on the importance of molecular structure. Many experiments previously conducted to look at single and dual ligand adsorption on preformed aluminum precipitates use aluminum chloride to form the precipitate (Pommerenk and Schafran 2005; Guan et al. 2007; Guan et al. 2006a; Guan et al. 2006b) and not alum. In the Pommerenk and Schafran (2005) study, sulfate was

shown to have 100% removal at low concentrations, yet the background competition of sulfate is not considered if alum is not used. The goal of this research was to evaluate the effect of a co-precipitating solid on removal and competition of low molecular weight (LMW) organic acids and fluoride. Using three structurally different low molecular weight organic acids in co-precipitating, competing systems with fluoride allowed for a broad analysis of ligand surface bonds and the role of precipitation in the removal for the dual ligand systems.

5.2 BACKGROUND AND SELECTION OF NOM SURROGATES

Considering a significant portion of NOM is comprised of carboxylic and phenolic functional groups, the LMW organic acids in Table 5-1 were used as NOM surrogates in this research. LMW organic acids adsorb to oxide surfaces through the formation of complexes between the phenolic, carboxylic, or amino groups and the metal ions of the oxide surface. Also important in the choice of LMW organics is the position and number of carboxylic and phenolic groups. Evanko and Dzombak (1998) performed an extensive study of organic acid adsorption onto to goethite and concluded that increasing numbers of carboxylic groups correlated with increasing removal, providing a base of work for comparison. Another important characteristic to improved removal was the position of a phenolic group ortho to a carboxylic group, influencing the choice of salicylic acid for this study.

Salicylic acid is an aromatic compound commonly found in natural waters. Ainsworth et al. (1998) investigated the binding of salicylic acid to alumina and proposed mixed monodentate and bidentate inner-sphere complexation. At low coverage of salicylate on the alumina surface, bidentate complexation dominated (Kasprzk-Hordon

2004). Phthalic acid has been shown to exhibit an inner-sphere, mononuclear bidentate, chelating ring when adsorbing to both goethite and boehmite under acidic conditions, influencing the overall stability of the metal oxide (Persson et al. 1998). This chelation is important when considering competition with fluoride and removal by non-crystalline materials. Finally, pyromellitic acid was selected since it has been reported to most closely represent humic acid in adsorption studies (Evanko and Dzombak 1998).

Table 5-1: Low molecular weight organic acids of interest

Name	Chemical Formula	Structure	pKa [a]
Salicylic Acid (2-hydroxy-benzoic acid)	$C_7H_6O_3$	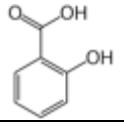	2.88 13.56
Phthalic Acid (1,2-benzenedicarboxylic acid)	$C_8H_6O_4$	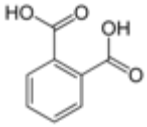	2.87 5.23
Pyromellitic Acid (1,2,4,5-benzene-tetracarboxylic acid)	$C_{10}H_6O_8$	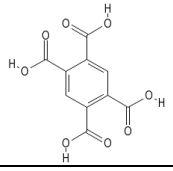	1.52 2.95 4.65 5.89

[a] Taken from Martell and Smith (1974) and corrected for an ionic strength of 0.01M.

5.3 RESEARCH APPROACH

The coagulation of NOM by aluminum salts involves a suite of chemical processes including aluminum hydrolysis, complexation, precipitation, and adsorption (Edzwald and Van Benschoten 1990). The removal of fluoride involves adsorption and, as Chapter 4 concluded, co-precipitation. To understand the competition between fluoride and organic acids for removal by coagulation processes using aluminum sulfate, an

experimental matrix of jar tests combined with spectroscopic analysis of precipitates and surfaces were conducted. A major focus of this chapter was experimentally determining the competition between fluoride and the LMW organic acids.

To test the differences in removal by adsorption versus co-precipitation, jar tests for macroscopic removals was a strong focus. The outline below details the analysis, what the analysis tested, and justification for using the specified approach. The detailed description of each analysis methodology from Chapter 3: Research Approach and Methodology is in the parenthesis following the analysis name.

Co-precipitation and Preformed jar tests (3.2.1)

To determine the removal efficiency differences for systems limited to adsorption and those where the precipitates form in the presence of fluoride and the LMW organic acids, the preformed precipitate (PRE) and co-precipitation (CPT) jar test experimental methods were used. Unless otherwise specified, all tests contain a background synthetic water matrix comprised of 3 meq/L alkalinity and 3 meq/L hardness and an ionic strength of 0.008 M. Jar test experiments were conducted at a target pH of 6.5 and only adjusted at the beginning of an experiment using 1.0 N HCl and 1.0 N NaOH unless indicated differently in the text or on the figure. Alum stock concentrations of 11.63 mMol and 23.26 mMol alum ($Al_2(SO_4)_3$*$12.8H_2O$) were used to dose the jars with coagulant at the beginning of the experiment.

X-Ray Diffraction Spectroscopy (XRD) (3.2.4)

XRD is an extremely useful analysis when analyzing crystalline samples as it is capable of identifying the solid and providing crystalline spacing in well formed materials or size or crystalline particles in those starting to form crystalline layers. In this

research XRD was used to test the amorphous phase of the precipitates at the conclusion of the experiment and solids handling.

5.4 Results and Discussion

Initial jar tests run to test the propensity of the LMW organics to bind to precipitating aluminum hydroxide surfaces during floc formation revealed that only pyromellitic acid experienced significant removal (Figure 5-2). LMW carboxylic acid adsorption on metal (hydr)oxides is typically classified into two distinct modes. The first is inner-sphere complexation that is characterized by strong direct bonding, similar to Structures C and D in Figure 5-1. The second is outer-sphere complexation in which the constituent is held by a weak electrostatic attraction or hydrogen bonding, as shown in Figure 5-1 Structures A and B. Salicylic and pyromellitic acids are cited as forming inner-sphere complexes with alumina and iron oxide surfaces (Johnson et al. 2005; Ainsworth et al. 1998; Phambu 2002; Pommerenk and Schafran 2005); yet, despite the same inner-sphere associations, pyromellitic acid achieves more removal than salicylic acid in an alum coagulation system.

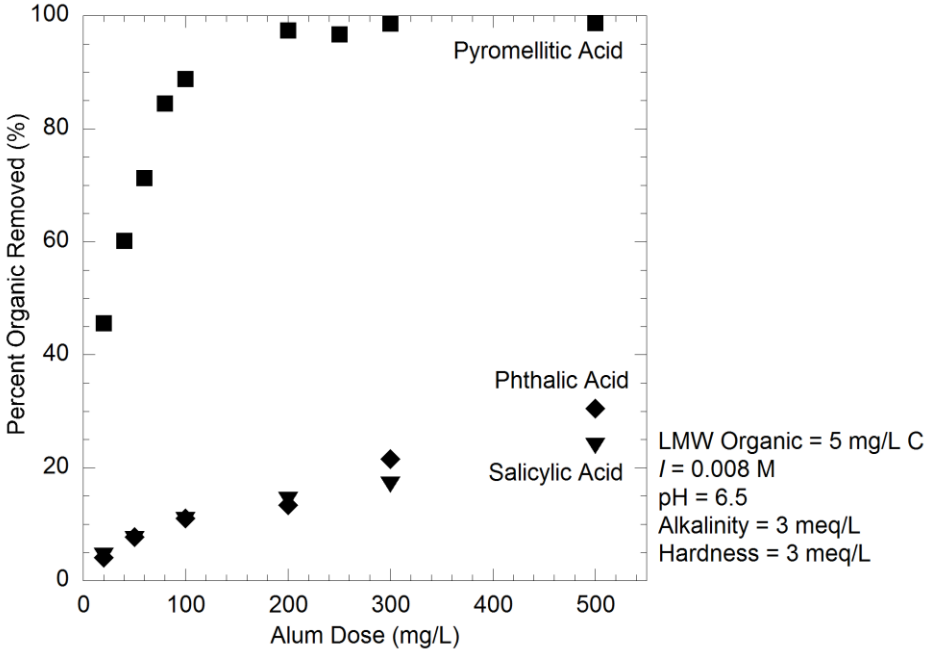

Figure 5-2: Removal of LMW organics by alum coagulation

Looking at salicylic removal more closely shows that even though only 32% of the total applied aluminum precipitated at the lower pH values, the greatest removals of LMW organics occurred in this lowest range with a maximum of 20% removed (q = 1.6885 mg C/mg Al) (Figure 5-3). Similarly, Ainsworth et al. (1998) saw decreasing adsorption of salicylic acid onto δ-Al_2O_3 with increasing pH; yet, they observed that these adsorption edges are concentration dependent. In this work, considerably less aluminum was used, resulting in a salicylic acid to aluminum molar ratio of 0.596:1 (C:Al) instead of the $10^{-5.58}$:1 (C:Al) ratio used to achieve 80% removal at pH 4 by Ainsworth et al. (1998). Their study determined a maximum adsorption density of salicylate of approximately 0.66 molecules/nm^2 at pH 5.8, lower than the Kummert and Stumm's (1980) reported maximum density of 1.3 molecules/nm^2 for adsorption onto δ-

Al_2O_3. Using the surface area determined for aluminum precipitates formed from 200 mg/L alum at pH 6.6 (see Table 4-2) and the adsorption density of salicylic at pH 6.6 (0.0332 mg C/mg Al, from Figure 5-2), an adsorbed density of 1.28 molecules/nm^2 is calculated. The removal density value calculated by this research suggests that closely packed surface adsorption is occurring in the alum precipitation system and it is achieving maximum removal considering the initial C:Al molar ratio. These highly packed surfaces at pH 4-6 are reported to be comprised of a mixture of monodentate and bidentate complexes with the carboxylate oxygen as well as outer sphere adsorption onto aluminum oxides (Ainsworth et al. 1998).

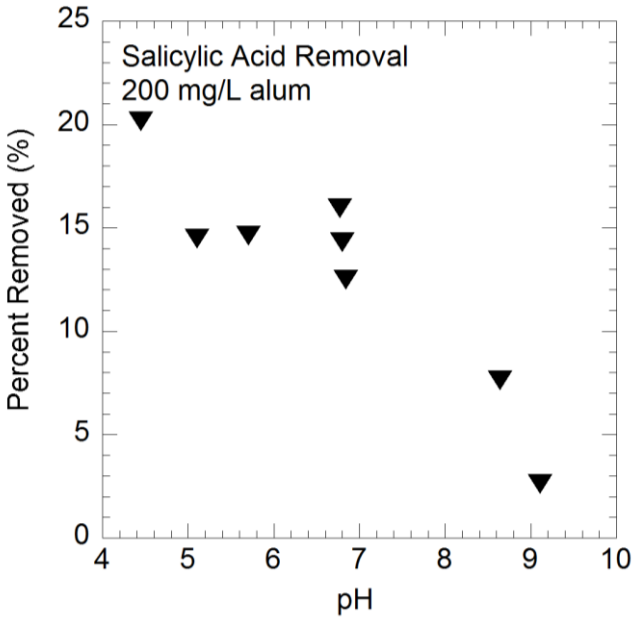

Figure 5-3: pH varied salicylic removal. 200 mg/L alum, initial concentrations of salicylic acid=5 mg/L C.

Phthalic acid, while achieving similar removal efficiency as salicylic acid, is reported to form slightly different bonds with oxide surfaces. A fully deprotonated outer-

sphere complex dominates adsorption of phthalic acid onto hematite at near-neutral pH (Hwang et al. 2007). Two fully deprotonated inner-sphere complexes increase in importance at low pH and can shift with relative importance as surface coverage increases. The contribution of the binuclear bidentate inner-sphere complexes can dominate at these low pH values, but decreased with increasing pH with mostly deprotonated outer-sphere complexes at near neutral pH (Hwang et al. 2007). These results are corroborated by the Persson et al (1998) study, which concluded that even though models predict outer-sphere complexes dominate for boehmite and aged γ-Al_2O_3, infrared spectroscopy data show a number of inner-sphere complexes still exist. Since the amorphous precipitates in this research most likely resemble the structure of boehmite (concluded from Chapter 4), phthalic acid adsorption is most likely dominated by outer-sphere bonds at pH 6.6. Considering the same specific surface area used for salicylic acid density calculations (200 mg/L alum, 186 m^2/g), phthalic acid reaches a surface density of 1.67 molecules/nm^2 on the alum precipitates formed at 200 mg/L alum.

Multicarboxylic ligands have shown high adsorption affinities for alumina (Kaspryk-Hordern 2004). Similarly, in this study, pyromellitic acid is the only chosen LMW organic to achieve over 40% removal with alum doses in the range of 20-500 mg/L alum (pH 6.6). This increased removal does not necessarily translate to surface groups involving more than two carboxylic groups, but more likely increased affinity due to the changing acidity of the organic. A 5.55 molecules/nm^2 density is achieved at a 200 mg/L alum coagulant dose assuming the same 186 m^2/g surface area as in the salicylic acid density calculations.

This calculation, however, is flawed for these molecules containing high molar concentrations of carbon. The distributions translate the removal of carbon to moles of the LMW organic without regard for the actual size of the molecule. Despite the

shortcoming, it provides a metric of comparison between organics on a molecule basis. According to the removal densities, the removal of the organics was highly dependent on the functional groups on the molecules rather than inner vs. outer sphere coordination. Increased removal corresponded to increased number of carboxylic groups, a result in agreement with Evanko and Dzombak's (1998) assessment of organic adsorption mechanism to goethite.

The results in Chapter 4 suggested that fluoride co-precipitated with aluminum and acted as a substitute for hydroxyl ions in the hydroxide lattice. This substitution would not disrupt the overall surface charge of the precipitate as long as hydroxide ions dominate the surface layer, and would therefore not have a significant effect on outer-sphere associations of the LMW organics with the precipitate. When fluoride was present, the removal of salicylic and phthalic acids were only slightly reduced despite salicylic acid primarily containing inner-sphere bonds and phthalic acids mostly outer-sphere (Figure 5-4). For these two systems, a maximum of a 6% decrease in salicylic removal and a maximum of 10% decrease in phthalic acid removal occur when fluoride is present at 5 mg/L. Pyromellitic acid exhibits a stronger affinity for removal, and the disruption of removal efficiency by fluoride is likely more complicated. At alum doses less than 200 mg/L, pyromellitic acid removal decreases by 10-30% when fluoride is present, yet over 90% of the added aluminum precipitated for the entire range of alum doses except for the 20 mg/L alum dose (65% aluminum precipitated).

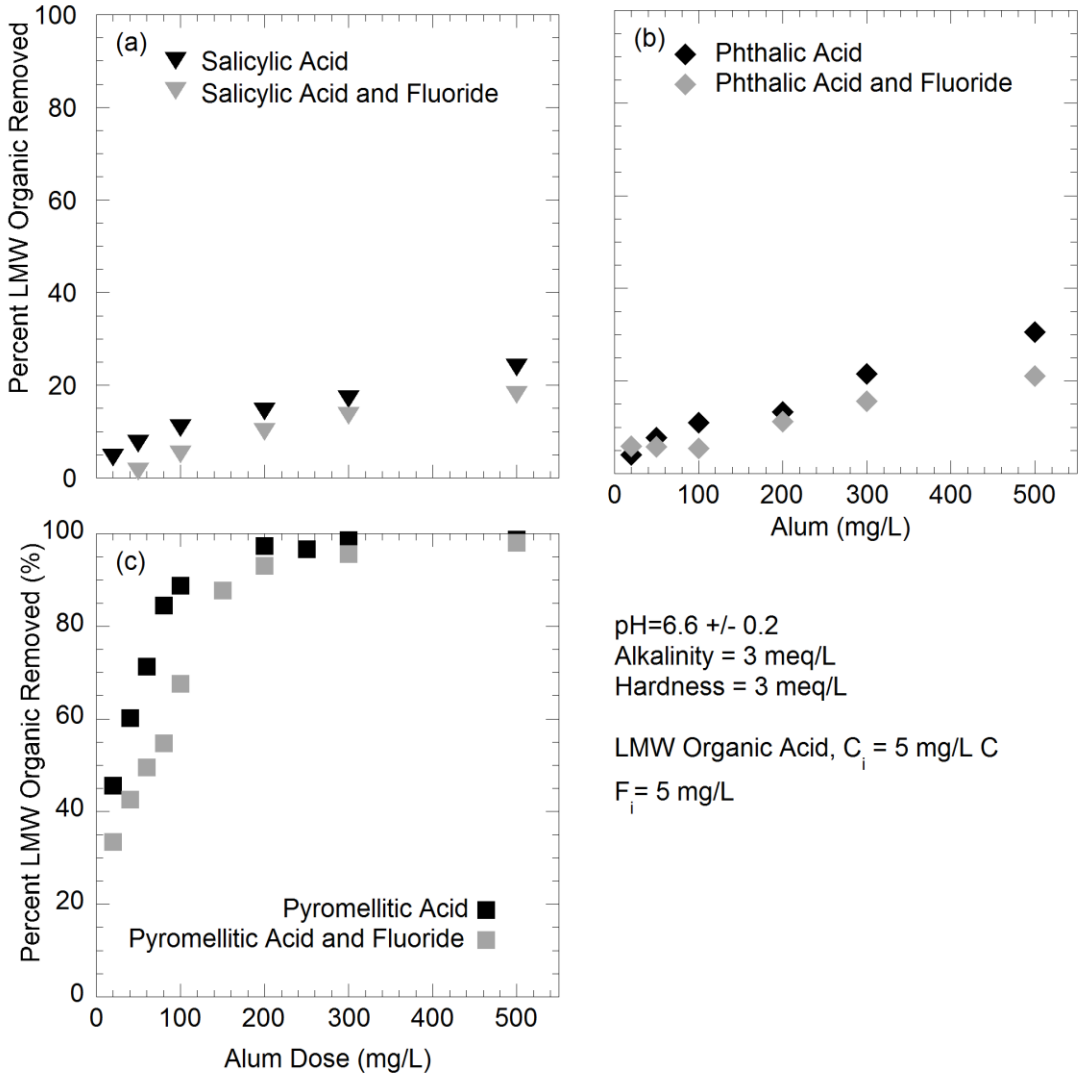

Figure 5-4: Impact of fluoride on removal of LMW organics by alum coagulation.

For the same experiments containing both LMW organics and fluoride, only pyromellitic acid significantly impacts fluoride removal (Figure 5-5). Phthalic and salicylic acid impact fluoride removal at doses less than 200 mg/L alum where both acids reduced fluoride removal by approximately 10% in this lower dose range. Similarly,

pyromellitic acid reduced fluoride removal when alum doses are less than 200 mg/L alum, but to a greater extent with a reduction of at least 20% in this range. Above 200 mg/L alum dose, competition with fluoride is minimal with little impact on fluoride removal observed.

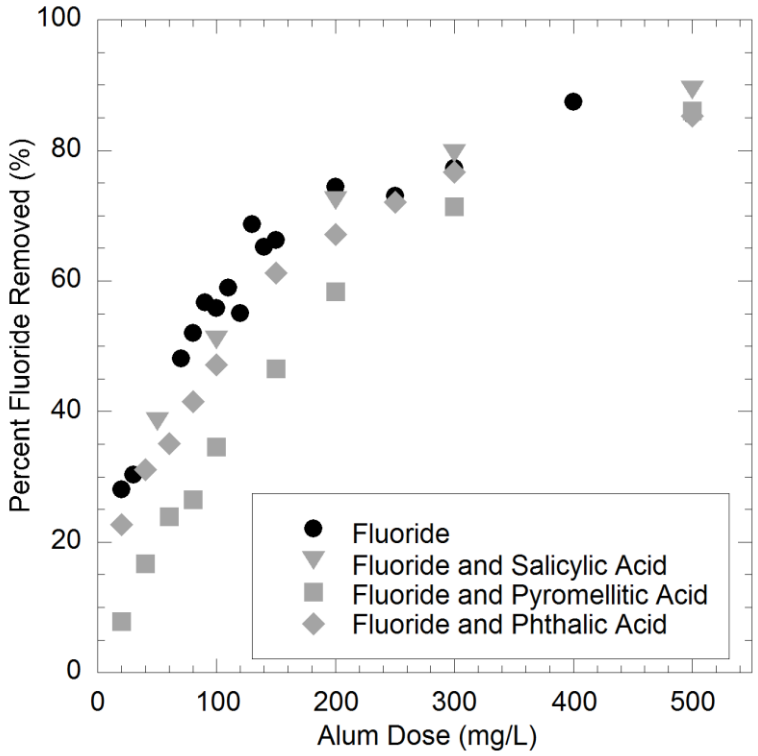

Figure 5-5: Impact of 5 mg/L C from LMW organics on fluoride removal: Alum doses varied and pH 6.6.

Even though the possible surface complexes for phthalic acid and pyromellitic acid would be identical (given the adjacent carboxylic groups as shown in Table 5-1), the results from Figure 5-4 and Figure 5-5 suggest that pyromellitic acid forms more inner-sphere complexes with the aluminum precipitate than does phthalic acid. The disruption

in the aluminum precipitate caused by fluoride incorporation into the solid would not interfere with electrostatic, outer-sphere associations with the solid since the overall charge would be the same; but it does change the arrangement of aluminum and hydroxide bonds, potentially interfering with inner-sphere complexes; this concept is illustrated in Figure 5-6. In Figure 5-6a, pyromellitic acid was able to bond to available sites on the surface when fluoride was not present, but the incorporation of fluoride into the structure and at surface sites decreased the density of pyromellitic acid removal, as shown in Figure 5-6b. The density of pyromellitic acid removed when fluoride and pyromellitic acid are present decreases to 3.16 molecules/nm^2 (surface area assumed the same as 200 mg/L alum CPT 5 mg/L fluoride, 294 m^2/g, from Table 4-2).

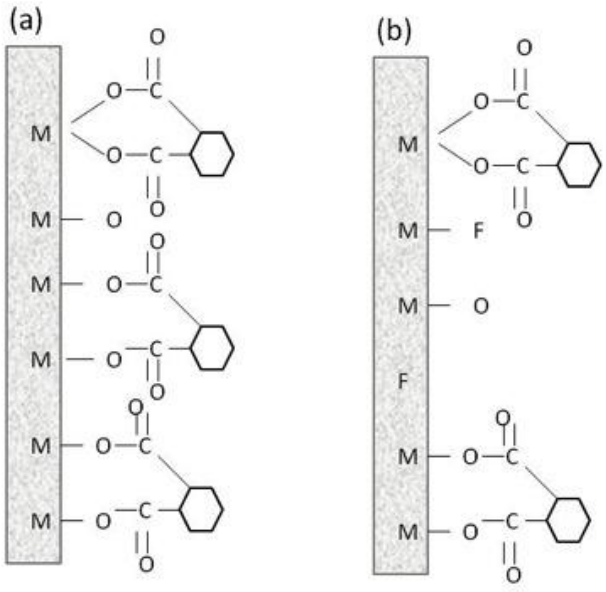

Figure 5-6: Potential inner-sphere disruptions caused by fluoride precipitating with alum: Comparing (a) Proposed inner-sphere bonds for pyromellitic acid during alum coagulation and (b) proposed inner-sphere bonds for pyromellitic acid during alum coagulation when fluoride is present.

The proposed complexes shown in Figure 5-6 largely address adsorption to the surface. As aluminum precipitates and flocs form during coagulation and flocculation, pyromellitic acid can occupy more surface as the flocs grow, becoming enmeshed in the flocs. This model of aluminum complexation to soluble organics followed by precipitation is typically attributed to complex organics (Huang and Shiu 1996; Dempsey et al. 1985; Semmens and Ayers 1985), but is applicable to pyromellitic acid as well. To test the competition between fluoride and pyromellitic acid further, preformed tests were conducted as outlined in the research approach and methodology in Chapter 3.2.1. Figure 5-7 compares removal efficiencies for fluoride (CPT and PRE) as presented in Chapter 4, pyromellitic acid (CPT and PRE), and fluoride and pyromellitic acid (CPT and PRE). In these experiments initial concentrations were 5 mg/L F and 5 mg/L C (pyromellitic acid) when included in the experiment. The experiments were conducted in an attempt to understand the competition between fluoride and pyromellitic acid and to further understand the binding mechanisms of pyromellitic acid.

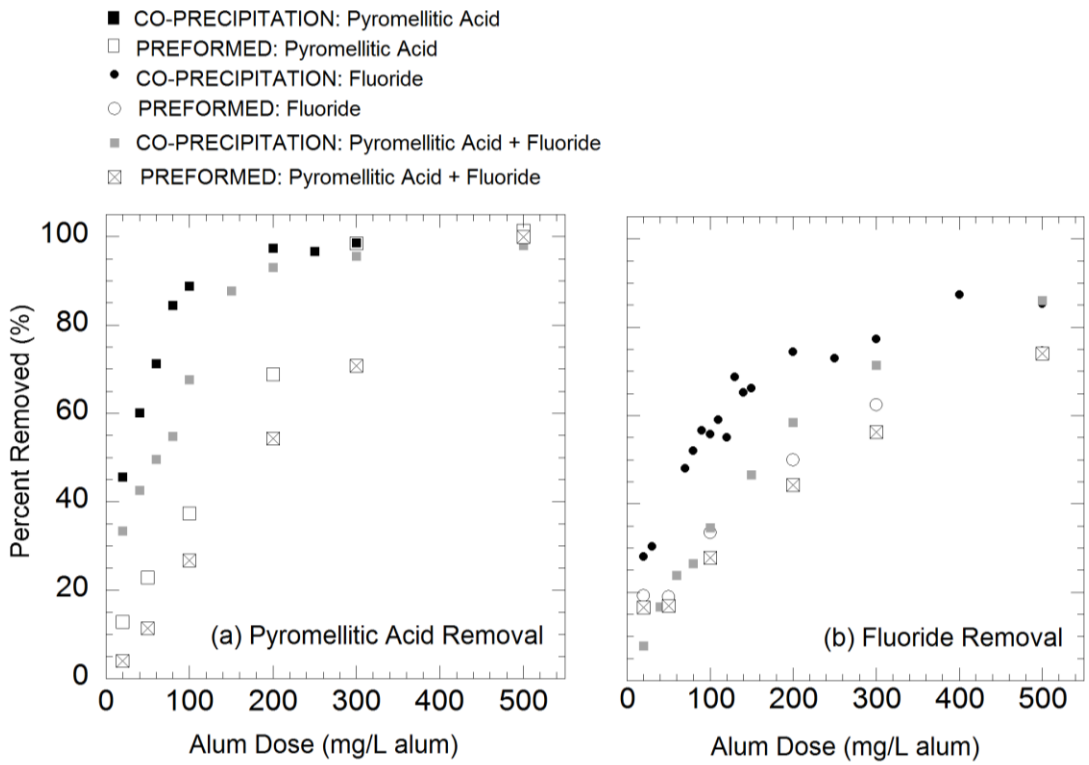

Figure 5-7: Effects of the precipitation process on removal at pH 6.6 and varying alum coagulant doses: Comparing CPT and PRE systems for pyromellitic acid and fluoride removal.

The results in Figure 5-7a-b clearly show that co-precipitation is incorporating significant amounts of each ligand. The decrease in ligand removed when single ligand systems of CPT and PRE tests are conducted confirms the importance of precipitation in removal. For example, an alum dose of 100 mg/L alum removed 60% less pyromellitic acid when limited to adsorption only in the PRE system (Figure 5-7a). Similarly, fluoride removal decreased by 25% when limited to adsorption only, as shown in Figure 5-7b. Comparing now CPT in single and dual ligand systems, the addition of a second ligand

reduced the removal of each ligand through the co-precipitation process. At high alum doses, the differences between removal with and without the presence of a second ligand diminished due to the presence of excess aluminum oxide precipitate. However, fluoride removal appears to plateau below 100% removal at doses greater than 400 mg/L alum in all systems, perhaps due to aqueous complexation. Similar results are evident for the PRE experimental results, which show that both ligands are competing for adsorption sites and adsorption removal is greater in the absence of a second ligand. At all alum doses tested, fluoride removed from the two PRE systems is in close agreement. This suggests that fluoride binds more strongly to the aluminum hydroxide surface when limited to adsorption competition; however, the close agreement in fluoride removal for CPT in the presence of pyromellitic acid and the two PRE experiments at alum doses ≤ 100 mg/L alum suggests that pyromellitic is preferentially incorporated into the co-precipitate when aluminum is limited in the system.

If pyromellitic acid forms a co-precipitate with aluminum, it is expected that the precipitate at the end of settling would still remain amorphous. XRD spectroscopy of the formed precipitates in Figure 5-8a-d all contained no peaks, confirming amorphous precipitates are formed once background peaks due to the quartz holder are removed. Aged crystalline inhibition is reported when analyzing precipitates formed in the presence of organics with multiple carboxylic functional groups after aging for over one month (Violante and Hwang 1985), further supporting the idea of a strong aqueous aluminum-organic complex preceding precipitation of the organic with aluminum. The amorphous properties of the co-precipitated pyromellitic solids after 1 hr 10 min were confirmed with a 12-hour x-ray scan of the precipitates to ensure no pseudo-oxides formed (Figure 5-9).

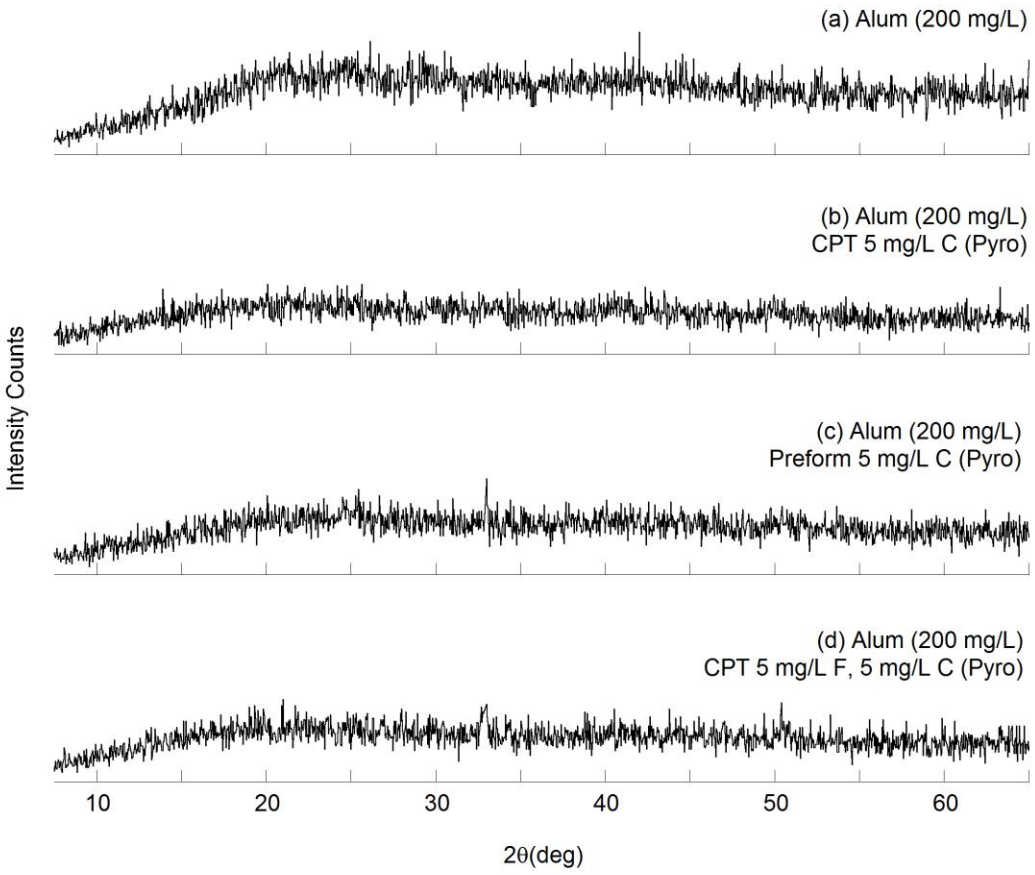

Figure 5-8: X-ray diffraction patterns for aluminum precipitates formed during CPT and PRE experiments with pyromellitic acid.

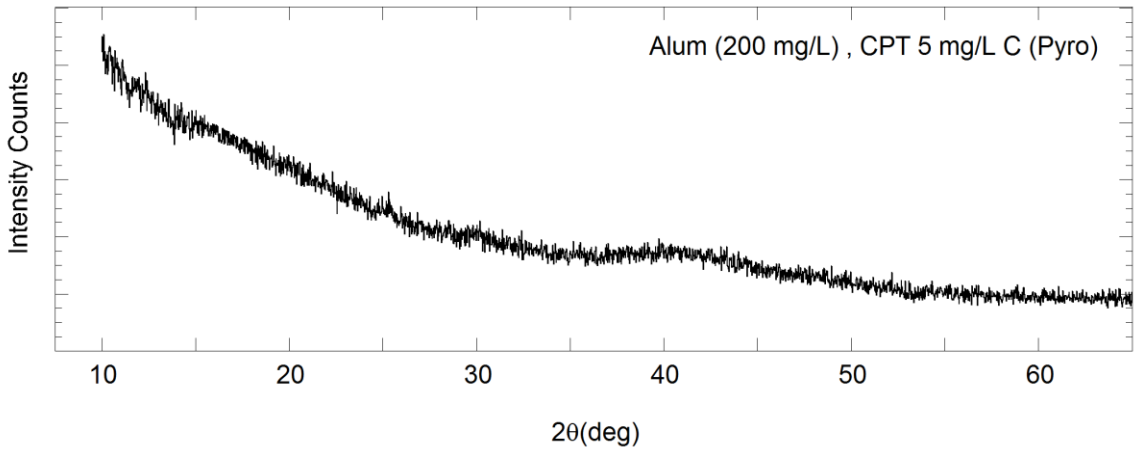

Figure 5-9: 12-hour x-ray diffraction scan of aluminum precipitates formed in the presence of 5 mg/L C pyromellitic acid, confirming amorphous precipitates.

The competition observed in Figure 5-7 between fluoride and pyromellitic acid in the CPT system was tested further using a series of CPT experiments with varying influent ligand doses at pH 6.6. The experiments were repeated with 100 mg/L and 200 mg/L alum doses to elucidate competition. First, consider the system where initial fluoride concentrations were varied from 1-10 mg/L and compared to systems also containing 5 mg/L C from pyromellitic acid, Figure 5-10. The experiments were conducted for 100 mg/L alum and 200 mg/L alum. Even though removal in these experiments was comprised of adsorption and co-precipitation, the results are presented as isotherms in which the mass of ligand removed per mass of adsorbent precipitated is plotted versus the final concentration of the ligand (i.e. the apparent equilibrium concentration). From Figure 5-10a and Figure 5-10b, it is clear that the isotherms are similar in the absence and presence of 5 mg/L C pyromellitic acid at these alum coagulation doses. The discrepancy between competition for removal in Figure 5-10a-b and Figure 5-7 is due to the normalization of removal by mass aluminum precipitated. To

compare the impact of the variable fluoride dose on pyromellitic acid removal, adsorption densities are compared in Figure 5-10c. The relationship between the fluoride and pyromellitic acid adsorption densities appears constant throughout the experimental range for the higher alum dose of 200 mg/L. However, the data for the 100 mg/L alum dose showed a decreasing trend in the adsorption density for pyromellitic acid as fluoride densities increased. This suggests that fluoride outcompetes pyromellitic acid for adsorption/co-precipitation binding sites on amass removed per mass aluminum precipitated basis.

Now, focusing on Figure 5-11, initial pyromellitic concentrations were varied from 1-10 mg/L and compared to systems also containing 5 mg/L fluoride. When the pyromellitic acid concentration was varied, the presence of 5 mg/L fluoride affected removal over the entire pyromellitic acid range (Figure 5-11a-b). In contrast to Figure 5-10, increasing pyromellitic acid concentrations did not affect the fluoride adsorption density for either alum dose so the adsorption of pyromellitic acid did not affect the capacity of the aluminum hydroxide for fluoride (Figure 5-11c).

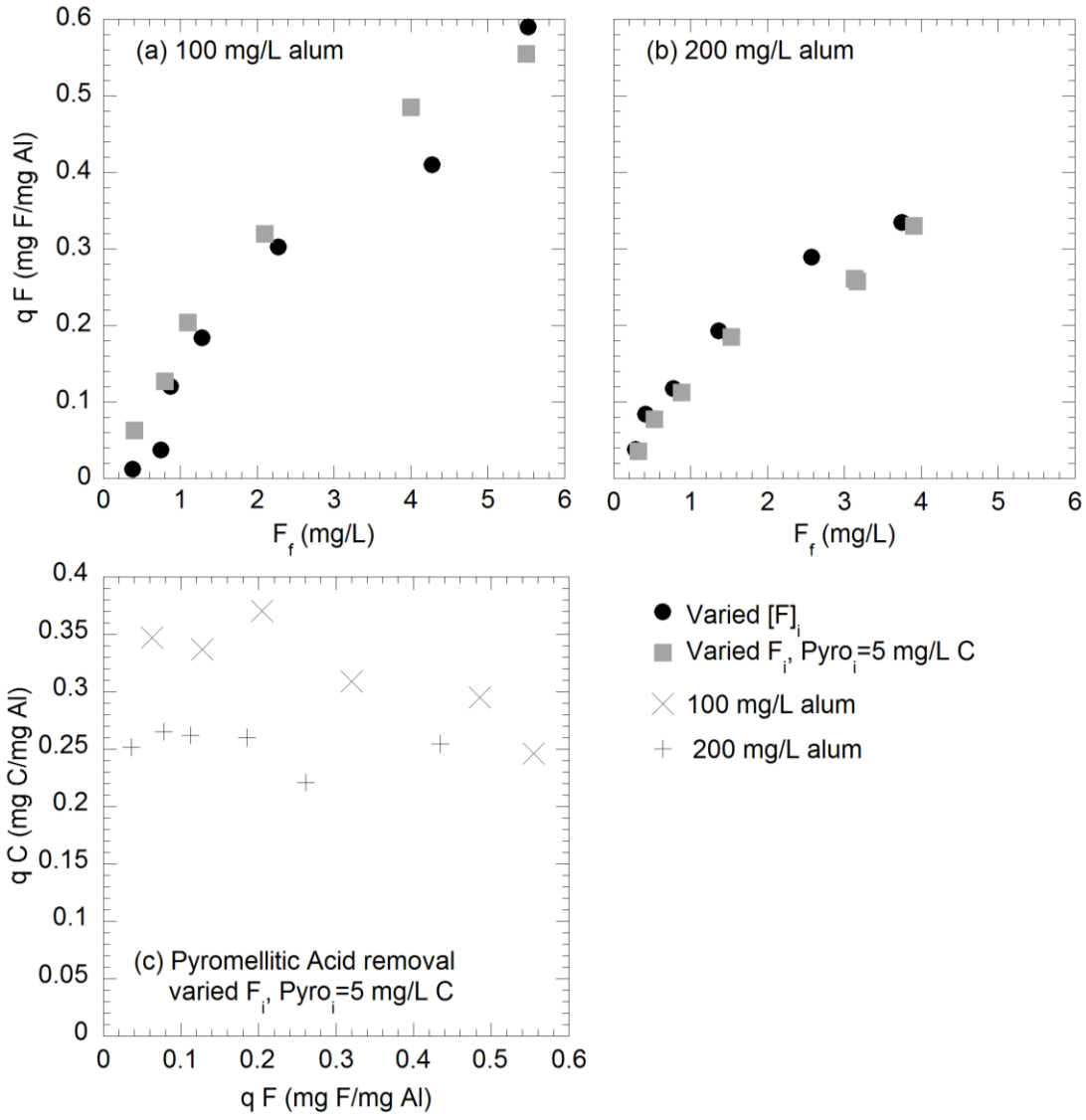

Figure 5-10: Comparison of pyromellitic acid impacts on fluoride removal at varying doses of influent fluoride concentrations: (a) fluoride removal density with 100 mg/L alum (b) fluoride removal density 200 mg/L alum. (c) Comparison of removal densities from varied fluoride on pyromellitic acid removal densities at 100 and 200 mg/L alum.

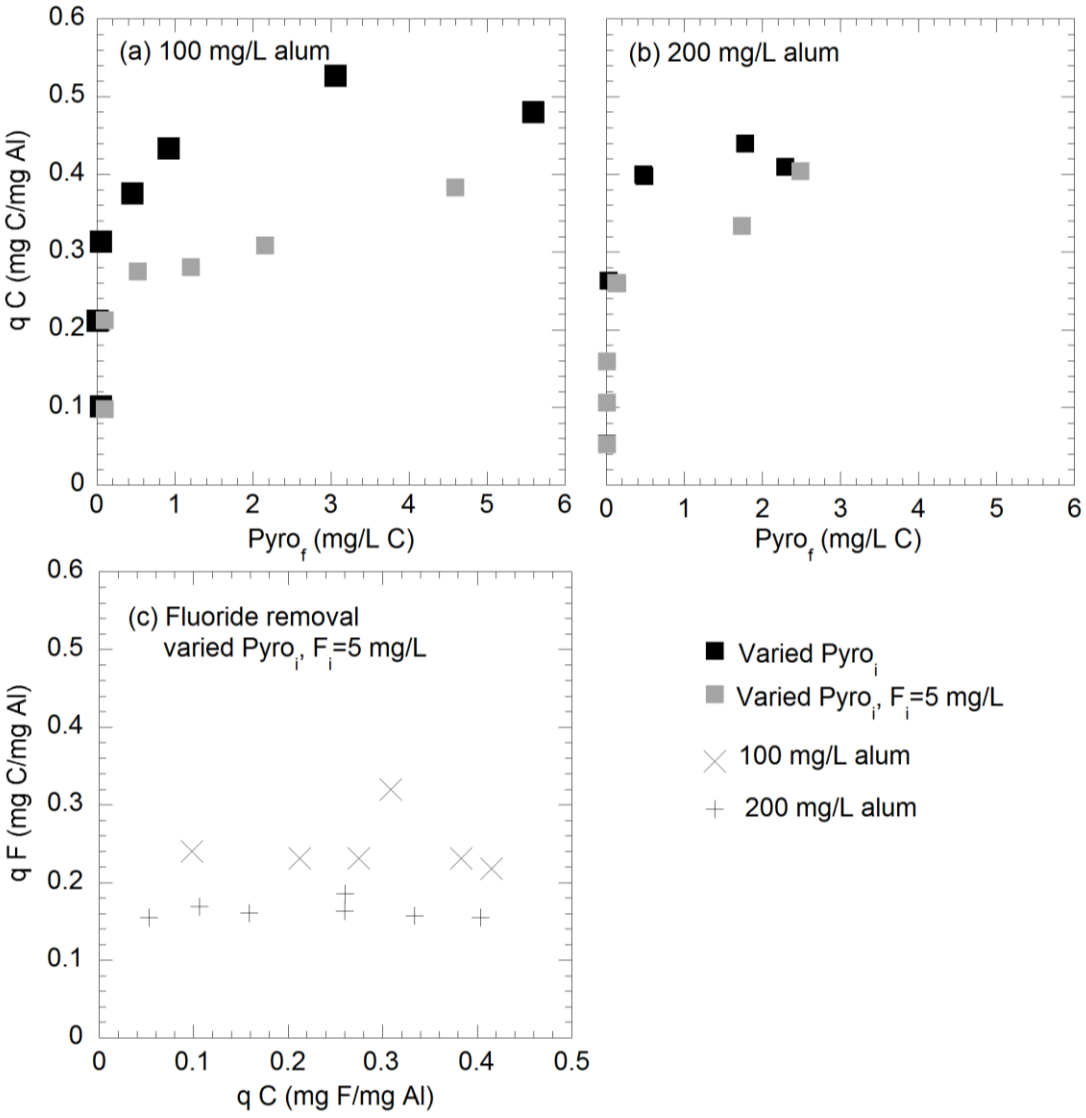

Figure 5-11: Comparison of fluoride impacts on pyromellitic acid removal at varying doses of influent pyromellitic acid concentrations: (a) organic removal density with 100 mg/L alum (b) organic removal density 200 mg/L alum. (c) Comparison of removal densities from varied pyromellitic acid on fluoride removal densities at 100 and 200 mg/L alum

The results from Figure 5-10 and Figure 5-11 indicate that fluoride is preferentially removed over pyromellitic acid. Drawing from the analysis of CPT and PRE results for pyromellitic acid, pyromellitic acid is bonded through inner-sphere complexes even when pyromellitic acid concentrations are increased. The fluoride incorporation and disruption of the precipitate structure was in competition with pyromellitic acid removal via co-precipitation or adsorption. When removal was normalized by mass aluminum precipitated, fluoride appeared to have preferential removal by alum CPT than pyromellitic acid.

5.5 CONCLUSIONS

The LMW organic acids chosen for this study are commonly found in soil and aquatic environments and contain basic functional groups of interest in modeling NOM removal. Even though pyromellitic acid and phthalic acid have similar structures and protonation of their ortho-carboxylic functional groups at pH 6.6, pyromellitic acid exhibits greater removal affinities when treated by alum coagulation. Removal of the LMW organics was highly dependent on the number of carboxylic groups and not the inner- or outer-sphere coordination. The coordination with aluminum was important when pyromellitic acid was tested in more depth to explore the co-precipitation mechanisms in dual ligand systems. The difference in inner versus outer-sphere complexation for pyromellitic acid resulted in a greater impact of fluoride on removal efficiencies of pyromellitic acid and pyromellitic acid on fluoride removal. Neither salicylic acid nor phthalic acid greatly influenced fluoride removal throughout the range of alum doses used for these experiments. The lack of impact on removal of either salicylic acid or phthalic acid suggests that neither of these molecules are significantly

co-precipitated and their bonding mechanisms during adsorption is different from fluoride.

A focused analysis on the competition between pyromellitic acid and fluoride concluded that in a CPT system, removals of both ligands are negatively affected by the presence of the other. In a PRE system, fluoride negatively impacts the removal of pyromellitic acid and is significantly affected by pyromellitic acid when at similar concentrations. For both fluoride and pyromellitic acid, the move from a CPT system to one that only considers adsorption greatly reduces removal. The reduction in pyromellitic acid removal between from CPT to PRE systems containing only the organic acid indicates that the aqueous complexes formed during the precipitation of aluminum are playing a significant role in pyromellitic acid removal. Similarly, there was a significant impact on fluoride removal when CPT and PRE are compared. The reduction in fluoride removal by pyromellitic acid in a dual ligand CPT system to that of a PRE fluoride only system suggests that pyromellitic acid was preferentially co-precipitated. As a result, the use of pyromellitic acid as a NOM surrogate seems more appropriate than salicylic or phthalic acid, which have both been proposed in the past (Vance et al. 1996).

The competition between fluoride and pyromellitic acid was further investigated in ligand dose tests and evaluated as mass removed per mass aluminum precipitated. Pyromellitic acid, when maintained at 5 mg/L C and increased from 1-10 mg/L C in the presence of fluoride, did not impact removal of fluoride. Fluoride, however, reduced pyromellitic acid removal at influent concentrations of 5 mg/L F. The results suggest that ligand incorporation into the forming precipitate is highly dependent on dose and the formation of aqueous complexes prior to precipitation. The limited impacts of pyromellitic on fluoride removal when considered on a mass aluminum precipitated basis was a result of diminished precipitation in fluoride systems.

The competition between pyromellitic acid and fluoride for both removal and co-precipitation indicates pyromellitic is a viable model for complex NOM. Analyses comparing removals of pyromellitic acid in sole and dual ligand systems with fluoride to those using natural organic matter are used to assess the ability to predict natural organic matter removal with a surrogate, low molecular weight organic and are presented in the next chapter.

Chapter 6: Competition between fluoride and natural organic matter during alum coagulation

6.1 INTRODUCTION

A common drinking water treatment plant undergoes rapid mix, coagulation/flocculation, sedimentation, filtration, and disinfection prior to entering the distribution system. Flocculation, or the process of aggregating smaller particles to form larger ones, began as an essential component for particle removal but has grown to also treat NOM and other organic and inorganic constituents. As the removal of more water impurities and contaminants were attempted through the flocculation treatment scheme, the process no longer solely involved physically bringing particles together. This higher dosage treatment process involving chemical reactions to achieve removal of non-particle constituents is called enhanced coagulation. In areas with high levels of fluoride, the competition for co-precipitation with aluminum and adsorption onto formed precipitates creates a multi-ligand system competing for removal. The effect of a co-precipitating solid on fluoride and natural organic removal is considered in this research.

Particle removal occurs by destabilization through the addition of a destabilizing agent, also known as a coagulant. Aluminum based destabilization agents mainly use two different methods to achieve particle removal: (1) charge neutralization of negatively charged particles by the positively charged metal hydrolysis species followed by the aggregation of destabilized particles and (2) the formation of a metal precipitate and/or sweep flocculation (Benjamin and Lawler 2013; Shin et al. 2008). Higher concentrations of particles allow for sufficient particle interaction after destabilization and, therefore, can undergo treatment at lower chemical concentrations. Fewer particles will require the

formation of precipitates to facilitate interaction through development of a sweep floc (Shin et al. 2008).

The process of removing NOM by coagulation with aluminum salts involves aluminum hydrolysis, aluminum complexation with the organics, precipitation, and adsorption reactions on the precipitate (Edzwald and Van Benschoten 1990). A study by Amirtharajah and Mills (1982) provides details on the method of particle removal (i.e., charge neutralization, sweep coagulation, combination sweep and adsorption), but considers only colloidal materials and not the additional effects of NOM. Effective treatment for NOM removal often requires high concentrations of aluminum, labeling the NOM removal process as enhanced coagulation; that is, the process uses more aluminum or iron salts than would be required for particle removal alone to create additional adsorption sites (surface area of the precipitated metal hydroxide) for NOM removal.

Chlorine, a widely used disinfectant, reacts with residual NOM, creating halogenated disinfection by-products (DBPs). Some of these by-products, especially trihalomethanes (THMs) and haloacetic acids (HAAs), are potentially carcinogenic. In 1998, as part of the Disinfectant/Disinfectant By-Product (D/DBP) Rule, the EPA started requiring treatment of total organic carbon (TOC, a common measure of NOM) due to the growing concern over DBP formation. Treatment goals based on TOC removal are dictated by U.S. EPA regulations which require utilities to reduce the TOC by a fixed percentage according to a matrix dependent on the raw water TOC and alkalinity (Table 6-1).

Table 6-1: Required removal of total organic carbon by enhanced coagulation for systems using conventional treatment. (EPA 815-R-99-012 1999)

Source Water TOC (mg/L)	Source Water Alkalinity (mg/L as $CaCO_3$)		
	0-60	60-120	>120
2.0-4.0	35%	25%	15%
4.0-8.0	45%	35%	25%
>8.0	50%	40%	30%

The regulations allow water utilities an exception to this rule if they reach the "point of diminishing returns," defined as less than 0.3 mg/L TOC removal per 10 mg/L addition of coagulant (EPA 815-R-99-012 1999). As more constituents are present in the raw water, each imparting a chemical demand, more consideration must be paid to optimizing chemical doses. With competition from fluoride, this point of diminishing returns might be reached far earlier than if no fluoride were in the water; that is, the fluoride competes for sites with the organics, so that less TOC removal per addition of coagulant would occur.

Northwest Texas is an area where high levels of fluoride are present in the groundwater leading to the practice of blending surface and groundwater to meet regulations. Water quality reports for the City of Midland show not only high fluoride levels present, but also relatively high influent levels (>5 mg C/L) of NOM (measured as dissolved organic carbon, DOC). According to the City of Midland 2008 Water Quality Report,, NOM is reduced by only approximately 10%, far less than the drinking water regulations require (Water System Data Sheet 2009; EPA 815-R-99-012 1999). The results presented in Chapter 5 suggest that the presence of fluoride can reduce adsorption and/or co-precipitation of organic matter thus, poor removal of DOC is possibly the result of elevated fluoride levels in the influent water.

Many experiments previously conducted to look at single and dual ligand adsorption on preformed aluminum precipitates use aluminum chloride to form the precipitate (Pommerenk and Schafran 2005; Guan et al. 2007) and not alum, therefore not considering the background competition with sulfate. Bose and Reckhow (1998) used alum to create their preformed flocs for fractionated NOM adsorption studies. The organics were allowed 24 hrs to react with the precipitates after formation in the presence of a 1mM sodium bicarbonate and 0.1 M ionic strength background solution. The most acidic fractions of NOM studied were less effective at forming surface complexes with the preformed aluminum precipitates compared to the other NOM fractions tested. Acidic fractions of NOM include weak hydrophobic acids, humic acid, fulvic acid, and hydrophilic acids (Bose and Reckhow 1998).

The research presented in this chapter evaluated the impact of fluoride on NOM removal in systems most closely resembling a treatment plant. It was hypothesized that competition between fluoride and NOM would influence the structure of the precipitate formed and decrease the removal of fluoride, NOM and particles. Based on the results of Chapters 4 and 5, fluoride co-precipitation depends on the affinity of the NOM to out-compete and preferentially bond with aluminum. The research also attempted to test the ability of using LMW organic acids as models for NOM that could mimic the impact of fluoride on NOM removal.

6.2 RESEARCH APPROACH

The research approach was designed to gain an understanding of the physicochemical processes operative during the coagulation-flocculation treatment process in systems containing fluoride and NOM. The chemical interactions of interest in

this phase of research occurred after the systems were dosed with the aluminum sulfate coagulant. . A brief description of the purpose of each test is provided below. The corresponding sections of Chapter 3: Research Approach and Methodology that contain the details of the analytical methods are identified within the parentheses following the analysis headings for each experimental procedure.

Co-precipitation jar tests (3.2.1, 3.2.5)

To determine the removal efficiency of NOM and impacts of competition between fluoride and NOM during water treatment, co-precipitation (CPT) jar test experimental methods were used. Unless otherwise specified, all tests contain a background synthetic water matrix comprised of 3 meq/L alkalinity and 3 meq/L hardness. Jar test experiments were conducted at a target pH of 6.5 and only adjusted at the beginning of an experiment using 1.0 N HCl and either 1.0 N or 2.5 N NaOH unless otherwise indicated in the text or on the figure. Alum stock solutions of 11.63 mMol and 23.26 mMol alum were used to dose the jars with coagulant at the beginning of the experiment. The impacts of fluoride and NOM on particle removal were also examined in this research phase so residual turbidity was also measured using procedures described in Chapter 3.

Electrophoresis analysis of precipitates (3.2.5)

Electrostatic repulsion of highly charged surfaces can prevent charge destabilization and turbidity removal. To understand the impact of fluoride and NOM on turbidity removal through particle destabilization, the zeta potential of particles at the conclusion of selected jar test experiments were conducted.

Titrations performed during the precipitation process (3.2.2)

Titrations of the systems with single (fluoride or NOM) and dual ligand doses (fluoride and NOM) were conducted by starting at an acidic pH and titrating with NaOH until a pH > 10 was reached. Measurements of pH were recorded after the electrode measurement stabilized (approximately 0.5 min after each addition of strong base) after each base addition. It was hypothesized that differences in the amount of base required to achieve higher pH values, through the pH range of optimal precipitation, would signify a change in precipitate chemistry. A titration of the background water matrix was used as a baseline from which to compare the alum only and alum with the particles and ligands. Paired with the titrations were residual aluminum analyses that were conducted in a separate set of 50 mL vials containing equal concentrations of coagulant, ligands, and base added to represent a complete titration curve. Together, these experiments helped elucidate the influence of each ligand and ligand combination on aluminum solubility and precipitation.

Potententiometric titrations of NOM (3.2.3)

NOM is a large, complicated compound. This research used NOM isolates from Lake Austin. Isolation of NOM fractions are separated based on molecular size and hydrophobicity, but these do not provide characterization of the functional groups. Using titrations of the NOM with strong acid and strong base, the charge equivalents of the NOM molecule allow for inference of the dominant functional groups.

6.3 RESULTS AND DISCUSSION

To understand the impact fluoride has on current treatment operations, four sets of jar tests were conducted, incrementally adding new contaminant parameters to each set.

The first test looked at simple alum coagulation when only particles (Min-u-sil 5, silica particles with a broad particle size distribution with 98% by weight being less than 5 μm in diameter) are present. To compare the impact of each ligand on turbidity, comparisons of the coagulant dose required to reduce turbidity to below 2 NTU are useful (defined here as the critical coagulant dose). In Figure 6-1a, for turbidity removal with only particles present; a critical coagulant dose of 30 mg/L alum was necessary. When 5 mg/L fluoride is present, coagulant dosing of at least 50 mg/L is needed to reduce the turbidity to less than 2 NTU. As concluded in Chapter 4, fluoride does form aqueous complexes with aluminum and, at these lower coagulant doses, can have a major impact on aluminum hydroxide precipitation. NOM, on the other hand, reduced the critical coagulant dose of the system to 20 mg/L alum when only present with particles. Unlike fluoride, the aluminum-organic complexes help destabilize and promote nucleation/precipitation in the system. This effect of NOM reducing the critical coagulant dose for water treatment has been reported in the past (Edzwald 1993). When both fluoride and NOM were present, the critical coagulant dose to destabilize particles and achieve residual turbidity below 2 NTU was double that needed in the presence of NOM alone; however, the required dose was still less than the 50 mg/L alum dose required for adequate turbidity removal in the presence of only 5 mg/L fluoride.

At pH 6.5, several different removal mechanisms dominate over the coagulant dose range of 10 - 50 mg/L alum (Table 6-2). Using the alum destabilization diagram created by Amirtharajah and Mills (1982), the zones of removal associated with pH 6.5 and the applied alum doses are tabulated in Table 6-2. As the aluminum dose increases, destabilization occurs above 20 mg/L alum dose which is consistent with the reduction in turbidity observed at that dose. Above that level the mechanism begins to include sweep flocculation, and at alum doses above 40 mg/L the mechanism of sweep flocculation

dominates. Thus, based on the analysis of removal zones described by Amirtharajah and Mills (1982), the mechanism for removal in the particle only system with 50 mg/L alum dose is primarily sweep floc in the absence of fluoride or NOM.

Table 6-2: Dominant coagulation mechanism for particle only system (interpreted from Amirtharajah and Mills (1982))

Alum Dose mg/L (Log [Al] in Mol)	Dominant coagulation mechanism at pH 6.5
10 (-4.457)	Little destabilization
20 (-4.155)	Adsorption destabilization
30 (-3.980)	Boundary between adsorption destabilization and sweep coagulation
40 (-3.855)	Sweep coagulation
50 (-3.758)	Sweep coagulation

Both fluoride and NOM undergo different reactions with aluminum over this small range of alum dose which can influence the removal of turbidity. The range of possible chemical reactions involved in coagulation of NOM by aluminum coagulants are summarized into the following four broad categories by Edzwald (1993):

1. Complexation of fulvic and humic acid with aluminum:

$$nHA + xAl \leftrightarrow Al_xHA_n$$

2. Organic competition with OH^- for hydrolysis of aluminum:

$$nHA + xAl^{3+} + 3H_2O \leftrightarrow Al_x(OH)_{3x-n}HA_n$$

3. Direct precipitation of Al-NOM after complexation and charge neutralization:

$$nHA + xAl \leftrightarrow Al_xHA_{n(s)}$$

4. Adsorption onto amorphous particles formed after coagulant dosing:

$$nHA + \equiv Al(OH)_{3(s)} \leftrightarrow nHA \equiv Al(OH)_{3(s)}$$

At near neutral pH, NOM is proposed to complex with aluminum creating a higher chemical demand to achieve reaction #4 presented above (Edzwald 1993). Therefore, given that the turbidity removal increases at lower alum doses when NOM is present, direct precipitation of Al-NOM is likely (reaction #3).

At the low alum doses investigated in Figure 6-1, fluoride reduced turbidity removal (Figure 6-1a) most likely through formation of aqueous fluoro-aluminum complexes, altering the availability of aluminum to precipitate at these low alum doses. When both fluoride and NOM are present, competition between Al-NOM precipitation and fluoro-aluminum complexation was apparent as the coagulant dose required to achieve a residual turbidity less than 2 NTU was between the 50 mg/L dose required in the presence of fluoride and the 20 mg/L dose required in the presence of NOM. Thus, it appears that neither ligand solely dictates the aluminum speciation in these dual ligand systems at low alum doses.

In the dual ligand systems, NOM and fluoride both experience reduced removal (Figure 6-1b-c). Removal of organic matter in systems without fluoride was greater than 60% at alum doses of 20 mg/L and higher as shown in Figure 6-1b. The presence of fluoride decreased organic matter removal, requiring a dose of at least 50 mg/L alum to achieve the same 60% removal. Fluoride reduced NOM removal by over 10% for each applied alum dose.

Fluoride removal increased with increasing dose of alum, but removals of only 50 percent were achieved at a of 50 mg/L in the absence of NOM. In the presence of NOM, fluoride experienced a greater impact on removal compared to NOM in the dual ligand system (Figure 6-1c). Not until a coagulant dose of 30 mg/L alum was delivered was fluoride removal observed in the dual ligand system. While fluoride may dictate the

aqueous complexation in these lower alum dose ranges, NOM still promoted turbidity removal and achieved significant organic removal as well.

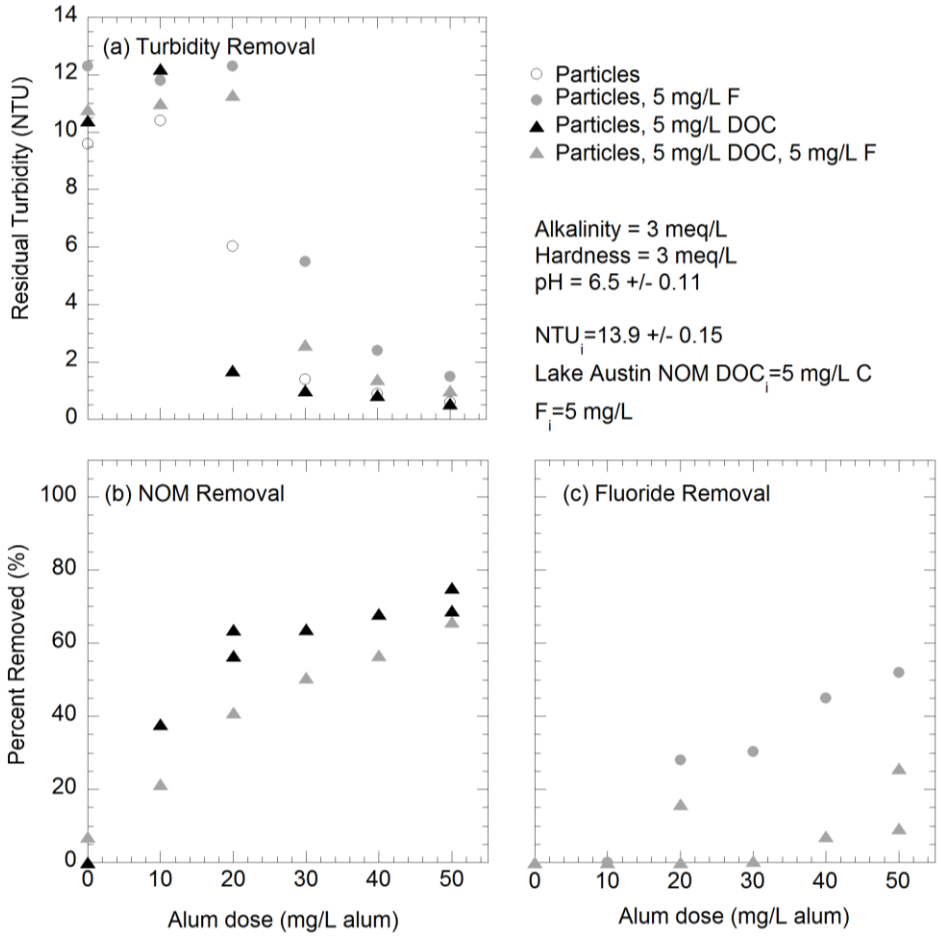

Figure 6-1: Critical coagulation dose evaluated for single and dual ligand systems (a) residual turbidity, (b) NOM removal, (c) fluoride removal.

These results suggest that, at low alum coagulant doses, co-precipitation with NOM is preferred over co-precipitation with fluoride. At 20 mg/L alum, turbidity removals vary greatly among the systems, while at 50 mg/L alum residuals of less than

2 NTU were achieved for all of the systems tested. The mechanism of particle removal at these two alum doses is evident from the residual aluminum concentrations, presented in Figure 6-2. At 20 mg/L alum (initial Al = 1.89 mg/L), where a large distribution in residual turbidity between the NOM only and the two systems containing fluoride existed, the residual aluminum concentrations are consistent with the observed high turbidity removal in the presence of NOM and the poor turbidity removal in the presence of 5 mg/L fluoride (Figure 6-2a). Only 40% of the aluminum precipitated in the two systems containing 5 mg/L fluoride which prevented turbidity removal. It should also be noted that, even with 40% of the solids precipitated, very little fluoride is removed as shown in Figure 6-1c.

In the experiments with 50 mg/L alum (initial Al = 4.71 mg/L), a greater difference in residual aluminum is observed for the systems containing fluoride (Figure 6-2b). At this alum dose, residual turbidity is less than 2 NTU for all systems. If only the coagulation regions presented by Amirtharajah and Mills (1982) are considered, then it is possible to consider the entire system as sweep floc; however, the residual aluminum concentrations (Figure 6-2b) contradict that conclusion. At 50 mg/L alum, residual aluminum concentrations are comparable to those observed for the 20 mg/L alum dose in the alum only and single ligand systems. If the residual aluminum concentration of approximately 0.7 mg/L is considered to be the amount of aluminum complexed by fluoride in aqueous solution, then it is expected that approximately 0.7 mg/L of residual aluminum would also be present in the dual, NOM and fluoride, system as well; however, the residual concentrations are less than those of the other three systems containing fluoride. The reduced residual aluminum concentration in the 50 mg/L alum, dual-ligand system supports the interpretation that an Al-NOM precipitate is the dominant removal mechanism for NOM at these low alum doses. The results also suggest that at higher

alum doses, there are sufficient aluminum hydroxide flocs present to reduce the impact of fluoride on NOM removal. Regardless, for both of the low alum doses tested, the presence of 5 mg/L fluoride led to fluoride concentrations that are in violation of the EPA SMCL for aluminum (0.05-0.2 mg/L Al).

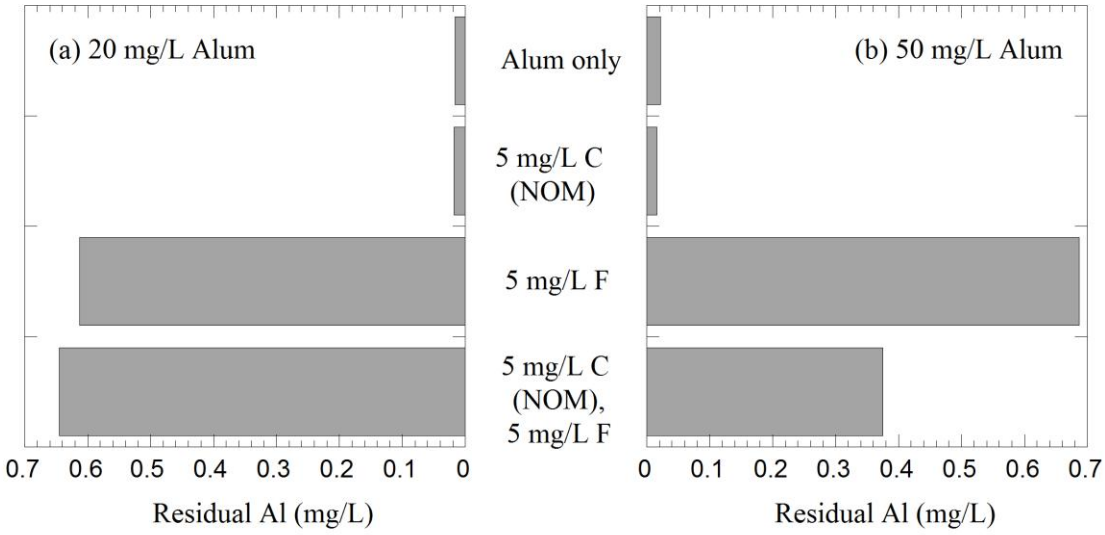

Figure 6-2: Residual aluminum for single and dual ligand systems at (a) 20 mg/L alum and (b) 50 mg/L alum.

Expanding the analysis to include higher alum doses, a more detailed analysis of the competition across a range of aluminum doses is possible (Figure 6-3). Considering first the impact of increased alum dose on NOM removal (Figure 6-3a), it is apparent that alum doses exceeding 200 mg/L alum reached the maximum possible removal of approximately 80% regardless of whether fluoride was present or not.

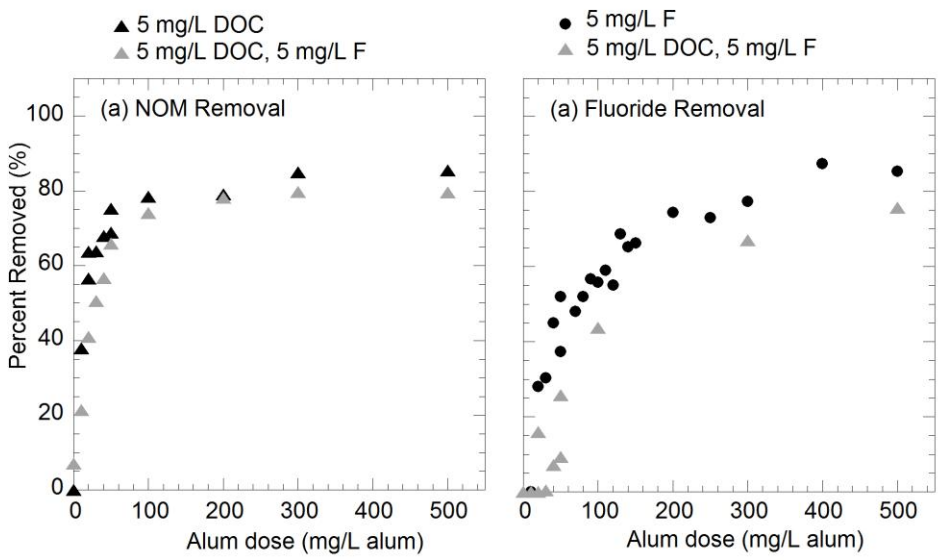

Figure 6-3: NOM and fluoride removal in single and dual ligand systems over a range of coagulant doses.

To properly interpret these results, it is helpful to consult the modified coagulation mechanism graphs developed by Dempsey et al. (1984). Dempsey et al. (1984) concluded that, for systems containing NOM, the mechanisms associated with coagulation are essentially the reverse of what Amirtharajah and Mills (1982) concluded for particle only systems. Dempsey et al. (1984) showed that in systems with 3.5 mg/L fulvic acid and a pH greater than 6, greater than 20% NOM removal begins at a log $[Al]_T$ of -4.2 M, consistent with results from this work. The highest aluminum concentration considered by Dempsey et al. (1984) is 8.53 mg/L Al (log -3.5 Mol), only slightly less than the 100 mg/L alum dose in this study. Using this mechanistic framework, it is plausible to

assume that both NOM systems, with and without fluoride, exhibit sweep flocculation as the alum concentration increases above 200 mg/L alum.

Fluoride removal, on the other hand, remains impacted across all alum doses considered in this research, as shown in Figure 6-3b. It was concluded in Chapter 4 that fluoride is replacing hydroxyl ions during precipitation, forming a co-precipitate in single ligand systems; but, dual ligand systems with pyromellitic created large competition for bonding with the precipitate. In Figure 6-3b, it is clear that fluoride removal decreased by approximately 15% in the system containing NOM across the entire applied range of alum. This sustained decrease in fluoride removal was most likely due to the change in surface charge NOM imparts on colloid and precipitate surfaces (O'Melia et al. 1999; Dentel 1988) that affects both fluoride adsorption and co-precipitation. At coagulant doses greater than 200 mg/L, the impacts of aqueous complexation with fluoride are severely reduced due to the availability of aluminum for fluoride complexation. After precipitates formed, the increased negative charge imparted by NOM on the surface of the precipitate at pH 6.6 was limiting the ability of fluoride to achieve further removal through adsorption.

Using particle electrophoresis on aluminum precipitates formed in a variety of different systems, the surface charge was calculated. The data in Figure 6-4 contain results for systems with and without initial turbidity to document the contributions of the Min-u-sil particles to the average particle surface charge. A 20 mg/L alum dose was selected for detailed analysis since this aluminum concentration experienced the largest variation in turbidity removal and only the NOM system achieved removals of turbidity lower than 2 NTU (refer to Figure 6-1a). In a study by Dentel (1988), decreased negative zeta potentials are correlated with improved floc strength and improved residual turbidity. To evaluate the zeta potential and the residual turbidity data gathered in this study, the

surface charges of each different solid phase were evaluated at pH 6.6 and are presented in Table 6-3 for comparison.

Table 6-3: Zeta potential for pH 6.5 and 20 mg/L alum

System Parameters	Zeta potential at pH 6.5
Alum only	27.3 +/- 7.5
Alum, 5 mg/L F	13.8 +/- 4.2
Alum, 5 mg/L C (NOM)	-12.6 +/- 12.4
Alum, 5 mg/L F, 5 mg/L C (NOM)	-20.7 +/- 6.5

The zeta potential at pH 6.5 decreased with each ligand addition to the system. In Figure 6-4a-d, the electrophoretic measurements from pH 4 to pH 9 were collected to understand the potential impact of precipitation on the average particle charge in the system. From Figure 6-4a, the addition of Minusil particles decreases the zeta potential of the aluminum precipitates slightly across the tested pH range. Measurements of surface charge were only collected for systems without particles when precipitates formed and were able to be analyzed, at pH greater than 6. Fluoride decreased the charge of the particles, as shown in Figure 6-4b, most likely due to changes to the precipitate structure identified in Chapter 4, altering the surface sites and characteristics of the precipitate. NOM imparted a large negative charge on the precipitates, as shown in Figure 6-4c, yet high turbidity removal is still achieved. The residual aluminum data presented earlier (Figure 6-2) suggest that an Al-NOM precipitate is possible at these low alum doses. The formation of this co-precipitate and the surface adsorption of NOM onto a formed aluminum hydroxide precipitate both potentially contribute to the lowered surface charge. The zeta potential for the dual ligand system is the lowest across the entire pH range

investigated (Figure 6-4d) suggesting that both fluoride and NOM impact the surface charge.

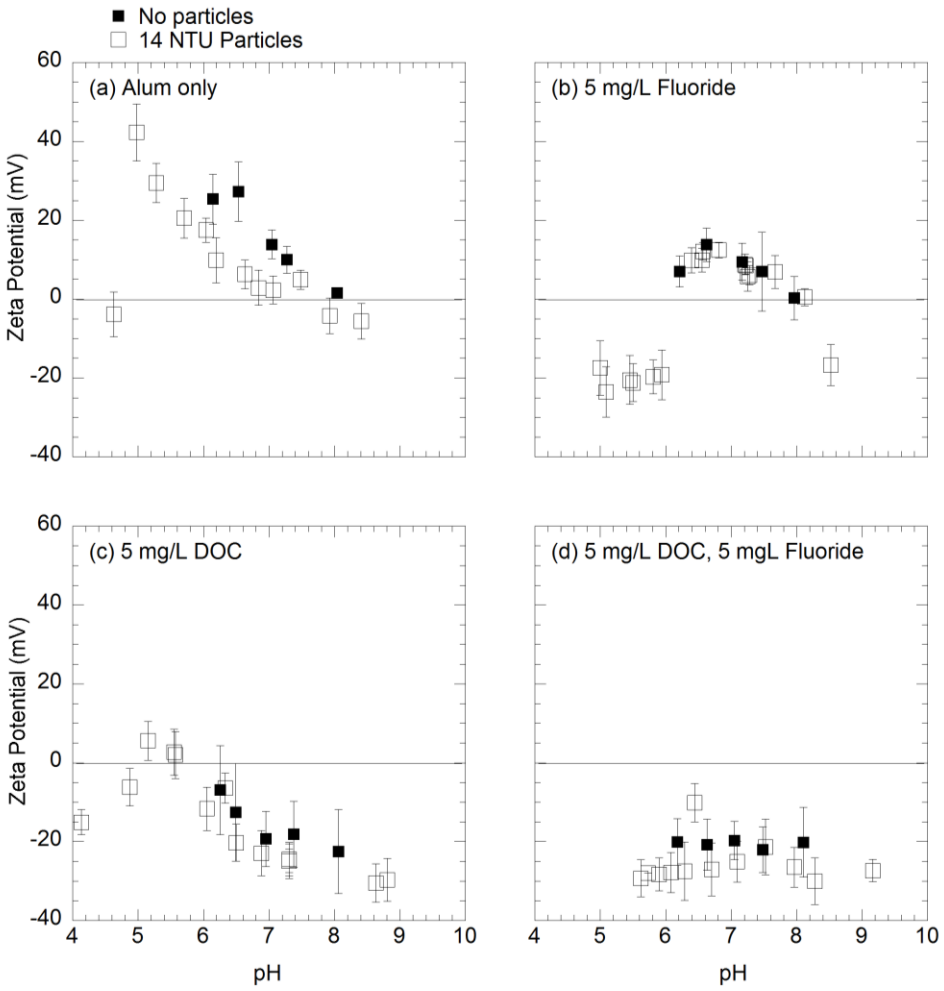

Figure 6-4: Electrophoresis measurements for 20 mg/L alum systems containing various combinations of ligands in single and dual ligand systems

The ability of the NOM to increase turbidity removal is most likely due to the large size of the NOM molecule, allowing for particles to overcome electrostatic repulsion. Referring back to the regions proposed by Dempsey et al. (1984), charge

destabilization occurs at this low applied aluminum concentration and near neutral pH, a removal mechanism for NOM in agreement with the zeta potential data and the ability to overcome electrostatic repulsion. The reduced fluoride removal in the presence of NOM that was observed across all alum doses tested is most likely due to the effect of the increased negative charge resulting from NOM attachment to the precipitate surface. A more in depth discussion of the zeta potential results in Figure 6-4 is presented later in this chapter following solubility analysis.

To further understand the nature of the negative charge imparted by NOM on the particle surface, a better characterization of the isolated Lake Austin NOM (fulvic acid) is necessary. Table 6-4 characterizes the raw water characteristics and the NOM chemistry by examining isolated fractions of the NOM, but it does not provide information regarding the dominant concentrations of functional groups.

Table 6-4: Raw water and NOM Extracts of Lake Austin water

Parameter	**Lake Austin**
Collection Date	7/22/09
pH	8.0
Alkalinity (mg $CaCO_3$/L)	164.5
$UV_{254\text{-nm}}$ (cm^{-1})	0.059
[DOC] (mg/L)	3.5
Turbidity (NTU)	4.5
$SUVA_{254}$ (L/mg-m)	1.76
HPOA (%)	35
HPOA $SUVA_{254}$ (L/mg-m)	2.9
TPIA (%)	20
TPIA $SUVA_{254}$ (L/mg-m)	1.7

Direct potentiometric titrations of 100 mg/L C solutions of the Lake Austin isolated NOM with a 0.10 M NaCl background electrolyte were performed and are plotted in Figure 6-5 to further elucidate the dominant properties of the Lake Austin NOM. The acidity due to carboxylic groups followed the definition of Ritchie and Perdue (2008) as the charge density changed from the very strong acidity region (those deprotonated at pH 3.0) to the strong acidity region (those protonated at pH 3.0 and deprotonated at pH 8.0). Phenolic functional groups were calculated as twice the difference in charge density between pH 8 and pH 10 (Ritchie and Perdue 2008). According to this definition, and using the average values measured for the forward and backward titrations, the charge density related to carboxylic groups is 29.76 +/- 0.7 meq/g-C and that related to phenolic groups is 3.34 +/- 0.8 meq/g-C. These results mean that Lake Austin NOM is dominated by carboxylic acidity; therefore, the NOM from this hydrophobic isolation is most likely more fulvic acid than humic acid.

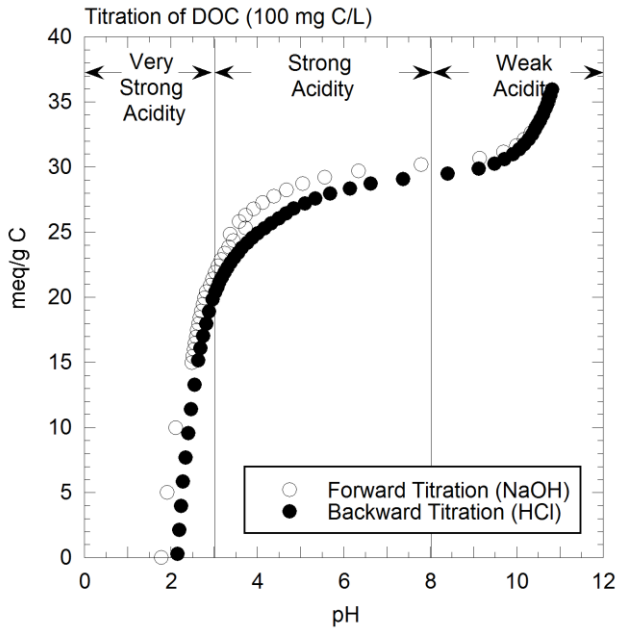

Figure 6-5: Potentiometric titrations of isolated Lake Austin NOM.

Fulvic acids are soluble at low pH while most humic acids are insoluble due to low carboxylic acid content (Pomes et al. 1999). Fulvic acids also have smaller molecular weights and higher charge densities, further confirming the increased negative charge from NOM on the particles formed by 20 mg/L alum.

To examine the alum coagulation/precipitation process of NOM and fluoride in more detail, titrations of the alum solutions containing NOM and fluoride were conducted. Comparison of these titration curves with those for alum alone and alum with fluoride (shown in Chapter 4) are instructive. For alum coagulant doses of 50 mg/L (Log $[Al]_T$ (M) = -3.758), the titration curves of these more complex solutions are expected to be identical to the curves for the alum only solution at acidic pH. Above a pH 4 where, according to Dempsey et al (1984), aluminum precipitation begins, a deviation from the alum only system is expected. If NOM is replacing OH^- ions during precipitation, then

small additions of base will result in larger incremental increases in pH than in the alum only system, similar to the results reported in Chapter 4 for the fluoride only system.

For the 50 mg/L alum dose, Figure 6-6a-b, regardless of initial ligand concentrations, an OH^- addition of 10 mMol was required to exceed the pH 4 barrier and to observe the expected separation in the curves. After exceeding pH 4, small additions of base do not result in the higher pH values observed in the fluoride only systems; instead, lower pH values were achieved. Even though NOM-Al precipitates are likely forming, NOM complexes with the aluminum ions are not replacing OH^- groups. Another form of co-precipitation is occurring.

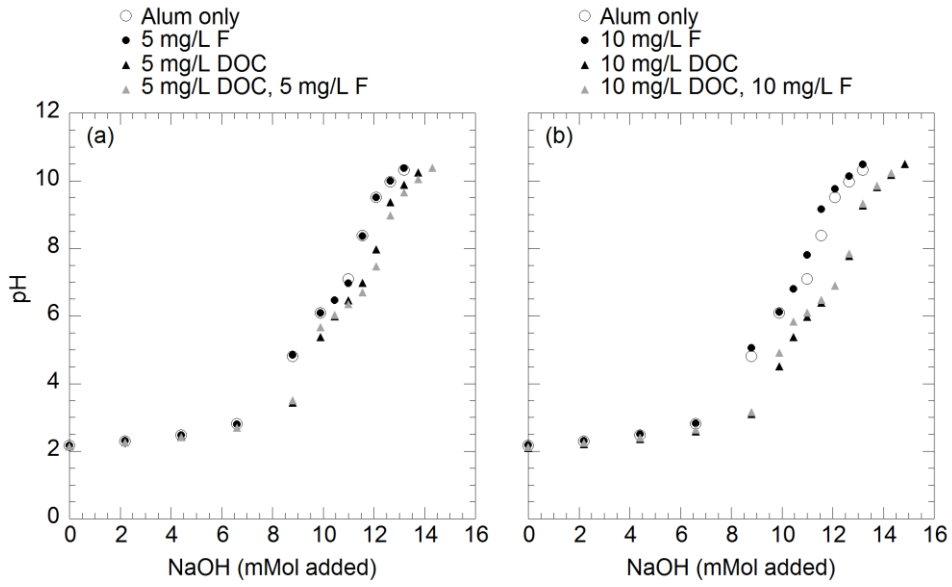

Figure 6-6: Titration of 50 mg/L alum in systems with varying combinations of NOM and fluoride (a) Initial concentration of 5 mg/L C NOM and 5 mg/L fluoride, (b) Initial concentrations of 10 mg/L C (NOM) and fluoride.

Increasing the alum dose to 100 mg/L, similar results are obtained, as shown in Figure 6-7a-b for 5 mg/L and 10 mg/L initial ligand concentrations. In all 4 sets of titrations, 10 mMol OH^- are required to increase the pH to above 4 for systems with NOM, regardless of whether or not fluoride was present. This consistent hydroxyl ion requirement suggests that precipitation of aluminum hydroxide and subsequent incorporation of NOM occurred rather than precipitation of a chemically different Al-NOM oxide.

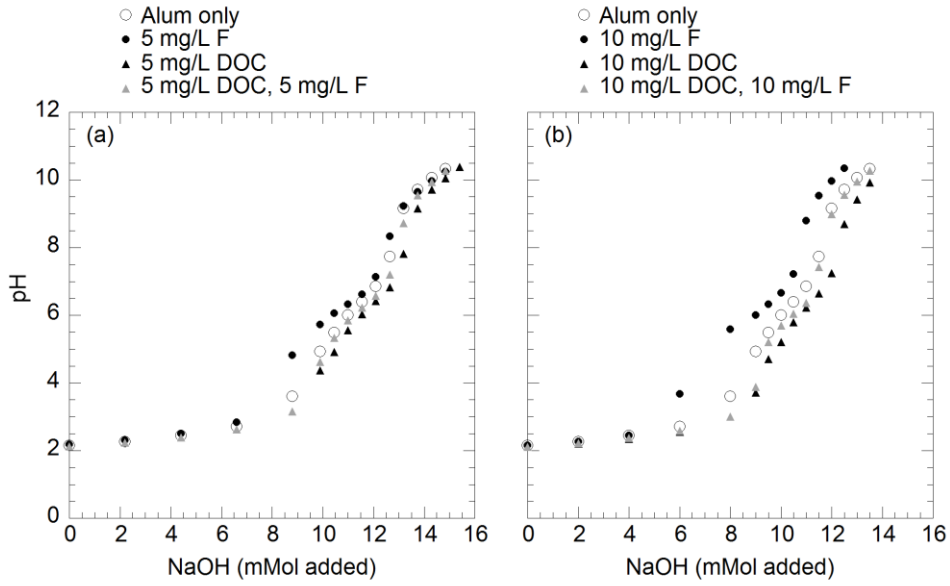

Figure 6-7: Titration of 100 mg/L alum in systems with varying combinations of NOM and fluoride (a) Initial concentration of 5 mg/L C NOM and 5 mg/L fluoride, (b) Initial concentrations of 10 mg/L C (NOM) and fluoride.

One explanation for the small differences in pH between NOM systems with and without fluoride is the neutralization of organic functional groups on the NOM as base is

added. While it was hypothesized that the low doses of NOM would not impart noticeable influence on the titrations, the neutralization may hide any difference that might be seen between the systems when fluoride and NOM are present.

While a deviation in pH occurred when NOM was titrated, it was not as hypothesized; therefore, aluminum solubility curves were experimentally determined using a 100 mg/L alum dose. The precipitation and solubility of aluminum were collected for single and dual ligand systems with fluoride and NOM (Figure 6-8a-c) and compared to the titration data. In Figure 6-8a, small additions of fluoride were capable of shifting the solubility curve of aluminum. An initial fluoride concentration of 0.5 mg/L fluoride was able to reduce the precipitation of aluminum below pH 6. As the initial fluoride concentration increased, the pH of maximum aluminum precipitation shifted to a higher pH value. When 5 mg/L C from Lake Austin NOM was present, the precipitation of aluminum was not impacted, as shown in the dual ligand (fluoride and NOM) systems, however, the results are more complicated (Figure 6-8c). Careful inspection of the 5 mg/L F data from Figure 6-8a and the dual ligand system data for 5 mg/L C and 5 mg/L F produced a curve that is between the fluoride only and NOM only systems. When 10 mg/L C and 10 mg/L F are present, the solubility curve is nearly identical to the 10 mg/L F curve in Figure 6-8a. According to these results, fluoride complexes with aluminum will dictate the solubility of the system, especially at higher fluoride concentrations.

The solubility results and titration results appear to contain contradictory information. Based on the titration data alone, little to no difference is observed in the NOM system with and without fluoride, yet the solubility curve provided evidence that fluoride is influencing the precipitation of aluminum. At this higher alum dose, the solubility curves confirm that the fluoride chemistry and the aqueous complexes formed

in the presence of fluoride are more important than the broadening of the pH ranges for precipitation in the presence of NOM. If an Al-NOM co-precipitate is formed, it does not preferentially form over the Al-F complexes.

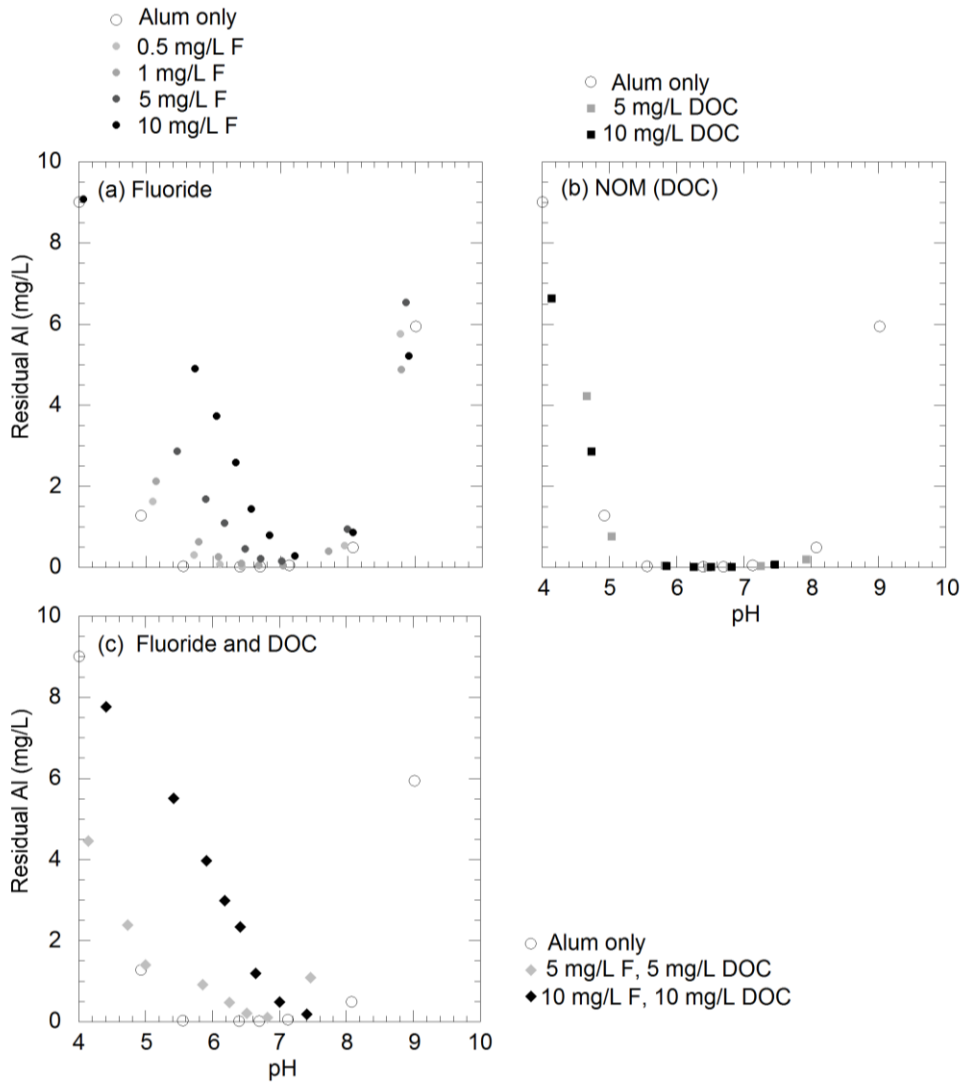

Figure 6-8: Solubility curves for 100 mg/L alum in the presence of varying ligand combinations.

Referring back to the zeta potential information for 20 mg/L alum, the pH ranges for precipitation are used to determine effective zeta potential values related to destabilization and are tabulated below in Table 6-5. The critical observation of this data set is that destabilization of particles occurs at lower effective zeta potential ranges when NOM is present in the system. The effective ranges are also narrowed for systems containing more than simply alum.

Table 6-5: Zeta potential (from 20 mg/L alum analysis) for optimal precipitation pH range (determined from 100 mg/L alum solubility curves)

System Parameters	Effective Zeta Potential Range (mV)
Alum only	+40 to 0
Alum, 5 mg/L F	+10 to 0
Alum, 5 mg/L C (NOM)	+5 to -25
Alum, 5 mg/L F, 5 mg/L C (NOM)	-20

In Chapter 5, it was concluded that only pyromellitic acid had a strong enough affinity with aluminum to achieve removals greater than 30% even in the higher alum dose ranges. Pyromellitic acid is also the LMW organic thought to yield the best approximation of humic fractions of NOM for adsorption onto iron oxides (Evanko and Dzombak 1998). The very strong acidity associated with the Lake Austin NOM supports the use of pyromellitic acid (pKa 1.52, 2.95, 4.65, 5.89) to appropriately capture the acidity of the NOM.

When compared to NOM in Figure 6-9a, pyromellitic acid has almost 20% greater maximum organic removal by alum for the high alum doses (greater than 100 mg/L alum). While this difference in overall removal is observed, the general trend of reaching a maximum in the 200-500 mg/L alum dose range is consistent for both

organics. Fluoride competition with the Lake Austin NOM isolates and pyromellitic acids, as shown in Figure 6-9b, follow a similar trend, but does show as much as 10% variation in reported fluoride removal in the dual ligand systems. Both the NOM and pyromellitic acid caused a decrease in fluoride removal that is sustained until approximately 200 mg/L alum. At this alum dose, pyromellitic acid competition with fluoride is diminished while NOM continues to negatively impact fluoride removal.

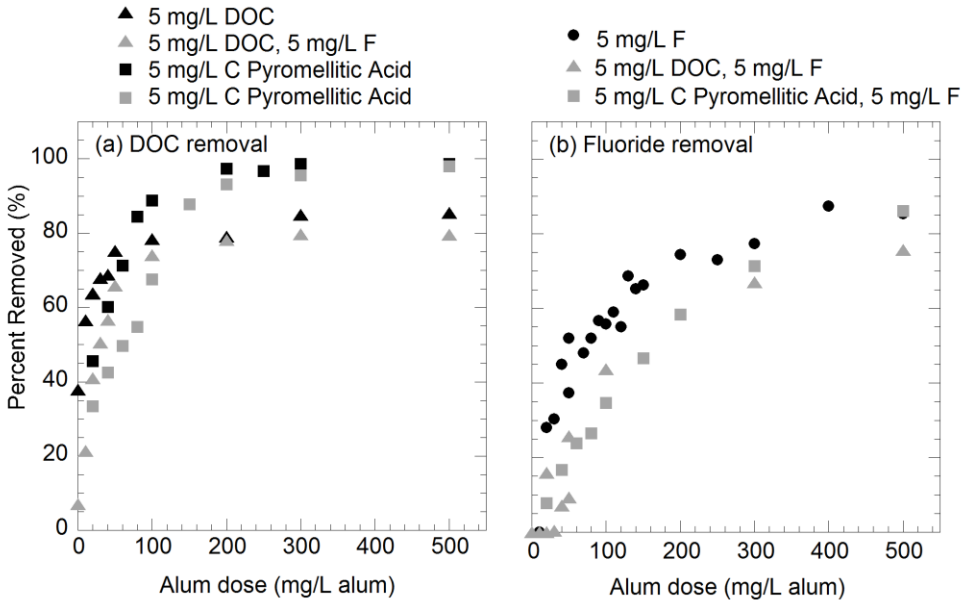

Figure 6-9: Comparison of NOM to LMW organic (pyromellitic) as a model surrogate over the 10-500 mg/L alum coagulant dose range: (a) percent organic removed, (b) percent fluoride removed.

The results in Figure 6-9a-b are re-plotted in Figure 6-10 to focus on coagulant doses below 200 mg/L alum and the ability of pyromellitic acid to model NOM at the

lower alum doses. There is a good correlation for both organic and fluoride removal between the pyromellitic acid data and the NOM results in this low alum dose range. In Figure 6-10a, NOM and pyromellitic acid removals in single and dual ligand systems are within 10% of each other at most alum doses. The competition between NOM and fluoride, as shown in Figure 6-10b, is also accurately mimicked by pyromellitic acid. At the lowest doses, the reduction in fluoride removal in the presence of an organic was similar to competition with pyromellitic acid. Pyromellitic acid is, therefore, a good LMW organic used to model complicated NOM competition with fluoride in an alum coagulation treatment system, especially at low alum doses. As doses exceed 200 mg/L alum, pyromellitic acid over predicts removal by NOM and is no longer a good choice of LMW organic as a model.

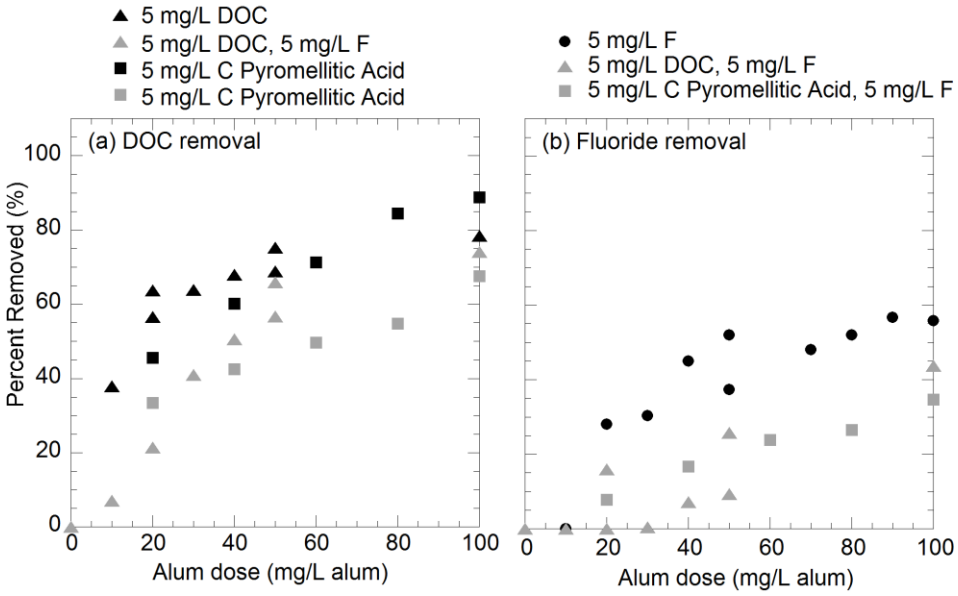

Figure 6-10: Comparison of NOM to LMW organic (pyromellitic) as a model surrogate: low dose alum coagulant range: (a) percent organic removed, (b) percent fluoride removed.

The impact of NOM on fluoride removal is most likely due to the negative charge imparted by the NOM on precipitate surfaces. Similarly, at these low alum doses, the ability of aluminum to achieve near complete removal via precipitation is impacted, reducing the NOM removal as well. NOM does improve precipitation in the dual ligand system, as observed in Figure 6-10, but a reduction in removal is still observed. This difference in results between these two systems suggests that a combination of Al-NOM precipitation and surface adsorption occurred in the NOM systems, with the dominant mechanism of removal across the alum dose range tested being adsorption.

6.4 CONCLUSIONS

Many treatment plants in the U.S. use alum coagulation to treat for NOM and turbidity. When fluoride was present, with and without NOM, the efficiency of turbidity removal was diminished. The presence of 5 mg/L of fluoride required doubling the alum coagulant dose that was required for a system with only NOM and particles to achieve turbidity levels of less than 2 NTU. The presence of fluoride, however, impacted more than just turbidity removal. Residual aluminum concentrations in systems employing alum doses less than 50 mg/L alum and containing 5 mg/L fluoride, with and without NOM, violate the EPA SMCL of 0.5-0.2 mg/L Al.

At these low alum doses, both adsorption and NOM co-precipitation with aluminum are mechanisms for NOM removal. The presence of NOM has a significant impact on particle surface charge which, in turn, affects turbidity removal. When compared to systems only containing the alum coagulant, the presence of NOM lowered the effective zeta potential range for precipitation, with and without fluoride present; therefore, destabilization of particles occurs at lower effective zeta potential ranges when

NOM is present in the system. This mechanism explains the improved turbidity removals observed in the presence of NOM.

The behavior and chemical competition between NOM and fluoride in alum coagulation systems are different for low and high alum doses administered during treatment. At low alum doses, preferential Al-NOM precipitation occurred over fluoride co-precipitation with aluminum. At a higher alum dose range, little competition is seen for NOM removal, yet there is a sustained impact on fluoride removal throughout the entire range of doses tested. This reduction may be due to competition for aluminum sites and the effect of NOM on aluminum hydroxide surface charge.

NOM is a complex structure that contains a variety of functional groups, aromatic rings, and aliphatic chains which vary depending on the source of the NOM. The identification of a surrogate, low molecular weight organic, to model NOM is important in order to simplify analyses of multi-ligand systems and create a uniform model for NOM removal. Pyromellitic acid acted as a good surrogate for NOM at alum doses less than or equal to 100 mg/L alum. At higher doses, including the 200 mg/L maximum NOM dose that yielded the highest NOM removals, pyromellitic acid over-predicted organic removal and may not be useful as a surrogate for NOM under these conditions. Pyromellitic acid mimicked competition with respect to fluoride in these higher alum dosed systems, followed trends in NOM removal, but over-predicted fluoride removal as alum doses increased above 200 mg/L alum.

The surface adsorption of fluoride on the precipitated aluminum solids is most likely impacted in both NOM and pyromellitic acid systems due to the negative charge imparted by the organics. Future research analyzing pyromellitic acid as a surrogate for NOM including a wider range of alum doses is needed. The microscopic analysis of the

oxide structure, before and after aging, for precipitates formed in the presence of NOM would greatly help with the evaluation of pyromellitic acid as a viable model.

Chapter 7: Stability of aluminum precipitates

7.1 INTRODUCTION

When alum is used as a coagulant in water treatment plants, an amorphous aluminum hydroxide precipitate is formed. We have established in previous chapters that, when fluoride and/or organic ligands are present during precipitation, these ligands can be incorporated into the amorphous structure of the precipitate (F) or adsorbed onto its surface (F or organics). Previous researchers have shown that, when ligands form inner- or outer-sphere complexes with oxide structures, dissolution of those oxides can result. However, little research has looked at how the surface coordination of fluoride in multi-ligand systems affects dissolution of amorphous precipitates. Therefore, the stability of co-precipitated aluminum oxides is poorly understood. The objective of the work reported in this chapter was to investigate the impact of fluoride on the stability of co-precipitates in the presence of low molecular weight organics.

7.2 BACKGROUND

The effects of ligand-promoted dissolution are important to the evaluation of surface bonding mechanisms. Furrer and Stumm (1986) proposed that, if proton and ligand-promoted dissolution occur as independent, parallel reactions, the dissolution kinetics can be superimposed and the dissolution rates are additive. They showed that, under acidic conditions, the surface concentrations of bidentate, inner-sphere chelates were proportional to the dissolution rate. It is hypothesized that the dissociation of aluminum precipitates at near neutral pH does not follow this parallel, independent dissociation model proposed by Furrer and Stumm (1986). Furrer and Stumm's

conclusion that certain outer-sphere coordinated organic ligands have little catalytic effect and could actually inhibit dissolution was confirmed by Johnson et al.'s (2004a) observations on the effects of maleate on corundum dissolution. Bidentate, binuclear bonds inhibit dissolution due to the high activation energy associated with the detachment of two metal cations from the mineral surface (Johnson et al, 2004b). Maleate inhibited dissolution regardless of pH and adsorption density. Oxalate, on the other hand, formed an inner-sphere, bidentate, mononuclear complex with corundum and promoted dissolution (Johnston et al. 2004b). In considering Suwanee River fulvic acid adsorption on boehmite, Yoon et al (2005) used desorption results to confirm ATR-FTIR surface spectroscopic interpretations for inner- or outer-sphere complexation; they found that, under acidic pH conditions, complicated NOM structures form outer-sphere bonds and inhibit dissolution of metal (oxyhydr)oxides.

Kraemer et al. (1998) re-evaluated Furrer and Stumm's independent and parallel model of dissolution and concluded that it failed in the multi-ligand system and was not completely consistent in the single ligand systems either. Fluoride enhanced the dissolution effects of organic acid HQS (8-hydroxyquinoline-5-sulfuric-acid), leading Kraemer et al. to hypothesize that a mixed surface complex of HQS, aluminum, and fluoride increased the rate of detachment. They also concluded that the pH not only affected the proton-promoted dissolution but impacted the ligand-promoted dissolution. As systems increase in pH, moving from acid environments to near neutral pH, the proton-promoted effects are reduced, becoming minimal at a pH > 7.5.

Most of the ligand-promoted dissolution work has utilized corundum, boehmite, δ-Al_2O_3, and other crystalline aluminum oxides. Xu et al. (2008) furthered the work by Huang's research group to consider the effects of a tannate/Al precipitate on the adsorption of arsenate. Desorption of arsenic in the presence of a competing ligand was

also used to quantify the relative strength of the bonds. It was discovered that the higher surface area tannate/Al oxides adsorbed more arsenate, but these bonds were weaker and desorption occurred more readily than with the aluminum oxides. The Xu et al. (2008) study, while attempting to understand the strength of bonds on mixed oxides, does not consider dissolution of the organic-aluminum solids as a measure of bond strength.

Thus far, this research has evaluated the effect of a co-precipitate on organic and fluoride removal in multi-ligand systems, competition in the co-precipitation process, and the ability to model NOM removal on a co-precipitate using and low molecular weight organic; but, the inner- and outer-sphere coordination of the LMW organics was not satisfactorily evaluated. Adsorption experiments from Chapter 5 proved that the number of carboxylic groups on an organic were more important to removal than bond coordination. The final research goal evaluated the impact of fluoride on co-precipitate stability through ligand-promoted dissolution. Analyses comparing the aluminum dissolution of oxides, aluminum precipitates, and co-precipitates formed in the presence of multiple ligand systems were used to further assess the removal mechanisms concluded in the previous chapters.

7.3 RESEARCH APPROACH

The following experiments are designed to understand the stability of ligand removal throughout the coagulation process. After the precipitate is formed and adsorption occurs, it is important to understand the duration of bond stability between the precipitate and adsorbed ligands to completely analyze the treatment system. Any

dissolution of aluminum during treatment could increase health risks to users. Using a modified jar test as outlined in the methodology, aluminum dissolution was tested.

Co-precipitation, Preformed, and Transferred preformed jar tests (3.2.1)

To determine the stability of removed ligands and the dissolution promoting effects, α-Al_2O_3 tests, as well as preformed (PRE), transferred preformed (T-PRE), and co-precipitation (CPT) jar tests were used. Unless otherwise specified, all tests contain a background synthetic water matrix comprised of 3 meq/L alkalinity and 3 meq/L hardness. Stock alum and α-Al_2O_3 solutions of 46.6 mMol Al and 40 mMol Al, respectively, were used to dose the jars with aluminum at the beginning of the experiment. Jar test experiments were conducted at a target pH of 6.5 and only adjusted at the beginning of each experiment using 1.0 N HCl and 1.0 N NaOH. Most experiments reported by earlier investigators on aluminum dissolution were conducted at an acidic pH, where the surface of the solid was quickly re-protonated allowing for continuous dissolution; however, drinking waters are not typically acidic.

7.4 RESULTS AND DISCUSSION

Ligand-promoted dissolution is typically explained within the context of oxides, and most of the reported research on aluminum oxides focuses on corundum (α-Al_2O_3). As shown in Chapter 4, the aluminum precipitates formed in this research remained amorphous throughout the entire removal process, and even after 46 days, only small boehmite crystals began to form. To compare the results in the co-precipitated system to the standard oxide dissolution investigation, jars with 349 μMol [Al] from α-Al_2O_3 were

used as a baseline (Figure 7-1). As shown in Figure 7-1a, none of the organics alone caused dissolution of the aluminum oxide, yet each system in the presence of fluoride (with or without organics) experienced ligand-promoted dissolution, as evidenced by the increasing residual aluminum concentrations with time. Dissociation in the corundum system was dictated by the fluoride in the system and not the LMW ligands. Dual ligand systems are often said to have additive, parallel paths of dissociation (Furrer and Stumm 1986); however, this phenomenon is not seen in these systems. In the LMW only systems, the existence of inner- or outer-sphere complexes did not impact residual aluminum concentrations. When both fluoride and the LMW organics were present, dissociation was equivalent to that seen in the fluoride only system.

The results for the removal of the organics in Figure 7-1b vary widely for the three different chosen LMW organics, with phthalic acid removed most effectively (and increasing with time) and salicylic acid removed least effectively; these same trends occurred in the presence or absence of fluoride. Interestingly, fluoride enhanced the removal of phthalic acid but reduced the removal of salicylic acid; fluoride had no effect on the removal of pyromellitic acid. As shown in Figure 7-1c, little removal of fluoride occurred in any of these systems, but the largest removal occurred in the system with no organics present to compete for sites on the corundum.

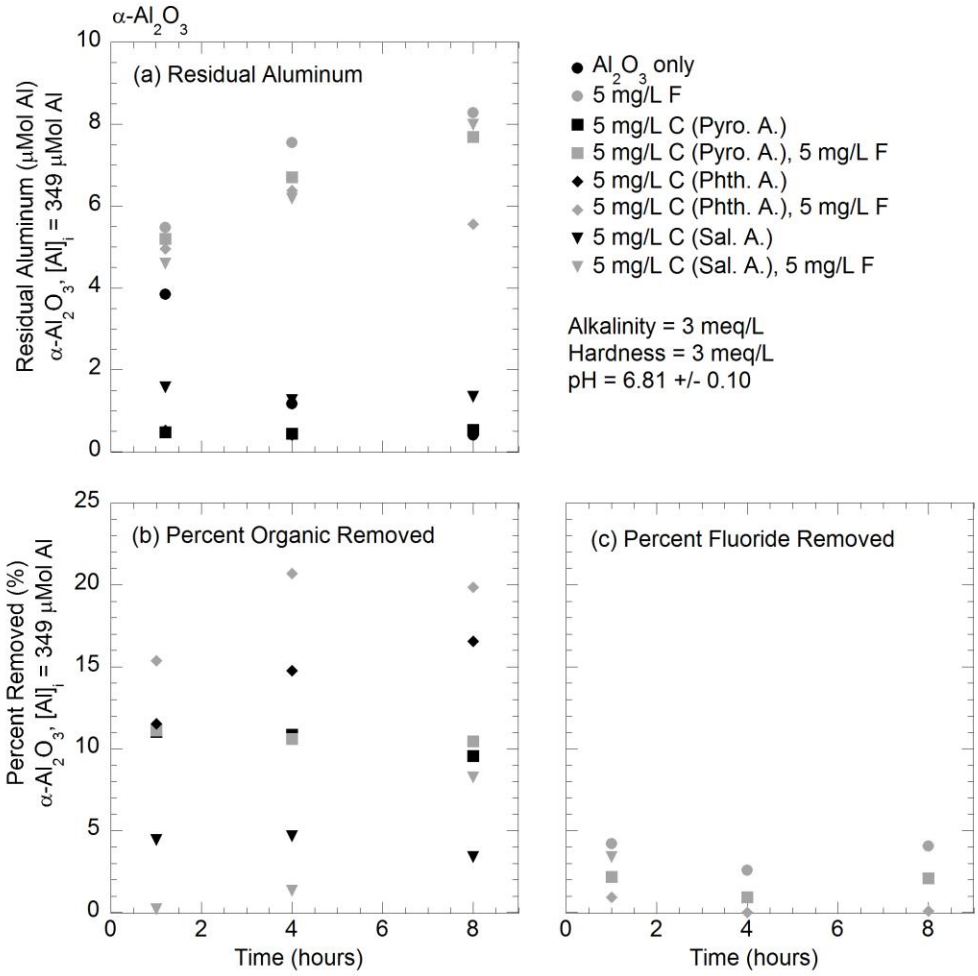

Figure 7-1: Stability of aluminum during treatment: α-Al_2O_3 ([Al] = 349 µMol, equivalent aluminum concentrations of a 100 mg/L alum dose). (a) Residual aluminum as a function of time, (b) percent organic removed, (c) percent fluoride removed.

The next set of experiments was designed to examine dissolution in a preformed aluminum hydroxide system, that is, one in which the competing ligands were not present

at the time of precipitation but were added in subsequently. To provide a baseline for comparison, residual aluminum concentrations of an aluminum hydroxide only system were measured. The residual aluminum concentrations at the time of the ligand dosing were less than 2 μMol Al in all of the solutions; in the system with no ligand addition, the Al concentration did not increase during the experiment. After the ligands were dosed, the residual concentrations were measured at 1 hour 10 min, 4 hours, and 8 hours. The results are presented in Figure 7-2.

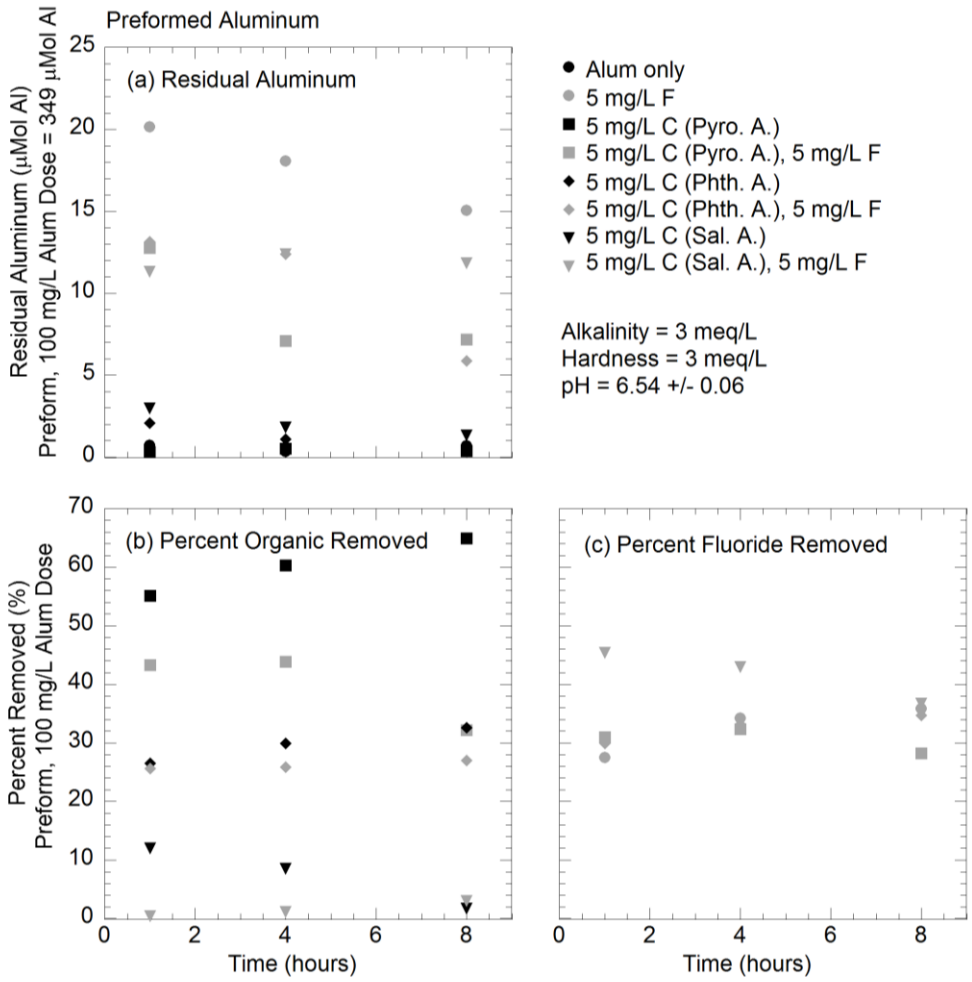

Figure 7-2: Stability of aluminum during treatment: preformed (PRE) aluminum precipitates using a 100 mg/L alum dose ([Al] = 349 µMol) (a) residual aluminum as a function of time, (b) percent organic removed, (c) percent fluoride removed.

Similar to the corundum experiments, the systems with only LMW organics showed little dissolution, although the aluminum concentrations are higher. The residual aluminum concentrations in systems that contained fluoride, on the other hand, differ from the results obtained during the corundum experiment. Initial dissociation of

aluminum from the system, at the 1 hr 10 min sampling time, ranged from 11 to 20 μMol Al, concentrations much greater than the initial dissolution from corundum. As the experiment continued, the suspensions containing fluoride apparently formed new precipitates throughout the experiment, as shown by the decreasing residual aluminum with time (Figure 7-2a).

The removal of the organics in single ligand systems, shown in Figure 7-2b, tended to increase slightly with time, except for the salicylic acid system which experienced steadily declining removal; as might be expected from the amorphous solid with its far greater surface area, the organics removal was much greater than in the corundum experiments for all three LMW organics. When fluoride was added, the removal of salicylic acid decreased to near zero. , The presence of fluoride caused a slight decrease in the removal of phthalic acid in comparison to the system with no fluoride. Pyromellitic acid displayed a significant decrease in removal after the first hour in the presence of fluoride, consistent with results presented in Chapter 5, but the competition between pyromellitic acid and fluoride for removal increased with time. This gap for pyromellitic acid removal with and without fluoride continued to widen with time, and after 8 hr, the difference in removal exceeded 30%.

The fluoride removal in these suspensions is shown in Figure 7-2c, and the solutions with the three LMW organics each exhibit different trends: fluoride removal increased slightly over time in the phthalic acid solutions, remained steady at approximately 30% in the presence of pyromellitic acid, and decreased over time for salicylic acid. These results are (reasonably) consistent with the trends in aluminum concentrations, suggesting that aluminum and fluoride (after the original dissolution of Al) are being co-precipitated onto the surface.

At these low aluminum concentrations and a near neutral pH, the degree of over- or undersaturation of the system with respect to aluminum can greatly influence the results. The corundum experiments should, in theory, have no residual aluminum at the start of the experiment. The preformed precipitates, however, are not transferred out of the jar nor are they washed, potentially leaving the system oversaturated with respect to aluminum hydroxide prior to ligand dosing. To compare the solubility of the systems, one must consider the difference in K_{s0} between amorphous aluminum solids and the most commonly used solubility constants. Most researchers use the K_{s0} of gibbsite when comparing the solubility of oxides during precipitation since amorphous precipitates are typically not considered. Comparing the difference between the solubility of gibbsite to that of amorphous precipitates (Figure 7-3 and Table 7-1), the preformed systems (at 10^{-6} M or slightly above) are undersaturated at the start of the experiment, even given the residual aluminum concentrations at the start.

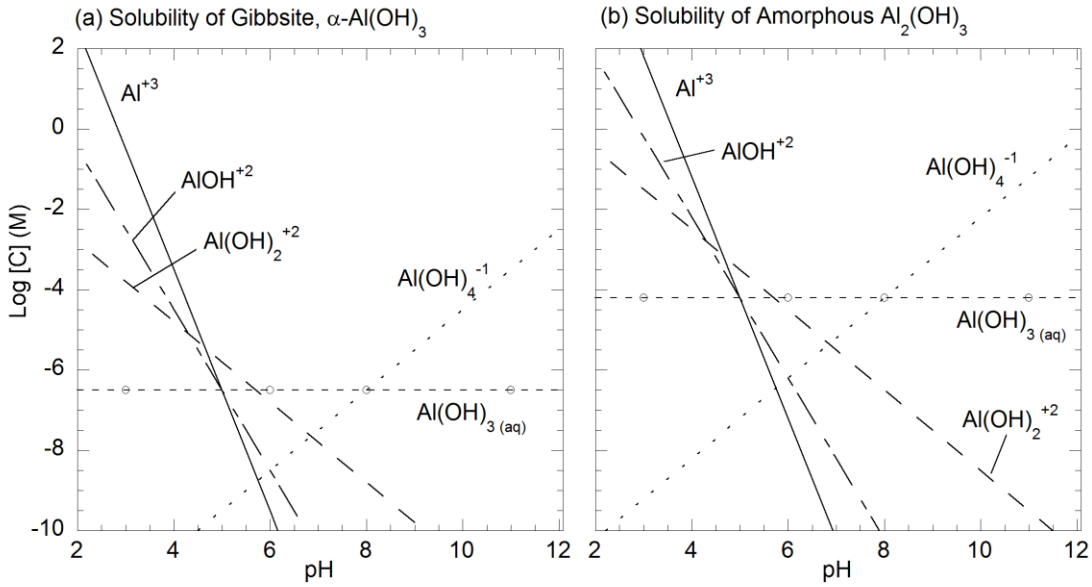

Figure 7-3: Solubility diagrams (a) gibbsite (α-$Al(OH)_{3(s)}$), (b) amorphous $Al(OH)_{3(s)}$ (stability constants are presented in Table 7-1).

Table 7-1: Stability constants for formation of complexes and solids

Components		β^a	α-$Al(OH)_{3(s)}$ log *K	$Al_2(OH)_{3(s)}$ log *K
	$Al(OH)_{3(s)}$		8.5[a]	10.8[b]
Species	Al^{+3}	---	8.5	10.8
	$AlOH^{+2}$	9	3.5	5.8
	$Al(OH)_2^{+}$	18.7	-0.8	1.5
	$Al(OH)_{3\,(aq)}$	27.0	-6.5	-4.2
	$Al(OH)_4^{-1}$	33.0	-14.5	-12.2

[a] Data from Morel (1983)
[b] Data from Nordstrom et al. (1990)

To eliminate the possibility that soluble aluminum in the jars at the time of ligand dosing was responsible for the trends noted, preformed precipitates were captured on a

0.45 μm filter and washed with 10 mL of D.I. water prior to transferring the solids to a system free of residual aluminum (referred to as "transferred preformed" or T-PRE experiments). After transfer, the precipitates were stirred at a high speed to break apart the compacted amorphous gel prior to ligand dosing. The results are presented in Figure 7-4.

Residual aluminum concentrations (Figure 7-4a) and trends in the T-PRE experiments including fluoride are similar to those seen in the preformed systems, with a gradual decline in the Al concentrations over time after an initial substantial dissolution (prior to the measurement at 1 hr 10 min). The residual Al concentrations in the fluoride only system are substantially lower than in the PRE experiment and are in greater agreement with the systems containing both fluoride and LMW organics in the PRE systems.

Little (3%) to no difference in organic removal was observed in the systems with and without fluoride by T-PRE precipitates, as shown in Figure 7-4b; as in the PRE experiments, removal of pyromellitic acid was best and that of salicylic acid worst. However, the removal of organics was substantially less in the T-PRE experiments (Figure 7-4b) than in the PRE experiments (Figure 7-2).

Fluoride removal (Figure 7-4c) was reduced by the presence of salicylic and pyromellitic acids, while fluoride had little impact on the removal of these organics. As in the PRE experiments, fluoride removal increased (i.e., fluoride concentration decreased) over time, coinciding with the decrease in Al residual; these results again suggest that a precipitate containing Al and F was being gradually formed in these jars.

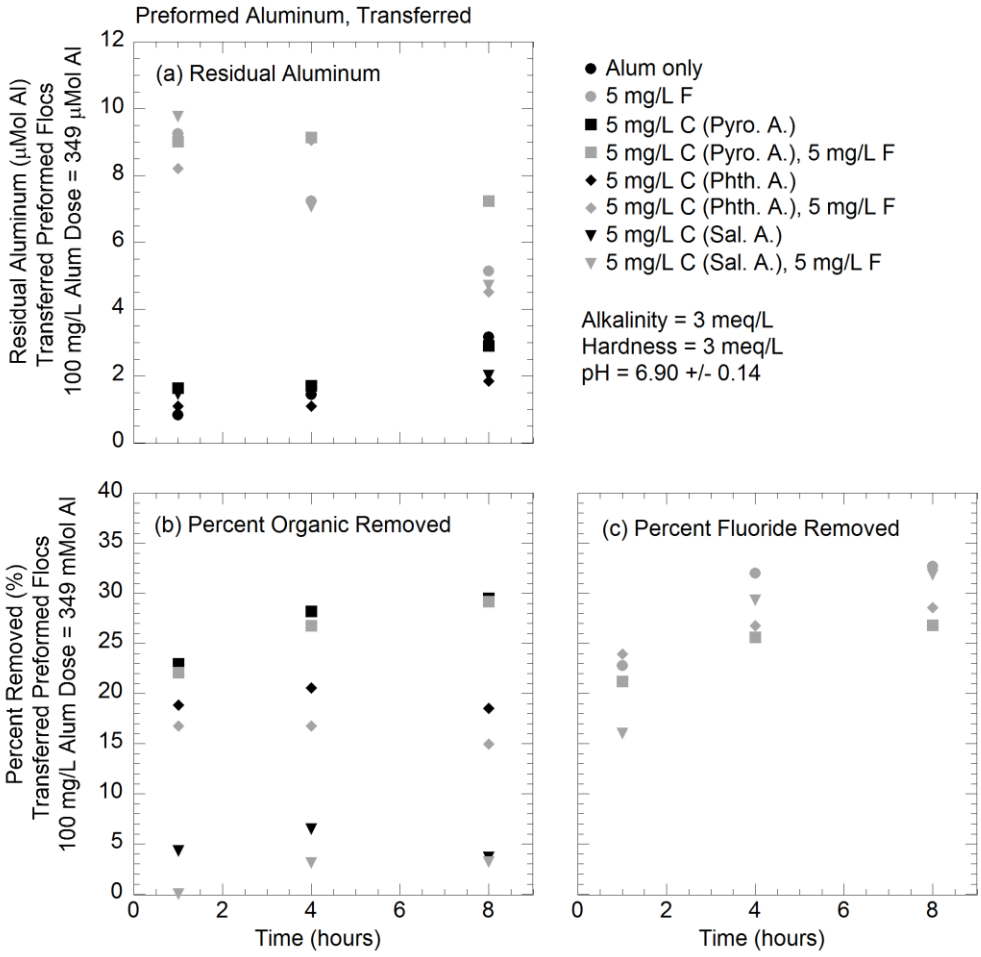

Figure 7-4: Stability of aluminum during treatment: preformed aluminum precipitates, transferred (T-PRE) using a 100 mg/L alum dose ([Al] = 349 µMol) (a) residual aluminum as a function of time, (b) percent organic removed, (c) percent fluoride removed.

While the results of the PRE and T-PRE tests have similar trends qualitatively, quantitative differences are evident. The act of filtering and transferring the precipitates created compacted pellets despite efforts to prevent gel transformation. After transfer, the pellets were mixed at a high speed to break up the pellet; however, significant large

pieces remained. While pellet compression did not greatly affect the residual aluminum concentrations with respect to the PRE experiments, it did impact removal of organics. The surface of the precipitates apparently decreased since the number and open configuration of the flocs were visually reduced. In Chapter 5, it was observed that the surface loading of pyromellitic acid was 44% less when moving from a CPT to a PRE precipitation system; therefore, it is conceivable that a reduction in surface area of the precipitates between the PRE and the T-PRE experiments would create a similar reduction. Future work determining methods of transferring the precipitates without significant alteration is needed to confirm no difference in the T-PRE and PRE systems.

From the aluminum solubility and precipitation results presented in the context of NOM precipitation in Chapter 6, it was observed that fluoride could increase the residual aqueous aluminum concentrations in solution at pH 6.6 after the standard 1 hr 10 min experiment. Chapter 4 conclusions regarding the formed Al-F co-precipitate included that fluoride prevented formed co-precipitates from growing during the flocculation process. Given these two sets of earlier observations, higher residual fluoride concentrations are expected at the conclusion of the 1 hr 10 min experiment. Predicting the stability of these formed co-precipitates, it was hypothesized that the presence of amorphous precipitates after 45 days of aging meant that the formed co-precipitate was stable and would not be as prone to dissolution. The PRE systems were predicted to be more susceptible to dissolution and have higher fluoride concentrations after 1 hr 10 min and would increase over time.

To fully test these predictions, the following sets of CPT experiments used the entire range of alum doses (20-500 mg/L) considered throughout this research instead of only a single dose. As a result of this difference in methodology, the figures use alum dose on the abscissa and differentiate the times with different markers. At the end of the

chapter, a final graph compares the CPT data to the α-Al_2O_3 adsorption, PRE, and T-PRE data presented earlier in this chapter.

To begin the CPT analysis, experiments were conducted with only fluoride present at 5 mg/L F for both CPT and PRE systems. Residual aluminum and percent fluoride removed for each are plotted as a comparison in Figure 7-5. Comparing the residual aluminum concentrations for the entire alum dose range for the CPT (Figure 7-5 a) to those for a PRE system with fluoride (Figure 7-5 c), the concentrations are higher for the PRE system across the alum dose range and over the entire 8 hr experiment, as expected. Alum doses of 100 mg/L or less for the CPT system experience an average 6 μMol decrease between the 1 and 8 hr samples, whereas the higher alum doses only experience an average 1.2 μMol decrease in residual aluminum. Despite this smaller fluctuation, the higher alum doses (≥200 mg/L alum) have lower aluminum residuals over the entire 8-hour experiment than those from alum doses < 200 mg/L alum. These aluminum residuals are also in close agreement with the average change over the 8-hour recorded for the alum only systems regardless of applied dose.

The percentages of fluoride removed in these two systems (Figure 7-5 b and d) are lowest at the start of the experiment and gradually increase as residual aluminum decreases. The variation in fluoride removal by the CPT system (Figure 7-5 b) over 8 hours is less (an average change of 3.5%) than in the PRE system (an average change of 6%) (Figure 7-5d). The greater fluctuations observed in both aluminum and fluoride for the PRE system are potentially a result of fluoride adsorption being less stable than co-precipitates formed with fluoride. These results (i.e., decreasing residual aluminum and fluoride over time) again suggest that a precipitate containing Al and F was being gradually formed in these jars, especially the PRE system, for the entire alum dose range tested.

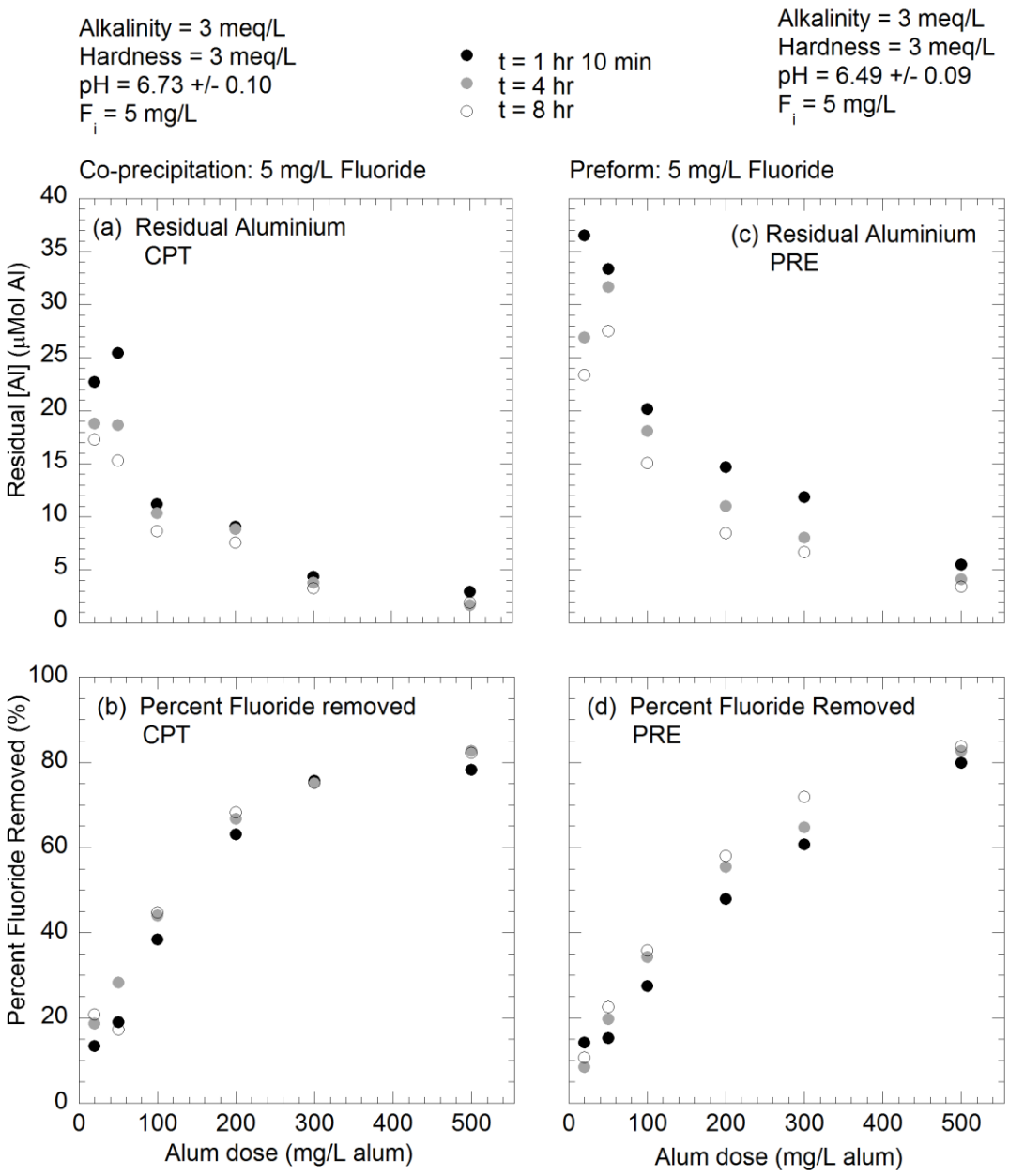

Figure 7-5: Solubility of aluminum precipitates over a range of coagulant doses with $[F]_i$=5 mg/L: comparison of CPT and PRE (a) dissolution of aluminum CPT, (b) percent fluoride removed by CPT precipitates, (c) residual aluminum of PRE precipitates, (d) percent fluoride removed by PRE precipitates.

To ensure the systems are at equilibrium at the end of the 8-hour experiment, the dissolution experiment was extended for 24 hr to test the trend further. The residual aluminum in the CPT system for the entire dose range of 20-500 mg/L alum does not change significantly (+/- 0.93 μMol Al) when extending from 8 hr to 24 hr; therefore, we can consider the system to be at equilibrium at the conclusion of the 8 hr experiments. Only fluoride removal at the higher alum doses is impacted by longer reaction times, with a slight decrease of 2-6% fluoride removed after 8 hours. Considering the time step, the decrease is minimal on a per hour basis, thus confirming that it was reasonable to stop the experiments after 8 hr.

Recalling the results from aging precipitates presented in Chapter 4 (see XRD results, Figure 4-8), aged precipitates form a boehmite structure with crystal sizes in the 25 Angstrom range, suggesting that this is the most likely arrangement at the amorphous level as well. Research by Nordin et al. (1999) used ^{19}F-NMR to understand the replacement of fluoride in boehmite and bayerite during adsorption. They concluded that fluoride created at least three different chemically distinct fluoride bonding sites. At high fluoride loading, surface aluminum ions coordinated with multiple fluoride ions at both edge terminal sites and paired bridging sites. Fluoride was also concluded to bridge two aluminum atoms at the bridging site (Nordin et al. 1999). This proposed model agrees with the conclusions from Chapter 4 regarding fluoride replacing hydroxyl ions in the precipitate structure and inhibiting hydroxyl bridging bonds and, as a result, altering precipitate growth.

Typical dissociation includes a proton-promoted dissolution step where protonation of a hydroxyl bridge forms a bridging water molecule. The water molecule leaves the surface as a hydration sphere for a detaching aluminum ion. The unbounded metal ion completes its coordination sphere through bonding to the hydrating water

molecule. The oxygen in highly ordered mineral phases is strongly coordinated to the metal ions, not allowing dissociation to occur. When fluoride occupies the bridging and terminal sites of an oxide structure, the dissociation is more complicated than can be expressed in a simplified rate law or definition. Fluoride's occupation of bridging sites weakened the bridging bonds formed, as shown by the inhibition of floc growth when fluoride was present (Figure 4-9). Nordin et al. (1999) also showed that several fluoride ions occupy a single site, increasing the charge density at a binding site, thus increasing the vulnerability of the aluminum to protonation and dissociation. The above detailed process of protonation and dissociation explains the higher residual aluminum concentrations after only 1 hr 10 min of reaction in all the experiments considered thus far, including the corundum experiments; however, it does not explain why aluminum residuals for PRE systems are greater than the CPT systems presented in Figure 7-5a and c.

The higher initial concentrations of aluminum in the preformed experiment are most likely due to surface adsorption first promoting aluminum dissociation followed by a reordered precipitate forming and precipitating. The dissociation from surface adsorption sites containing fluoride must be more favorable than dissolution from a bridging or terminal site occupied by fluoride. Furthermore, the lower residual aluminum concentrations in the CPT system suggest that dissociation and re-ordering of precipitates is not as large of an influence as it is in the preformed experiments. The co-precipitate has already formed a structure in which fluoride has replaced many of the bridging hydroxyl groups, thereby creating a more stable structure given the concentration of the fluoride. However, since the residual aluminum concentrations continue to decrease along with residual fluoride, it is possible that the released hydroxyl groups help destabilize the aqueous aluminum-fluoride complexes over time, promoting further

precipitation over the 8-hour experiment. At the end of 8 hours for the higher alum dose (200 mg/L dose, Figure 7-5a and c), both the CPT and PRE systems contained approximately 8 μMol/L residual aluminum, suggesting that little additional ordering within the precipitate re- occurred past this 8 hour period.

If both the explanation that fluoride can occupy multiple sites as proposed by Nordin et al. (1999) and the conclusions in this study that fluoride has the ability to replace hydroxyl ions in the precipitate structure are accepted, then the interaction of LMW organics with the precipitate over time can be predicted as strongly influenced by the fluoride in the system. Salicylic acid is, according to this work, considered to form primarily inner-sphere bonds with aluminum precipitates at near neutral pH. The CPT results for salicylic acid alone, Figure 7-6a-b, and salicylic in a dual ligand system with fluoride, Figure 7-6c-e, are more complex than the fluoride only results. Salicylic acid promoted aluminum dissolution over 8 hr when present alone in the system (Figure 7-6a) and corresponded to increasing organic concentrations as well (decreased percent removals), Figure 7-6b.

The dual ligand, salicylic acid and fluoride, system contained the highest residual aluminum concentrations, shown in Figure 7-6c, after only 1 hr 10 min and decreased with time, similar to the CPT fluoride only system (Figure 7-5a); however, the decreasing residual aluminum concentrations coincided with decreased organic and fluoride removal (increasing concentrations of both ligands). The variation in organic removal, Figure 7-6d, is only a 5% decrease while fluoride removals diminish by as much as 15% (Figure 7-6e). The dual ligand, CPT is most likely functioning similarly to the salicylic acid only system: decreased constituent removals indicate dissolution except that the residual aluminum continues to decrease with time. Most likely, a fresh aluminum precipitate is forming in the system that is not a co-precipitate with either salicylic acid or fluoride.

Salicylic did not compete with fluoride for either adsorption or co-precipitation in previous experiments, and, therefore, the competition during the re-precipitation of aluminum was unexpected.

Similar to salicylic acid, pyromellitic acid was assumed to form primarily inner-sphere complexes with the aluminum precipitates, except that pyromellitic acid achieves higher levels of removal than salicylic acid using aluminum precipitates formed during coagulation experiments. The stronger association between pyromellitic acid and the aluminum solids for removal do not translate into higher aluminum residuals than salicylic acid, Figure 7-7a. While the residual aluminum increases only slightly (an average 2.1 μMol increase), the increase is an observed trend over the entire range of coagulant doses used in the experiment. Overall, the increased residual aluminum resulted in a higher residual organic concentration as well (Figure 7-7b), similar to the salicylic acid system. Pyromellitic acid experiences a slight decrease in removal (increase in residual organic concentrations) over the 8 hours. This set of results is consistent with a ligand-promoted dissolution analysis.

In the dual ligand systems with pyromellitic acid and fluoride, the same aluminum residual trend was observed in that the residual concentrations decreased over the 8-hour experiment. The initial residual aluminum concentrations were less in the pyromellitic acid and fluoride system than one with salicylic acid, as shown in Figure 7-7c. Unlike in the salicylic system, when pyromellitic acid and fluoride are present, little to no fluctuation in organic removal occurred (Figure 7-7d). Fluoride concentrations, shown in Figure 7-7e, experienced a decrease in removal (increase in residual concentrations) similar to the results in the salicylic acid dual system. Fluoride removals were less than in the salicylic acid system, consistent with results presented in Chapter 5, and the competition between fluoride and pyromellitic acid exists over the 8-hour experiment.

The re-precipitation of dissolved aluminum is not forming a co-precipitate with fluoride in these dual ligand systems that include inner-sphere bonding organic acids.

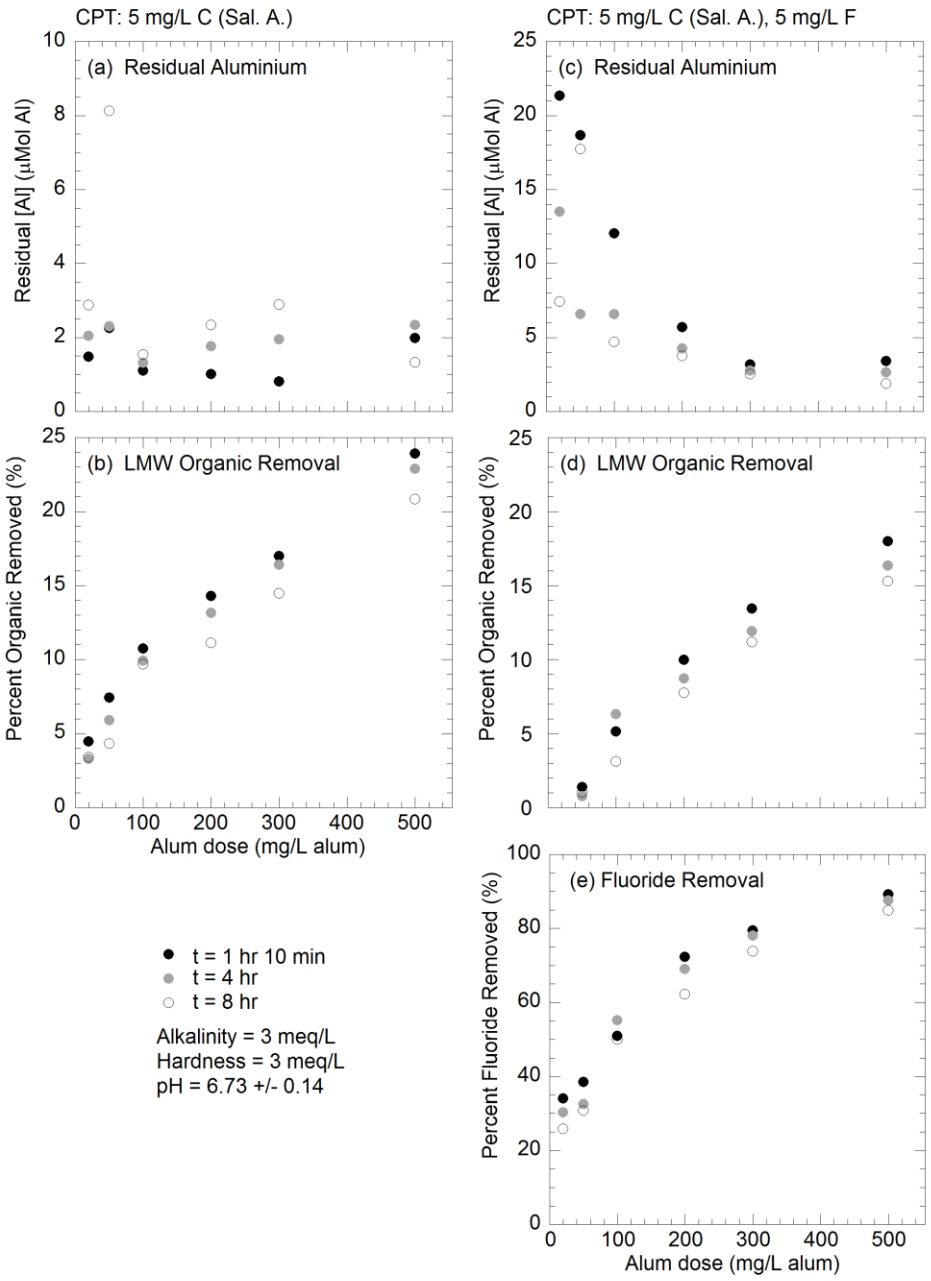

Figure 7-6: Solubility of CPT aluminum precipitates over a range of coagulant doses, C_i=5 mg/L salicylic acid, F_i = 0 and 5 mg/L (a) residual aluminum concentration F_i = 0 mg/L, (b) percent organic removed F_i = 0 mg/L (c) residual aluminum concentration F_i = 5 mg/L, (d) percent organic removed F_i = 5 mg/L, (e) percent fluoride removed F_i = 5 mg/L.

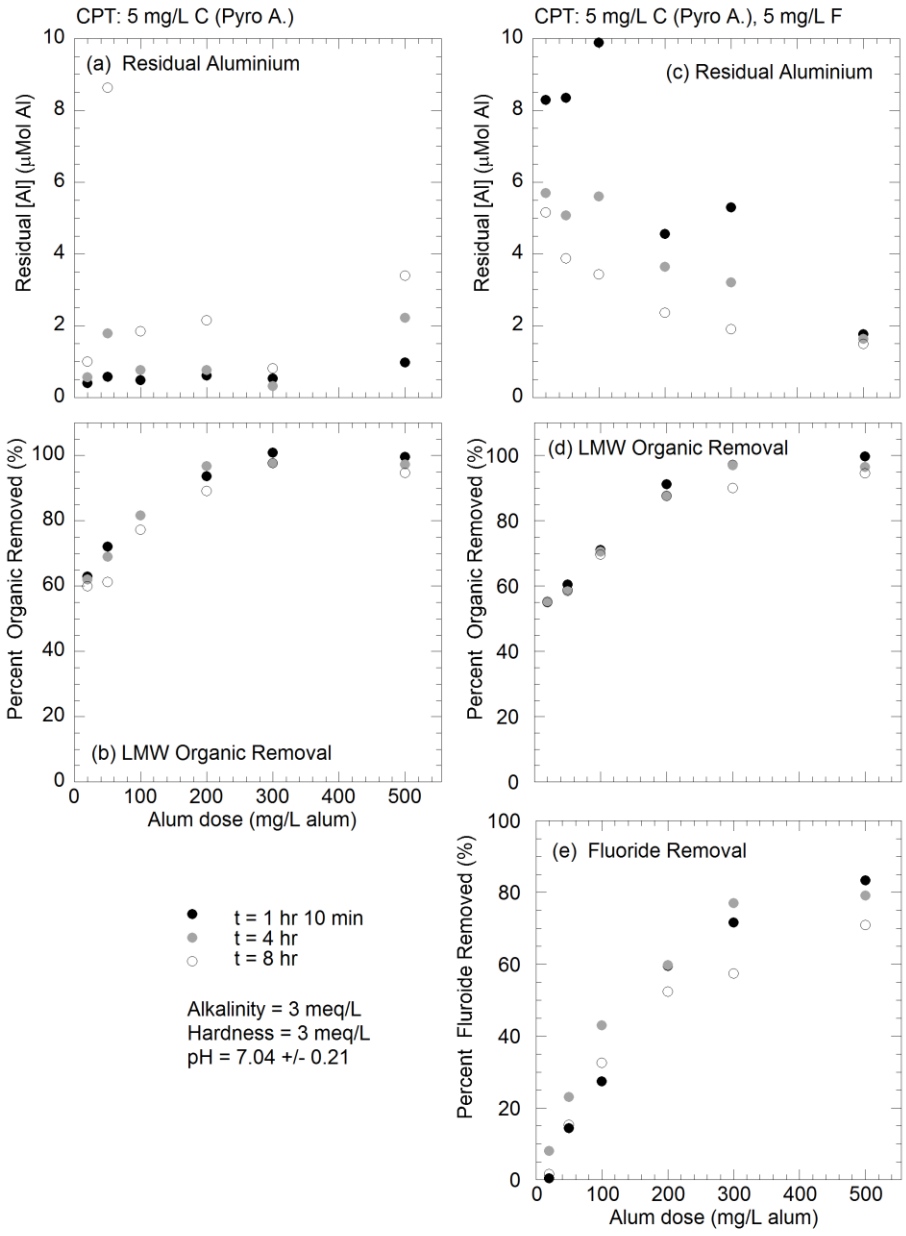

Figure 7-7: Solubility of CPT aluminum precipitates over a range of coagulant doses, C_i=5 mg/L pyromellitic acid, F_i = 0 and 5 mg/L (a) residual aluminum concentration F_i = 0 mg/L, (b) percent organic removed F_i = 0 mg/L (c) residual aluminum concentration F_i = 5 mg/L, (d) percent organic removed F_i = 5 mg/L, (e) percent fluoride removed F_i = 5 mg/L.

Phthalic acid, unlike salicylic and pyromellitic, is proposed to form more outer-sphere than inner-sphere bonds with the precipitated aluminum oxide at near neutral pH. These proposed outer-sphere bonds appear to have a greater influence on residual aluminum concentrations than affinity of the organic for removal. In Figure 7-8a, the residual aluminum concentrations of a phthalic only system presented no clear trend over the 8-hour experiment. At doses of 200 mg/L alum and less, aluminum residuals generally increase over time, consistent with the results from the other two organic acids. Only the 100 mg/L alum dose showed any significant fluctuation in residual aluminum concentrations over the observed period, but this is most likely a result of the experimental pH changing. After the 1 hr 10 min, the pH was measured as 6.3 and increased to 6.51 for the remainder of the experiment. The increased pH would result in increased precipitation. Once at 6.51, the pH did not change and neither did the residual aluminum concentrations for the 100 mg/L alum dose jar. At alum doses greater than 200 mg/L alum, little to no effect on residual aluminum concentrations are observed. Residual concentrations of phthalic acid, on the other hand, fluctuate greatly over the entire alum dose range and the 8-hour experiment as shown in Figure 7-8b. The residual phthalic acid concentrations increase over the time period (shown as a decrease in removal in Figure 7-8b), with changes as great as 15% less by the conclusion of the experiment. Percent organic removed decreased after the first 1 hr 10 min of contact, but fluctuated after that initial reduction in removal and showed no definitive trend. The fluctuations were most likely due to the variation in pH (+/- 0.34) between jars and over the entire time analyzed, suggesting that the process, even at near neutral pH, is extremely sensitive to pH.

When phthalic acid is included in the dual ligand experiments with fluoride, residual aluminum concentrations no longer follow a decreasing trend with time. In Figure 7-8c, the aluminum concentrations increase over time for all alum concentrations

except the highest used (500 mg/L alum). Focusing on what has been considered a low alum dose throughout this work, less than 200 mg/L alum dose, the dual ligand system with phthalic acid and fluoride greatly increase residual aluminum concentrations with as much as a 40 μMol Al increase (1.1 mg/L Al) for the 50 mg/L alum dose. This increase in aluminum concentrations violates the SMCL for aluminum by the conclusion of the experiment. Phthalic acid is the only LMW organic that is proposed as binding primarily through outer-sphere associations. The outer sphere bonding was possibly the cause for the different residual aluminum trends when fluoride was present. Outer-sphere bonding can locally lower the effective electrical charge of a positively charged mineral surface, increasing proton concentrations in the diffuse electrical double layer, and, thereby, increasing the rate of protolytic attack on bridging metal-oxygen bonds (Johnson et al. 2004). Fluoride has been reported to enhance the reactivity of the Al(III)-O bond, similar to labilization impacts for ligands (Phillips et al. 1997). It is believed that the incorporation of fluoride into the precipitate reduced the bond strengths of terminal water molecules and the outer-sphere, electrostatic bonding of phthalic acid is able to labilize the water molecules and promote dissolution

The residual ligand concentrations are, again, more complicated to interpret. Phthalic acid removals, Figure 7-8d, generally decreased over the entire 8-hour experiment; however, there is no definitive trend across the time intervals other than the general decrease in concentration from 1 hr 10 min to 8 hr. The fluoride removal data, Figure 7-8d, shows a general increase in removal (decrease in residual concentrations) over the entire alum dose range except for the two lowest doses tested. Percent fluoride removed, Figure 7-8e, increased with time at the coagulant doses greater than 50 mg/L alum. At doses less than 50 mg/L alum, the aqueous aluminum-fluoride complexes could have prevented continued removal as more aluminum was dissolved from the solid. Since

fluoride removal was not diminished as residual aluminum concentrations increased, it is believed that proton promoted dissolution did not use fluoride in completing the coordination spheres of aluminum as dissociation occurred.

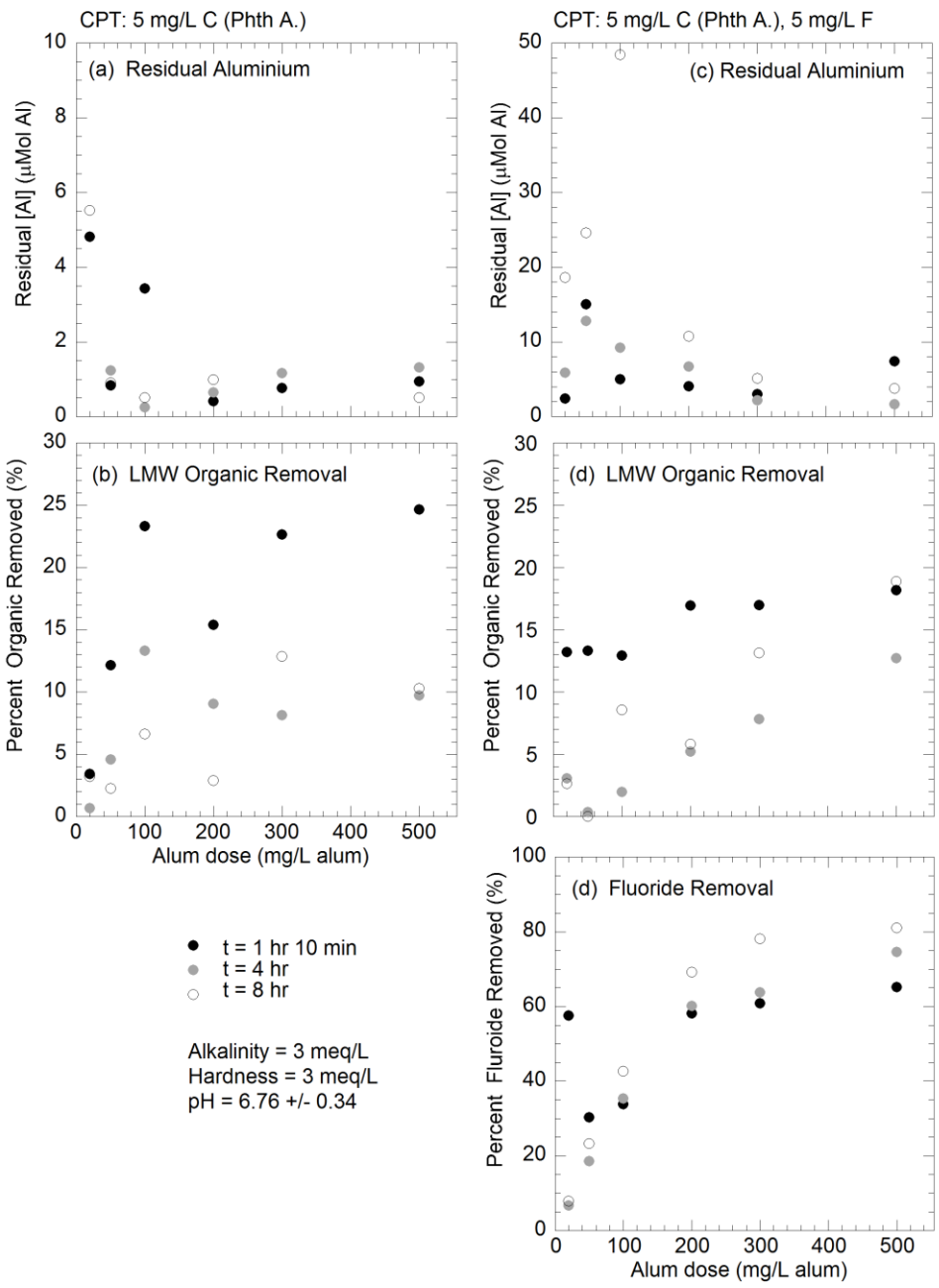

Figure 7-8: Solubility of CPT aluminum precipitates over a range of coagulant doses, C_i=5 mg/L phthalic acid, F_i = 0 and 5 mg/L (a) residual aluminum concentration F_i = 0 mg/L, (b) percent organic removed F_i = 0 mg/L (c) residual aluminum concentration F_i = 5 mg/L, (d) percent organic removed F_i = 5 mg/L, (e) percent fluoride removed F_i = 5 mg/L..

To compare the CPT aluminum results to PRE and T-PRE data gathered as part of this work, the residual aluminum data was plotted vs. time for the two coagulant doses closely investigated as part of this work: 100 mg/L alum and 200 mg/L alum (Figure 7-9a-b and Figure 7-9c-d, respectively). To highlight the increasing residual aluminum data associated with the phthalic acid and fluoride system, phthalic acid data are plotted separately for each coagulant dose. The residual aluminum for the 100 mg/L alum coagulant dose and the dual phthalic acid and fluoride system required a larger scale in order to plot the 8 hour data point close to 50 μMol residual aluminum (Figure 7-9b). The residual aluminum concentrations for the 100 mg/L alum systems containing fluoride and LMW organics (Figure 7-9a) were similar to those measured during the PRE experiments with concentrations approximately 13 μMol after 1 hr 10 mins and steadily decreased to approximately 5 μMol after 8 hours. The fluoride only experiments had less residual aluminum concentrations over the entire CPT range than in the PRE experiments, suggesting that incorporation of fluoride is more stable and occurs at the time of precipitation during the CPT while aqueous fluoro-aluminum complexes maintain a higher residual aluminum concentration in the PRE systems.

The residual aluminum concentrations for the 200 mg/L alum, Figure 7-9c-d, further illustrate that as the concentrations of alum dose are increased, the associated effects of the ligands, especially fluoride, on residual concentrations are diminished. While the trends for the organic acids with fluoride, Figure 7-9c, and those for phthalic acid with fluoride, Figure 7-9d, are similar to the rest of the results presented, the concentrations are lower. The decrease in the overall trend makes it easier to ignore the impacts of the organic acids and fluoride on aluminum precipitation; however, at concentrations less than 200 mg/L alum (alum doses considered more typical of a

treatment plant), the associated effects of inner- and outer-sphere bonded organics and fluoride are more obvious. These results further the conclusion that it is important to consider concentrations relevant to treatment when conducting these experiments.

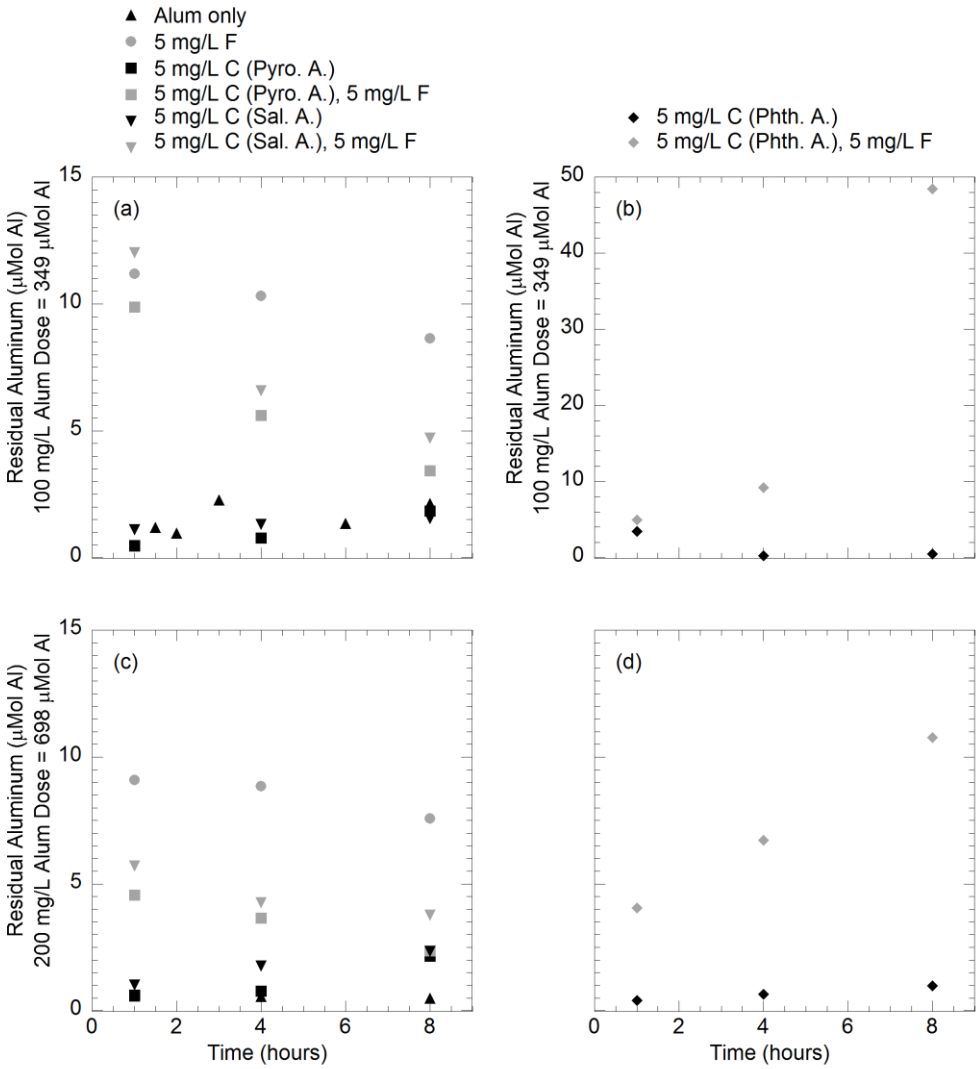

Figure 7-9: Comparison of CPT aluminum solubility for select coagulant doses: 100 mg/L (a, b) and 200 mg/L (c, d) alum doses. Residual aluminum concentrations in the phthalic acid systems are plotted separately to highlight the dissolution effects of a phthalic and fluoride CPT system (b, d).

7.5 CONCLUSIONS

Salicylic acid (proposed inner-sphere complexes) and pyromellitic acid (proposed mixed inner- and outer-sphere, primarily inner-sphere complexes) do not have significant differences for the dissolution of aluminum in the co-precipitated system, contrary to what has been reported in the past for systems using crystalline aluminum oxides. The work of Yoon et al. (2005), in which aluminum dissociation is used as an indicator of inner- or outer-sphere complexation, does not apply when the solids are co-precipitated and when organics are co-precipitated in the presence of fluoride. When fluoride is present, precipitation is not only reduced due to aqueous complexation but precipitation appears to continue to occur over time as well. Only phthalic acid experiences ligand-promoted dissolution in the presence of fluoride in the co-precipitation system.

Outer-sphere bonding caused an accelerated detachment of aluminum due to a lowered effective electrical charge generated by positively charged mineral surfaces and ions in the Stern layer (Johnson et al. 2004). The reduction of charge in the Stern layer promoted increased proton concentrations in the diffuse electrical double layer, increasing the rate of protolytic attack on bridging metal-oxygen bonds (Johnson et al. 2004). Fluoride has been reported to enhance the reactivity of the Al(III)-O bond, similar to labilization impacts for ligands (Phillips et al. 1997). It is believed that the incorporation of fluoride into the precipitate reduced the bond strengths of terminal water molecules and the outer-sphere, electrostatic bonding of phthalic acid is able to labilize the water molecules and promote dissolution. The phthalic acid-fluoride, dual ligand CPT scenario examined as part of this research is the only combination where the fluoride chemistry was not the sole dictating factor on the residual aluminum concentrations. The

ability of NOM to form inner- versus outer-sphere complexes with the formed aluminum flocs during alum coagulation will impact the residual aluminum concentrations as a function of detention time in produced drinking water. The complexity of NOM creates a concern that, if the NOM in the system is outer-sphere oriented at near neutral pH, elevated levels of aluminum might be present in the treated water.

From Chapter 5, pyromellitic acid, a primarily inner-sphere organic acid, closely modeled Lake Austin NOM in multi-ligand systems in competition with fluoride for co-precipitation and removal. By extension, it is concluded that NOM would not experience ligand-promoted dissolution. Additional research is required to test the applicability of pyromellitic acid as an NOM surrogate and its impact on dissolution.

Chapter 8: Conclusions

The goals of this study were to (1) evaluate how co-precipitating aluminum solids in the presence of fluoride affects the characteristics of the solid precipitate, (2) evaluate the effect of a co-precipitating solid on removal and competition of low molecular weight organics and fluoride, (3) evaluate the effect of a co-precipitating solid on removal and competition of natural organic matter and fluoride, and (4) evaluate the stability of co-precipitated aluminum in the presence of low molecular weight organics and fluoride.

8.1 Fluoride Co-Precipitation

This research verified the presence of a co-precipitate in the presence of fluoride at alum doses that are relevant to water treatment processes; that is fluoride is incorporated into a solid that is predominantly $Al(OH)_{3(s)}$. Determination of precipitate structure from an amorphous solid is not a straightforward process. Conclusions regarding the precipitate were only possible after the analysis of the combined results from several types of measurements because the amorphous characteristics of the precipitates obscured many of the results or conclusions from particular analyses.

In the presence of fluoride, the flocs formed were smaller in diameter, higher in specific surface area, and more negatively charged than those formed in the absence of fluoride. Further, the Al-F bond strength increased with increasing fluoride. These results are consistent with conclusions from previous studies suggesting that fluoride occupies edge and bridge sites in the amorphous oxide structure when a co-precipitate is formed. The data from this dissertation supports the previous work in that replacement of hydroxyl ions by fluoride ions at these bonding sites inhibited bridging hydroxyl bonds from forming, creating a smaller precipitate with a greater surface area.

Removal of fluoride was greater in the co-precipitation system than in a system with preformed $Al(OH)_{3(s)}$ that minimizes co-precipitation; therefore, it is extremely important that treatment predictions are not extrapolated from adsorption-based laboratory research to coagulation-based treatment schemes. Using adsorption-only data will result in an underestimation of removal and, most likely, excess chemicals being used during treatment.

The changing particle and floc sizes caused by fluoride incorporation into the precipitate can potentially lead to detrimental water quality with regard to parameters other than fluoride residual concentrations in treated water. The decreased particle size has the potential to limit particle-particle collisions in systems, leading to less floc growth and a potential decrease in the ability of the flocs to settle. When turbidity was included in the experiments, the presence of fluoride meant that more aluminum coagulant was required to reduce turbidity to less than 2 NTU. Fluoride decreased the surface charge of the particles formed during co-precipitation due to a change in the precipitate structure and surface binding sites on the aluminum surface.

8.2 Effect of a Co-Precipitating Solid on Removal and Competition of Low Molecular Weight Organics

Pyromellitic acid achieved over 90% removal in a co-precipitating system at alum doses greater than 100 mg/L alum. When adsorption only was considered in the PRE experiments in which ligands were added after $Al(OH)_{3(s)}$ had precipitated, pyromellitic acid removals decreased by 60%. In the presence of fluoride, there was a significant decrease in removal of pyromellitic acid, believed to be directly related to competition with fluoride in the removal methods. In these dual ligand systems, pyromellitic acid removals decrease due to a reduction in co-precipitation of the organic acid and reduction

in adsorption as fluoride competes for co-precipitation with aluminum and for adsorption sites on the formed aluminum hydroxide surface. There was also an impact of the pyromellitic acid on fluoride co-precipitation, and the presence of both ligands led to less fluoride co-precipitation with aluminum. The lack of impact on removal by either salicylic acid or phthalic acid suggests that neither of these molecules are significantly co-precipitated and their bonding mechanism during adsorption is different from that of fluoride.

Salicylic acid and pyromellitic are reported to form both inner and outer sphere surface complexes on iron and aluminum oxides at neutral pH, but are predominantly inner-sphere at a pH of 6. In contrast, phthalic acid also forms inner and outer-sphere surface complexes with aluminum oxide surfaces, but is predominantly outer-sphere above pH 5. However, the impact of fluoride on these organic acids appears to be more highly dependent on the functional groups on the organics rather than their inner vs outer sphere coordination. Phthalic acid removal is slightly greater than salicylic acid removal even though it undergoes a greater degree of outer sphere coordination. Pyromellitic acid is the only organic acid tested that achieved removals over 30%. Removal appears to be dependent on the number of carboxylic groups, as indicated by comparison of surface coverage from precipitates formed from 200 mg/L alum at pH 6.5. The coverage increased in accordance with increasing carboxylic group: salicylic acid with one carboxylic group (1.28 molecules/nm^2) to phthalic acid (1.67 molecules per nm^2) to pyromellitic acid (5.55 molecules/nm^2). All of the carboxylic groups are deprotonated at pH 6.5, so the molecules have increasing negative charge with increasing carboxylic groups.

8.3 Competition Between Fluoride and Natural Organic Matter and the Ability to Model Removal using a Low Molecular Weight Organic Acid

To examine the competition between fluoride and isolated fractions of NOM from Lake Austin, several experiments were required. The behavior and chemical competition are different for low and high ranges of alum doses administered during treatment. In CPT systems operated at alum doses less than 200 mg/L alum (low doses), NOM was preferentially precipitated but still experienced lowered removal due to competition in systems in which fluoride was present. The preferential NOM co-precipitation appeared to inhibit fluoride co-precipitation in the dual ligand system. When the alum doses increased so that the system was no longer limited by available aluminum, NOM removals with and without fluoride converged and plateaued at a maximum removal while fluoride removals remained impacted by NOM competition.

Pyromellitic acid only accurately, mimicked NOM behavior in the low alum coagulant dose ranges of 100 mg/L alum or less. At doses above 100 mg/L, NOM removal and pyromellitic acid removal both plateau at a maximum value; however, the maximum removal for pyromellitic acid is near 100% while that of NOM was only 80%. At these higher alum doses, the use of pyromellitic acid as a surrogate is no longer consistent with NOM as pyromellitic acid will over-predict organic removal; however, the competition with respect to fluoride removal remains similar over the entire alum range tested. Given this information, the surface adsorption of fluoride on the precipitated aluminum solids is most likely impacted in both systems due to the negative charge imparted by the organics. Future research analyzing pyromellitic acid as a model compound for NOM, including a wider range of alum doses for surface characterization and surface charge analysis, is needed. The microscopic analysis of the oxide structure,

before and after aging, for precipitates formed in the presence of NOM would greatly help with the analysis of pyromellitic acid as a viable surrogate.

8.4 Stability and Dissolution of Amorphous Aluminum Precipitates

Salicylic acid and pyromellitic acid do not show significant differences in residual aluminum over time despite the differences in percent organic removed for each; therefore, the stability of the bonds must be more closely related to bonding mechanisms with the aluminum precipitates than the percent coverage achieved by the organic during removal. When fluoride was present, considerable dissolution occurred after 1 hr 10 min, but then re-precipitation proceeded. The residual fluoride concentrations for the PRE system were greater than in the CPT system after 1 hr, suggesting dissolution of the preformed aluminum solids occurred after addition of fluoride.

Phthalic acid is the only LMW organic acid tested for which literature data suggested outer-sphere bonding at pH 6.5 with aluminum oxide surfaces and is the only organic acid tested that experienced increasing aluminum concentrations in the presence of fluoride in the co-precipitation system. It is believed that the increasing aluminum concentrations with time are from proton-promoted dissolution that has been accelerated. The accelerated detachment of aluminum was due to the outer-sphere bound phthalic acid creating a lowered effective electrical charge generated by positively charged mineral surfaces and ions present in the Stern layer (Johnson et al. 2004). The reduction of charge in the Stern layer promoted increased proton concentrations in the diffuse electrical double layer, increasing the rate of protolytic attack on bridging metal-oxygen bonds (Johnson et al. 2004). Fluoride has been reported to enhance the reactivity of the Al(III)-O bond, similar to labilization impacts for ligand enhanced dissolution (Phillips et al.

1997). The incorporation of fluoride into the precipitate reduced the bond strengths of terminal water molecules and the outer-sphere, electrostatic bonding of phthalic acid is able to labilize the water molecules and promote dissolution. It was proposed that this was not observed in the other systems, especially the pyromellitic acid system, due to the competition for the surface adsorption sites and aluminum co-precipitation with the, inner-sphere, organic acid.

It is important to understand the dominant bonding mechanisms of NOM to avoid elevated aluminum residual concentrations in the presence of fluoride. Furthermore, treatment plants with fluoride present must closely monitor residual aluminum concentrations since concentrations were highest after 1 hour 10 min for most systems with fluoride and amorphous precipitates.

8.5 IMPLICATIONS FOR DRINKING WATER TREATMENT PLANTS

The ability of NOM to form inner- versus outer-sphere complexes with the formed aluminum flocs during alum coagulation will impact the residual aluminum concentrations in produced drinking water as a function of detention time. If the NOM in the system is outer-sphere oriented at near neutral pH, aluminum dissolution is more likely, requiring plant operators to continuously monitor the residual aluminum concentrations (regulated by a SMCL) at their treatment facility, particularly if longer detention times are utilized.

Incorporation of NOM or fluoride into the precipitating aluminum hydroxide can have significant influence on treatment depending on the coagulant dose applied. The effects of fluoride on the aluminum co-precipitate is most apparent at environmentally relevant and treatment relevant ratios of Al:F captured by alum doses equal to or less than

200 mg/L alum in this research. At the lower alum doses, fluoride imparted a negative charge on formed precipitates at near neutral pH and detrimentally affected particle removal. The presence of fluoride also created a larger demand for the alum coagulant to achieve turbidity < 2 NTU. The measured differences in particle size and OH^- replacement indicated that co-precipitate formation was diminished at high alum doses; therefore, it is necessary to study the impact of fluoride on alum coagulation at these relevant aluminum-fluoride ratios. The change in the aluminum precipitate properties can potentially lead to detrimental water quality with regard to parameters other than high residuals of fluoride in treated water. For example, plants operating alum coagulation with low doses of alum and the presence of fluoride in the influent water should closely track the residual aluminum concentrations in produced water.

The ability to achieve adequate fluoride, NOM, and turbidity removal will be a challenge for treatment plants if/when the EPA MCL for fluoride is reduced.

8.6 FUTURE WORK

Future work further investigating the precipitate characteristics of $Al(OH)_{3(s)}$ co-precipitated with fluoride and NOM is needed. This research focused largely on understanding the role of fluoride in co-precipitation and resulting competition with organics due to the co-precipitate. The surface of the precipitate and the mechanisms through which an amorphous, aluminum-fluoride solid can be represented in a chemical model is lacking.

Using LMW organic as surrogates for complicated NOM is a promising approach; however, a method of determining which LMW organics are best for the given NOM of one's area has not been defined. If a definitive analysis method of the local

NOM is determined, then extrapolation of conducted research using LMW organic surrogates could occur. Further analysis of the use of pyromellitic acid to model Lake Austin NOM is needed as well, especially regarding turbidity removal and zeta potential measurements.

Fluoride's occurrence in the environment is not diminishing; rather, as Christian et al. (2011) proved, it is increasing even in areas not geologically prone to elevated levels of fluoride, and we can only expect it to continue to increase. If fluoride continues to accumulate in the environment from natural or anthropogenic causes and/or the regulated MCL is reduced to align with both the WHO limits and U.S. fluoridation limits at treatment plants, fluoride treatment will be required for more than just those located over contaminated groundwater. Tracking aqueous aluminum species, AlF_x complexes, and residual, free fluoride and aluminum concentration is necessary. The associated health effects of complexed Al-F species on the development of Alzheimer's Disease and other detrimental conditions will help inform decisions regarding proper treatment and regulation of fluoride in the future.

Fluoride remains an interesting contaminant since it is supplemented into people's diet to promote healthy bone and teeth, but we must ask how much is enough. Increasing fluoride in the wastewater and water-reuse stream will increase concentrations in the environment. The treatment of fluoride and natural organic matter must continue to be researched and defined. The pathways of removal for fluoride and the organics were inferred largely from the suite of tests performed. Direct analysis of the preformed precipitate would provide more detailed confirmation of the removal pathways and bonding mechanisms proposed by this research.

Appendix

Appendix 1: Fourier Transform Infrared (FTIR) Spectroscopy

A-1.1 Background

Researchers have had success using ATR-FTIR spectra to look at single ligand and competitive, two ligand adsorption onto oxides over a wide pH range (Axe et al. 2006; Liendergren and Persson 2010; Noren and Persson 2007; Yoon et al. 2004; Yoon et al. 2005; Johnston et al. 2004a, Johnson et al. 2004b; Johnson et al. 2005). Lindergren and Persson (2010) have been able to use ATR-FTIR to test benzenecarboxylic acids possessing 1- to 5- functional groups to show the importance of type and position of functional groups in surface bonding to goethite and competition with phosphate for adsorption. Their research concluded that the competition for hydrogen bonding sites, and not inner sphere surface sites, were what determined the removal of ligands during competitive adsorption. As functional groups increased to three or more, adsorption became more favorable, a conclusion also drawn by Evanko and Dzombak (1998).

Described in this appendix is the FTIR analysis of the removal process when amorphous (co-)precipitates are formed during alum coagulation.

A-1.2 Research Approach

Several attempts were made by this research to analyze the formed co-precipitates and adsorption onto aluminum hydroxide precipitates by several Fourier Transfer Infrared (FTIR) (Bruker IFS 66v/S) analyses. The Bruker IFS 66v/S is a vacuum pump system that decreases the background peaks associated with carbon dioxide. Liquid

nitrogen was used to cool the detectors and purge the system of carbon dioxide. After filling the chamber with liquid nitrogen, the system was allowed 15-20 minutes to reach thermal stability. Initial analysis of the precipitates used attenuated total reflectance (ATR), however this wet-mount method did not produce peaks that were identifiable due to the interaction with water. Two different ATR holders, a zinc selednide (ZnSe) and germanium (Ge) were used in an attempt to obtain spectra with limited noise. Even after subtraction of the water peaks was attempted, this method of analysis did not produce any useable results.

Freeze dried solids were stored in desiccators for analysis by Fourier Transfer Infrared (FTIR) (Bruker IFS 66v/S, Ettlingen, Germany) transmission and diffuse reflectance spectroscopy (DRIFTS). Freeze dried samples intended for analysis by DRIFTS and transmission FTIR were subjected to a standard KBr preparation technique (Smith 1996). The dried precipitate solids and oven dried KBr were ground separately using an agate mortar and pestle and then combined in mix ratios by agitation with a spatula. Using this approach, the sample and KBr were mixed, but the grinding time was not increased so as to control experimental fluctuations. Initial mix ratios varied from 0.01%-1% precipitate and KBr to test peak strength and minimize required precipitate mass. A final mix ratio of 0.1% was used in the pressed pellets.

The DRIFTS samples were placed in the sample cup and the edge of the spatula drawn across the top one time to create a level surface. All FTIR spectra were collected at 4 cm^{-1} resolution for approximately 40-400 scans per spectrum with scans adjusted as necessary. This technique is similar to that followed by Yu et al (2007). DRIFTS analysis produced spectra that contained a substantial amount of interference from the matrix water and amorphous composition of the solids. Transmission analysis used samples pressed into KBr-sample disks using a hydraulic press and stored on 9.5 mm Econo

Cards for transfer and storage. The transmission data produced useable data in the fingerprint region of 1500-650 cm^{-1} and in the region of 2000-1500 cm^{-1}. In 2000-1500 cm^{-1}, principal bands due to the C=C and C=O were analyzed. Any peaks, however, contained in the 2500-4000 cm^{-1} region were obscured by the large characteristic O-H stretching in the 3200-3650 cm^{-1} range and not used for analysis.

A-1.3 RESULTS AND DISCUSSION

The spectra produced by DRIFT spectroscopy was collected in Kubelka-Munk units following the Kubelka and Munk theory developed to describe diffuse reflectance process for powdered samples (Stuart 2004). The spectra were not well resolved below 1300 cm^{-1}. The best results were obtained using the hydraulic press to create the KBr pellets and analyzing the solids as transmission spectroscopy. Minimal corrections and processing were performed on collected spectra and, when processes such as baseline corrections, were used, consistency was ensured. The spectra comparing corundum to precipitated aluminum solids are presented in Figure A1-1. The grey lines overlaying the figure mark the peaks of the corundum. Corundum spectra can range in resolution, especially in the "fingerprint" region of less than 1500 cm^{-1} (van der Marel and Beutelspacher 1976). The most resolved peaks should occur at approximately 595, 640, and 775 cm^{-1}. In the acquired spectrum, only the 640 and 775 cm^{-1} peaks are present. The peak around 1025 cm^{-1} is only present in spectra acquired by other researchers (van der Marel and Beutelspacher 1976).

When compared to the precipitates formed from 200 mg/L alum, the peaks shift slightly. The strongest peak occurs at 600 cm^{-1}, but resolution below 500 cm^{-1} was too poor to determine peaks in this lowest range. The peak present in the corundum at around

1025 cm^{-1} was more defined in the formed precipitate and is a strong peak often associated with boehmite.

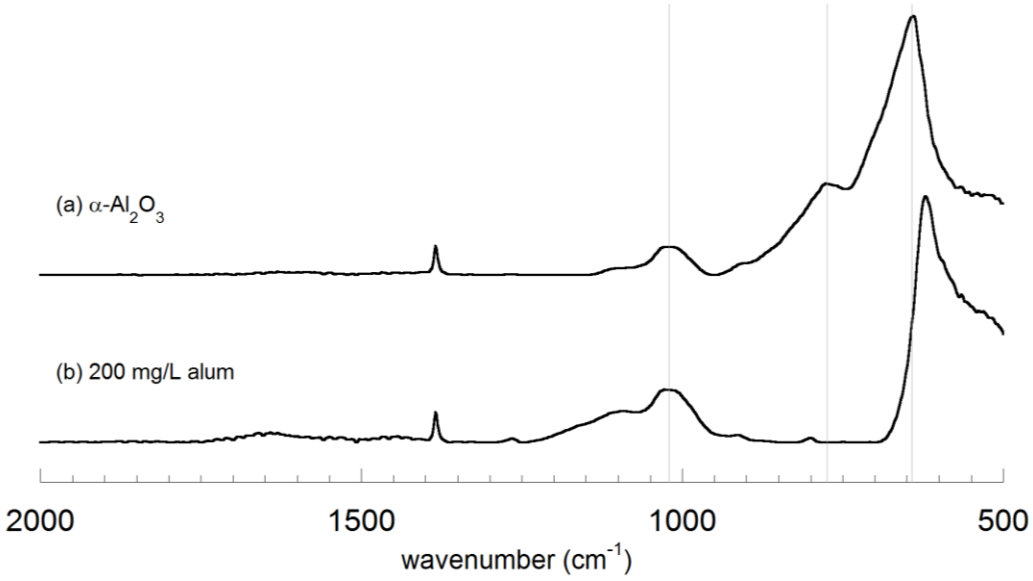

Figure A1-1: FTIR spectra for corundum and precipitated aluminum solids from 200 mg/L alum.

Using Figure A1-1b as a reference, the formed spectrum collected from the formed co-precipitates can all be compared to analyze for structural changes. The analysis of amorphous precipitates is not common and, therefore, does not have good reference spectra for comparison. The work done by Gong et al. (2012) does provide a set of data for comparison, but the low resolution of the acquired spectra from amorphous precipitates makes analysis difficult and conclusions are only speculations.

Figure A1-2a-e presents the data for the 200 mg/L alum only system (a) as a baseline comparison to the varying CPT and PRE systems. Focusing first on the

pyromellitic acid systems (b, d, and e), there is a set of peaks that is consistent throughout all three spectra. The peak at 1500 +/- 25 cm^{-1} is typically attributed to skeletal stretch of aromatic compounds (Smith 2011). The peak is consistent throughout all three systems with pyromellitic acid. The bond could possible account for electrostatically bound aromatic compounds, signifying outer-sphere associated pyromellitic acid. Pyromellitic acid is thought to primarily associate with aluminum through inner-sphere bonding. The small, weak signal associated with this peak is potential confirmation that pyromellitic is primarily inner-sphere and that the outer-sphere associations are not disrupted by fluoride in the system. The peeak at ~1655 (1600 in presented spectra) is associated with C=O stretch, intramolecular hydrogen bonds for aromatic compounds (Smith 2011). This peak is believed to represent the inner-sphere associations between pyromellitic acid and the aluminum surface. Presence of the 1500 cm^{-1} and 1655 cm^{-1} bands in the presence of fluoride, as shown in Figure A1-2e, suggest that the inner-sphere bonds still exists in the presence of fluoride. No significant change in spectra from CPT systems containing pyromellitic acid (Figure A1-2b) to PRE systems with pyromellitic acid (Figure A1-2d), are observed with regards to these two bonds associated with the aromatic ring.

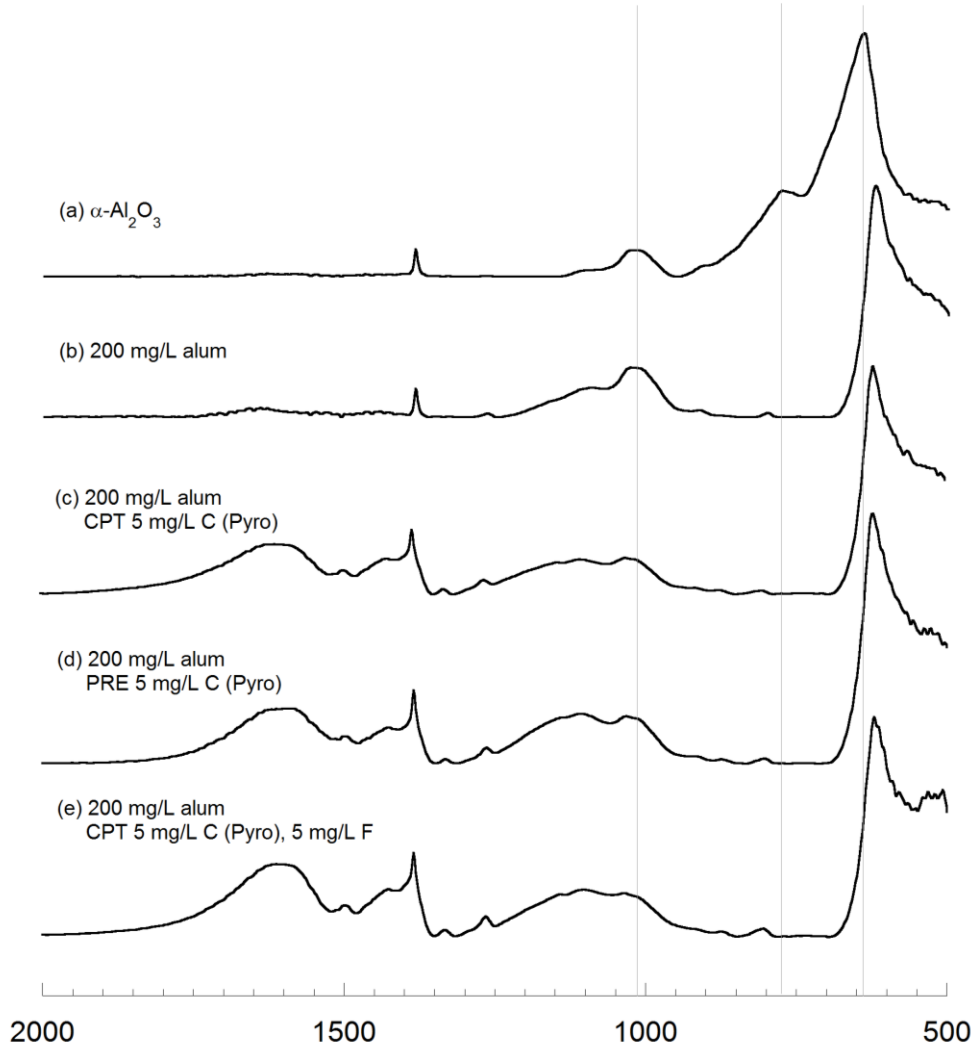

Figure A1-2: FTIR spectra of the pressed KBr pellets for precipitates formed by 200 mg/L alum. (a) 200 mg/L alum only, (b) CPT with 5 mg/L C from pyromellitic acid, (c) CPT with 5 mg/L F, (d) PRE with 5 mg/L C from pyromellitic acid, and (e) CPT dual ligand system with 5 mg/L F and 5 mg/L C from pyromellitic acid.

The strongest peaks associated with the aluminum (O…OH) related peaks are the two present at 1125 cm^{-1} and 1625 cm^{-1}. It is believed that the 1125 cm^{-1} peak represents

strong surface water bonds and the 1625 cm^{-1} peak is associated with the weaker, surface bound OH^- since it is not present in the corundum spectra (Figure A1-1a). Focusing first on the peak at 1125 cm^{-1}, several shifts occur when different ligands are present and the systems are operated as CPT or PRE systems. The peak significantly shifts to a higher wavenumber in the presence of fluoride in the CPT system (Figure A1-2c). This shift potentially represents the formation of different bonds in the precipitant than the typical O…OH bonds; however, more analysis and FTIR work with the formed precipitates is needed to confirm. In the pyromellitic acid only systems, the 1125 peak is present in both the CPT (Figure A1-2b) and PRE (Figure A1-2d) systems, but is significantly diminished in the CPT system. This decrease in the peak intensity hints at more inner-sphere, strong bonds with pyro forming during CPT and the displacement of the aluminum (O…OH) bonds.

The peak at 1625 cm^{-1} only observed in CPT, fluoride only system (Figure A1-2c). It is possible that this peak is present, but very weak, in systems containing pyromellitic acid and obscured by the peaks associated with the aromatic ring.

A-1.4 CONCLUSIONS

Work is often conducted using FTIR as an analysis tool to interpret inner- or outer-sphere associations with metal oxide structures (i.e., Noren and Persson, 2007; Wang et al. 2003; Nakamoto 2008; Johnson et al. 2004; Yoon et al. 2004; Hwang et al. 2007). Those researchers using FTIR as an analysis of precipitated aluminum, age the precipitates for increased resolution of peaks (Violante and Huang 1985; Xu et al. 2010; Yu et al. 2007). The use of this analysis on amorphous precipitates requires further method development before making definitive conclusions. There are slight, qualitatively

observed, shifts in the spectra comparing single and dual ligand systems and PRE and CPT experimental systems; however, they are not as definitive as the results presented in Chapter 4 supporting the formation of a fluoride co-precipitate. FTIR remains a valid tool for analysis of oxide structures, but is not viable to reliably analyze bonding associations with amorphous precipitates.

References

Aiken, G.R., McKnight, D.M., Thorn, K.A, & Thurman, E.M. (1992). Isolation of hydrophilic organic acids from water using nonionic macroporous resins. *Organic Geochemistry, 18*(4), 567-573.

Ainsworth, C., Friedrich, D., Gassman, P., Wang, Z., & Joly, A. (1998). Characterization of salicylate-alumina surface complexes by polarized fluorescence spectroscopy. *Geochimica et Cosmochimica Acta*, *62*(4), 595-612.

Amirtharajah, A., & Mills, K.M. (1982). Rapid-mix design for mechanisms of alum coagulation. *Journal (American Water Works Association), 74*(4), 210-216.

Aoba, T., & Fejerskov, O. (2002). Dental fluorosis: Chemistry and biology. *Critical Review of Oral Biological Medicine, 13*, 155-170.

Arora, H., LeChevallier, M., & Dixon, K. (1997). DBP occurrence survey. *Journal (American Water Works Association), 89*(6), 60-68.

Beltrán-Aguilar, E., Barker, L., & Dye, B. (2010). *Prevalence and Seveity of Dental Fluorosis in the United States, 1999-2004*. National Center for Health Services Data Brief, *53*, 1-8.

Benjamin, M. & Lawler, D. (2012) *Water Quality Engineering: Physical/Chemical Treatment Processes*. Wiley, N.Y., N.Y. (in final preparation)

Biber, M., & Stumm, W. (1994). An *In-Situ* ATR-FTIR Study: The Surface Coordination of Salicylic Acid on Aluminum and Iron(III) Oxides. *Environmental Science Technology*, *28*(5), 763-768.

Black, G.V., & Mckay, F. (1916). Mottled Teeth: An Endemic Developmental Imperfection of the Enamel of the Teeth Heretofore Unknown. *Dental Cosmos 58*, 129-156. (accessed May 20, 2007).

Bose, P., & Reckhow, D.A. (1998). Adsorption of natural organic matter on preformed aluminum hydroxide flocs. *Journal of Environmental Engineering*, *124*(9), 803-811.

Burdon, J. (2001). Are the Traditional Concepts of the Structures of Humic Substances Realistic? *Soil Science*, *166*(11), 752-769.

Carton, R.J. (2006). Review of the 2006 United States National Research Council Report: Fluoride in drinking water. *Fluoride, 39*(3), 163-172.

Center for Disease Control and Prevention (CDC). (2006). *Community Water Fluoridation.* http://www.cdc.gov/fluoridation/statistics/2006stats.htm. (accessed July 12, 2011)

Cho, J., Amy, G., & Pellegrino, J. (1999). Membrane filtration of natural organic matter: Initial comparison of rejection and flux decline characteristics with ultrafiltration and nanofiltration membranes. *Water Research*, *33*, 2517–2526.

Christian, L.N., Banner, J.L., & Mack, L.E. (2011). Sr isotopes as tracers of anthropogenic influences on stream water in the Austin, Texas area. *Chemical Geology, 282*, 84-97.

Churchill, H.V. (1931). Occurrence of fluorides in some waters of the United States. *Industrial and Engineering Chemistry, 23*, 996-998.

City of Midland. (2000-2008). *Water Quality Reports*. http://www.midlandtexas.gov/ (accessed on 22 October 09).

Crapper McLachlan, D. C. (1986). Aluminum and Alzheimer's Disease. *Neurobiology and Aging*, *7*, 525-532.

Davis, J. (1982). Adsorption of natural dissolved organic matter at the oxide/water interface. *Geochimica et Cosmochimica Acta*, *46*, 2381-2393.

Dean, H.T. (1934). Classification of Mottled Enamel Diagnosis. *Journal of the American Dental Association, 21*, 1421-1426.

Dean, H.T., Arnold, F.A., & Evolve, E. (1942). Domestic water and dental caries. *Public Health Reports, 56*, 761-792.

Dempsey, B., Hueymeei, S., Tanzeer Ahmed, T.M., & Mentink, J. (1985). Polyaluminum chloride and alum coagulation of clay-fulvic acid suspensions. *Journal (American Water Works Association)*, *77*(3), 74-80.

Dempsey, B.A., Ganho, R.M., & O'Melia, C.R. (1984). The Coagulation of Humic Substances by Means of Aluminum Salts. *Journal (American Water Works Association)*, *76*(4), 141-150.

Dentel, S. K. (1988). Application of the Precipitation-Charge Neutralization Model of Coagulation. *Environmental Science and Technology*, *22*, 825-832.

Department of Health and Human Services. (1993). *Fluoridation Census,* Department of Health and Human Services: Atlanta, Georgia.

Ding, L., Marinas, B.J., Schideman, L.C., & Snoeyink, V.L. (2006). Competitive effects of natural organic matter: parametrization and verification of the three-component adsorption model COMPSORB. *Environmental Science & Technology*, *40*(1), 350–356.

Drever, J., & Stillings, L. (1997). The role of organic acids in mineral weathering. *Colloids and Surfaces A: Physicochemical and Engineering Aspects*, *120*, 167-181.

Driscoll, C.T., Baker, J.P., Bisogni, J.J., & Schofield, C.L. (1980). Effect of aluminium speciation on fish in dilute acidified water. *Nature*, *284*, 160-164.

Edzwald, J.K. (1993). Coagulation in drinking water treatment: particles, organics, and coagulants. *Water Science and Technology, 27*(11), 21-35.

Edzwald, J.K., & Van Benschoten, J.E. (1990). Aluminum Coagulation of Natural Organic Matter. In *Chemical Water and Wastewater Treatment,* Eds. H.H. Hahn and R. Klute. Pp 341-359.

Eggleton, R. A. & Fitzpatrick, R. (1988). New data and a revised structural model for ferrihydrite. *Clays & Clay Minerals*, *36*, 111-124.

Elliott, J. C. (1994). *Structure and Chemistry of the Apatites and Other Calcium Orthophosphates*, New York: Elsevier Science Pub Co.

Environmental Protection Agency (EPA). (1999). *Enhanced Coagulation and Enhanced Precipitative Softening guidance manual*, 815-R-99-012 ed. EPA, Office of Water: Environmental Protection Agency, 1999.

Environmental Protection Agency (EPA). (2003). *Six-year review chemical contaminants health effects technical support document*, 822-R-03-008 ed. EPA: Environmental Protection Agency, 2003.

Environmental Protection Agency (EPA). (2007). "EPA Ground Water & Drinking Water." US Environmental Protection Agency. http://www.epa.gov/ogwdw000/hfacts.html (accessed July 27, 2010).

Environmental Protection Agency (EPA). 2010. *Secondary Drinking Water Regulations: Guidance for Nuisance Chemicals*. EPA 816-F-10-079. *http://water.epa.gov/drink/contaminants/secondarystandards.cfm.*

Environmental Protection Agency (EPA). 2010b. *Fluoride: Dose-response analysis for non-cancer effects*. EPA Health and Ecological Criteria Division. 820-R-10-019.

Evanko, C.R., & Dzombak, D.A. (1998). Influence of structural features on sorption of NOM-analogue organic acids to geothite. *Environmental Science and Technology, 32*, 2846-2855.

Fawell, J., Bailey, K., Chilton, J., Dahi, E., Fewtrell, L. & Magara, Y. (2006). *Fluoride in Drinking-water (World Health Organization Drinking Water)*, (1 ed.). Geneva: World Health Organization.

Flaten, T. P. (2001). Aluminium as a risk factor in Alzheimer's disease, with emphasis on drinking water. *Brain Research Bulletin*, *55*(2), 187-196.

Fluoride Action Network. (n.d.) Index to natural levels of fluoride in US drinking water. *Fluoride Action Network*. Retrieved July 27, 2010, from www.fluoridealert.org/pesticides/levels/index.html

Furrer, G., & Stumm, W. (1986). The coordination chemistry of weathering: I. Dissolution kinetics of gamma-Al2O3 and BeO. *Geochimica et Cosmochimica Acta, 50*, 1847-1860.

Goldberg, S. Davis, J.A., & Hem, J.D. (1996). The surface of aluminum oxides and hydroxides. In *The Environmental Chemistry of Aluminum*, Eds G. Sposito. Lewis Publishers: Boca Raton. 271-332.

Gong, W-X, Qu, J-H, Liu, R-P, & Lan, H-C. (2012). Effect of aluminum fluoride complexation on fluoride removal by coagulation. *Colloids and Surfaces A: Plysiochemical and Engineering Aspects, 395*, 88-93.

Gregg, S. & Sing, K. (1967). *Adsorption, surface area, and porosity.* London, New York, Academic Press, 1967.

Gregg, S.J., & Sing, K.S.W. (1967). *Adsorption, surface area, and porosity.* London, New York, Academic Press, 1967.

Guan, X-H, Chen, G-H, & Shang, C. (2007). ATR-FTIR and XPS study on the structure of complexes formed upon the adsorption of simple organic acids on aluminum hydroxide. *Journal of Environmental Sciences, 19*, 438-443.

Guan, X-H, Li, D-L, Shang, C., & Chen G-H. (2006b). Role of carboxylic and phenolic groups in NOM adsorption on mineral: a review. *Water Science and Technology*, *6*(6), 155-164.

Guan, X-H, Shang, C., & Chen, G-H. (2006a). ATR-FTIR investigation of the role of phenolic groups in the interaction of some NOM model compounds with aluminum hydroxide. *Chemosphere, 65*, 2074-2081.

Gurdak, J., McMahon, P., Dennehy, K., & Qi, S. (2009). Water Quality in the High Plains Aquifer, Colorado, Kansas, Nebraska, New Mexico, Oklahoma, South Dakota, Texas, and Wyoming, 1999–2004. *U.S. Geological Survey Circular*, *1337*, 1-63.

Hao, O.J., & Huang, C.P. (1986). Adsorption Characteristics of Fluoride onto Hydrous alumina. *Journal of Environmental Engineering, 112*, 1054-1069.

Hemingway, B.S., & Sposito, G. (1996). Inorganic aluminum-bearing species. In *The Environmental Chemistry of Aluminum*, Eds G. Sposito. Lewis Publishers: Boca Raton. 81-116.

Hu, C.Y., Lo, S.L., & Kuan, W.H. (2005). Effects of the molar ratio of hydroxide and fluoride to Al (III) on fluoride removal by coagulation and electrocoagulation. *Journal of Colloid and Interface Science, 283*, 472-476.

Huang, C., & Shiu, H. (1996). Interactions between alum and organics in coagulation. *Colloids and Surfaces A: Physiochemical and Engineering Aspects, 113*, 155-163.

Huang, W-J, Fang, G-C, & Wang, C-C. (2005). The determination and fate of disinfection by-products from ozonation of polluted raw water. *Science of the Total Environment*, *354*. 261-272.

Hudak, P.F. (2009). Elevated fluoride and selenium in West Texas groundwater. *Bulletin of Environmental Contamination and Toxicology, 82*(1): 39-42.

Hunter, R.J. (2001). Measureing zeta potential in concentrated industrial slurries. *Colloids and Surfaces A: Pysiochemical and Engineering Aspects*, *195*, 205-214.

Hwang, S.H., & Lenhart, J.J. (2009). Surface complexation modeling of dual-mode adsorption of organic acids: Phthalic acid adsorption onto hematite. *Journal of Colloid and Interface Science*, *336*, 200-207.

Hwang, Y.S. & Lenhart, J.L. (2008). Adsorption of C4-dicarboxylic acids at the hematite/water interface. *Langmuir*, *24*, 13934-13943.

Hwang, Y.S., Liu, J., Lenhart, J., & Hadad, C. (2007). Surface complexes of phthalic acid at the hematite/water interface. *Journal of Colloid and Interface Science*, *307*, 124-134.

International Programme on Chemical Safety (IPCS). (2002). *Environmental Health Criteria 227: Fluorides*, Geneva: World Health Organization.

Isa, J. (2011). EPA and HHS Announce New Scientific Assessments and Actions on Fluoride. Agencies working together to maintain benefits of preventing tooth decay while preventing excessive exposure. http://yosemite.epa.gov/.(accessed 19 June 2011).

Jacangelo, J.G., DeMarco, J., Owen, D.M., & Randtke, S.J. (1995). Selected processes for removing NOM: an overview. *Journal (American Water Works Association)*, *87*(1): 64-77.

Johnson, S.B., Yoon, T.H., & Brown Jr., G.E. (2005). Adsorption of Organic Matter at Mineral/Water Interfaces: 5. Effects of adsorbed natural organic matter analogues on mineral dissolution. *Langmuir*, *21*, 2811-2821.

Johnson, S.B., Yoon, T.H., Slowey, A.J., & Brown Jr., G.E. (2004a). Adsorption of Organic Matter at Mineral/Water Interfaces. 2. Outer-sphere adsorption of maleate and implications for dissolution processes. *Langmuir*, *20*, 4996-5006.

Johnson, S.B., Yoon, T.H., Slowey, A.J., & Brown Jr., G.E. (2004b). Adsorption of Organic Matter at Mineral/Water Interfaces: 3. Implications of surface dissolution for adsorption of oxalate. *Langmuir*, *20*, 11480-11492.

Jones, E. (2010) EPA Administrator Jackson Outlines New Vision for Clean, Safe Drinking Water. Environmental Protection Agency 03/22/2010.

Kazprzyk-Hordern, B. (2004). Chemistry of alumina, reactions in aqueous solution and its application in water treatment. *Advances in Colloid and Interface Science*, *110*, 19-48.

Kitis, M., Karanfil, T., Wigton, A., & Kilduff, J.E. (2002). Probing reactivity of dissolved organic matter for disinfection by-product formation using XAD-8 resin adsorption and ultrafiltration fractionation. *Water Research*, *36*, 3834-3848.

Kraemer, S.M., Chiu, V.Q., & Hering, J.G. (1998). Influence of pH and competitive adsorption on the kinetics of ligand-promoted dissolution of aluminum oxide. *Environmental Science and Technology, 32*, 2876-2882.

Kummert R. & Stumm W. (1980). The surface complexation of organic acids on hydrous gamma-Al2O3. *Journal of Colloid and Interface Science*, *75*, 373–384.

Kwong, N., Kee, K.F., & Huang, P.M. (1981). Comparison of the influence of tannic acid and selected low-molecular-weight organic acids on precipitation products of aluminum. *Geoderma*, *26*, 179-193.

Leng, Y. (2008). Materials characterized: Introduction to microscopic and spectroscopic methods. Wiley and Sons: Singapore.

Li, Y. et al. (2001). Effect of long-term exposure to fluoride in drinking water on risks of bone fractures. *Journal of Bone and Mineral Research. 16*(5), 932-939.

Licsko, I. (1993). Dissolved Organics Removal by Solid-Liquid Phase Separation (Adsorption and Coagulation). *Water Science and Technology, 27*(11), 245-248.

Lindergren, M. & Persson, P. (2010). Competitive adsorption involving phosphate and benzenecarboxylic acids on goethite—Effects of molecular structures. *Journal of Colloid and Interface Science*, *343*, 263-270.

Lindsay, W.L., & Walthall, P.M. (1996). The solubility of aluminum in soils. In *The Environmental Chemistry of Aluminum*, Eds G. Sposito. Lewis Publishers: Boca Raton. 333-418.

López Valdivieso, A.L., Reyes Bahena, J.L., Bahena, Song, S., & Herrera Urbina, R. (2006). Temperature effect on the zeta potential and fluoride adsorption at the alpha-Al2O3/aqueous solution interface. *Journal of Colloid and Interface Science, 298*, 1-5.

Marel, H. W., & Beutelspacher, H. (1976). *Atlas of infrared spectroscopy of clay minerals and their admixtures*. Amsterdam: Elsevier Scientific Pub. Co.

Martell, A. E., & Smith, R. M. (1974). *Critical Stability Constants*, Plenum Press: New York.

Martinez, C. E. & McBride, M. B. (1998). Coprecipitates of Cd, Cu, Pb and Zn in iron oxides: Solid phase transformation and metal solubility after aging and thermal treatment. *Clays and Clay Minerals*, *46*, 537–545.

Maurice, P. (2009). *Environmental Surfaces and interfaces from the nanoscale to the global scale*. Wiley: Hoboken, NJ.

McKay, F.S. (1925). Mottled enamel: A fundamental problem in dentistry. *The Dental Cosmos, 67*, 847-860.

McKay, F.S. (1927). Mottled Enamel: The chemical determination of the discoloration known as the "Brown Stain." *The Dental Cosmos, 69*, 736-738.

McKay, F.S., & Black, G.V. (1929). The establishment of a definite relation between enamel that is defective in its structure, as mottled enamel, and the liability to decay. *The Dental Cosmos, 58*, 627-644.

Morel, F. (1983). *Principles of aquatic chemistry*. Wiley-Interscience: Michigan.

Nordin, J.P., Sullivan, D.J., Phillips, B.L., & Casey, W.H. (1999). Mechanisms for fluoride-promoted dissolution of bayerite and boehmite: F-NMR scpectroscopy and aqueous surface chemistry. *Geochimica et Cosmochimica Acta*, *63*(21). 3513-3524.

Nordstrom, D.K., & May, H.M. (1996). Aqueous equilibrium data for mononuclear aluminum species. In *The Environmental Chemistry of Aluminum*, Eds G. Sposito. Lewis Publishers: Boca Raton. 39-80.

Noren, K. & Persson, P. (2007). Adsorption of monocarboxylates at the water/goethite interface: The importance of hydrogen bonding. *Geochimica et Cosmochimica Acta*, *71*. 5717-5730.

O'Melia, C.R., Becker, W.C., & Au, K-K. (1999). Removal of humic substances by coagulation. *Water Science and Technology*, *40*(9), 47-54.

Pernitsky, D., & Edzwald, J.K. (2006). Selection of alum and polyaluminum coagulants: principles and applications. *Journal of Water Supply: Research and Technology—AQUA*, *55*(2), 121-141.

Persson, P., Nordin, J., Rosenqvist, J., Lövgren, L., Öhman, L., & Sjöberg, S. (1998). Comparison of the Adsorption of o-Phthalate (γ-AlOOH), Aged γ-Al2O3, and Goethite (α-FeOOH). *Journal of Colloid and Interface Science*, *206*, 252-266.

Phambu, N. (2002). Adsorption of carboxylic acids on submicrocrystalline aluminum hydroxides in aqueous solution, Part 1: qualitative study by infrared and raman spectroscopy. *Applied Spectroscopy*, *56*(6), 756-761.

Phillips, B., Casey, W., & Neugebauer Crawford, S. (1997). Solvent exchange in AlFx(H2O)(aq) complexes: Ligand-directed labilization of water as an analogue for ligand-induced dissolution of oxide minerals. *Geochimica et Cosmochimica Acta, 61*(15), 3041-3049.

Plankey, B.J., & Patterson, H.H. (1988). Effect of fulvic acid on the kinetics of aluminum fluoride complexation in acidic waters. *Environmental Science and Technology, 22*(12), 1454-1459.

Pomes, M.L., Green, W.R., Thurman, E.M., Orem, W.H., & Lerch, H.E. (1999). DBP Formation Potential of Aquatic Humic Substances. *Journal (American Water Works Association)*, *91*(3), 103.

Pommerenk, P., & Schafran, G.C. (2002). Effects of prefluoridation on removal of particles and organic matter. *Journal (American Water Works Association)*, *94*(2), 99-108.

Pommerenk, P., & Schafran, G.C. (2005). Adsorption of inorganic and organic ligands onto hydrous aluminum oxide: evaluation of surface charge and the impacts on particle and NOM removal during water treatment. *Environmental Science and Technology, 39*(17), 6429-6434.

Prakash A., & MacGregor D.J. (1983) Environmental and Human Health Significance of Humic Materials: An Overview. In *Aquatic and Terrestrial Humic Materials, Eds. Christman, R and Gjessing, E.T.* pp. 481-490.

Rebhun, M., & Lurie, M. (1993). Control of Organic Matter by Coagulation and Floc Separation. *Water Science and Technology, 27*(11), 1-20.

Reddy, R.D. (2009). Neurology of endemic skeletal fluorosis. *Neurology India, 57*(1), 7-12.

Richardson, S. D. (1998). Drinking Water Disinfection By-products. In *The Encyclopedia of Environmental Analysis and Remediation*, John Wiley & Sons: New York, Vol. 3, p 1398.

Ritchie, J.D., & Perdue, E.M. (2008). Analytical constraints on acidic functional groups in humic substances. *Organic Geochemistry, 39*, 783-799.

Semmens, M.J., & Ayers, K. (1985). Removal by coagulation of trace organics from Mississippi River Water. *Journal (American Water Works Association)*. *77*(5), 79-84.

Shin, J.Y., Spinette, R.F., & O'Melia, C.R. (2008). Stoichiometry of coagulation revisited. *Environmental Science & Technology, 42*(7), 2582-2589.

Smith, B.C. 1996. *Fundamentals of Fourier Transform Infrared Spectroscopy.* 2nd Ed. CRC Press: Hoboken.

Srinivasan, R., Sorial, G. A., Ononye, G., Husting, C., & Jackson, E. (2008). Elimination of persistent odorous compounds from drinking water. *Water Science & Technology: Water Supply*, *8*(2), 121-127.

Strunecka, A., & Patocka, J. (2002). Aluminofluoride complexes in the etiology of Alzheimer's Disease. *Structure & Bonding*, *104*, 139-180.

Stuart, B. (2004). *Infrared spectroscopy: fundamentals and applications*. Chichester.: John Wiley.

Szekeres, M., Tombacz E., Ferencz K., & Dekany I. (1998). Adsorption of salicylate on alumnina surfaces. *Colloids and Surfaces A: Physiochemical and Engineering Aspects, 141*, 319-325.

Texas Commission on Environmental Quality (TCEQ). (2011). Public Water System Database. http://www10.tceq.state.tx.us (accessed on 21 August 2011).

Tripathy, S.S., Bersillon, J-L, & Gopal, K. (2006). Removal of fluoride from drinking water by adsorption onto alum-impregnated activated alumina. *Separation and Purification Technology, 50*, 310-317.

Van der Heide, P. (2011) *X-ray photoelectron spectroscopy: An introduction to principles and practices.* Wiley: New Jersey

Vance, G.F., Stevenson, F.J., & Sikora, F. (1996). Environmental chemistry of aluminum-organic complexes. In *The Environmental Chemistry of Aluminum*, Eds G. Sposito. Lewis Publishers: Boca Raton. 39-80.

Violante, A., & Huang, P. (1992). Effect of Tartaric Acid and pH on the Nature and Physiochemical Properties of Short-range Ordered Aluminum Precipitation Products. *Clays and Clay Minerals*, *40*(4), 462-469.

Violante, A., & Huang, P.M. (1985) Influence of inorganic and organic ligands on the formation of aluminum hydroxides and oxyhydroxides. C*lays and Clay Minerals, 33*(3), 181-192.

Water System Data Sheet. (2009). PSW 165001: City of Midland Water Purification Plant. *Texas Commission on Environmental Quality:* http://www10.tceq.state.tx.us/iwud/reports/index.cfm?fuseaction=RunWSDataSheetreport&RequestTimeout=500&pwsid=1650001 (accessed 22 October 09).

Wu, W.W., Chadik, P.A., Davis, W.M., Delfino, J.J., & Powell, D.H. (2000). The effect of structural characteristics of humic substances on disinfection by product formation in chlorination. In *Natural Organic Matter and Disinfection By-Products: Characterization and control in drinking water.* Eds Barrett,S.E., Krasner, S.W., Amy, G.L. American Chemical Society: Washington D.C.: 109-121.

Xu, R.K., Yu, G., Kozak, L.M., & Huang, P.M. (2008). Desorption kinetics of arsenate adsorbed on Al (oxy)hydroxides formed under the influence of tannic acid. *Geoderma*, *148*, 55-62.

Xu,. R.K., Hu, Y.F., Dynes, J.J., Zhao, A.Z., Blyth, R.I.R., Kozak, L.M., & Huang, P.M. (2010). Coordination nature of aluminum (oxy)hydroxides formed under the influence of low molecular weight organic acids and a soil humic acid studied by X-ray absorption spectroscopy. *Geochimica et Cosmochimica Acta*, *74*, 6422-6435.

Yoon, T.H., Johnson, S.B., & Brown Jr., G.E. (2005). Adsorption of Organic Matter at Mineral/Water Interfaces. IV. Adsorption of Humic Substancesat Boehmite/Water Interfaces and Impact on Boehmite Dissolution. *Langmuir. 21*, 5002-5012.

Yu, G., Saha, U.K., Kozak, L.M. & Huang, P.M. (2007). Combined effects of tannate and ageing on structural and surface properties of aluminum precipitates. *Clays and Clay Minerals.* &(4). 369-379.

Zoschke, K., Engel, C., Boernick, H. & Worch, E. (2011). Adsorption of geosmin and 2-methylisoborneol onto powdered activated carbon at non-equilibrium conditions: Influence of NOM and process modeling. *Water Research*, *45*(15), 4544-4550.

Zutic, V., & Stumm, W. (1984). Effect of organic acids and fluoride on the dissolution kinetics of hydrous alumina. A model study using the rotating disc electrode. *Geochimica et Cosmochimica Acta, 48*, 1493-1503.

Vita

Katherine Alfredo was born in Brooklyn, NY and was educated in the New York City public education system. Katherine graduated from Fort Hamilton High School's Honors Academy and obtained her B.E. in Civil Engineering from The Cooper Union for the Advancement of Science and Art in NY, NY. While at Cooper Union, Katherine worked internships at local engineering companies as well as in Italy at *Universita degli Studi di Firenze*. After graduating from The Cooper Union, Katherine traveled to Ghana, West Africa, where she studied the problems and health risks associated with elevated levels of fluoride in groundwater. A year later, Katherine began graduate school at the University of Texas at Austin (UT) in the Environmental and Water Resources Engineering Department. Funded by the National Science Foundation (NSF) Graduate Research Fellowship Program, Katherine began her research on fluoride treatment. After completing her M.E., Katherine traveled back to Ghana on a U.S. Student Fulbright Fellowship to research fluoride-related issues on a community level. After completing her tenure in Ghana as a Fulbright Fellow, Katherine returned to UT and commenced her Ph.D. research in Civil Engineering. While in pursuit of her Ph.D., Katherine was engaged in K-12 science outreach developed while a fellow in the NSF GK-12 Graduate STEM Fellowship initiative at UT Austin.

Permanent email: Katherine.alfredo@fulbrightmail.org

This dissertation was typed by Katherine Ann Alfredo.